BALTIMORE 3, MARYLAND

DISCLAIMER

This work was done under Contract
AT(30-3)-217, sponsored by the
Division of Reactor Development,
U. S. Atomic Energy Commission.

Strontium-90 Fueled Thermoelectric Generator Power Source

Five-Watt U. S. Navy Weather Station

Final Report

MND-P-2707

Approved by:

James J. Keenan

Asst Project Engineer

LEGAL NOTICE

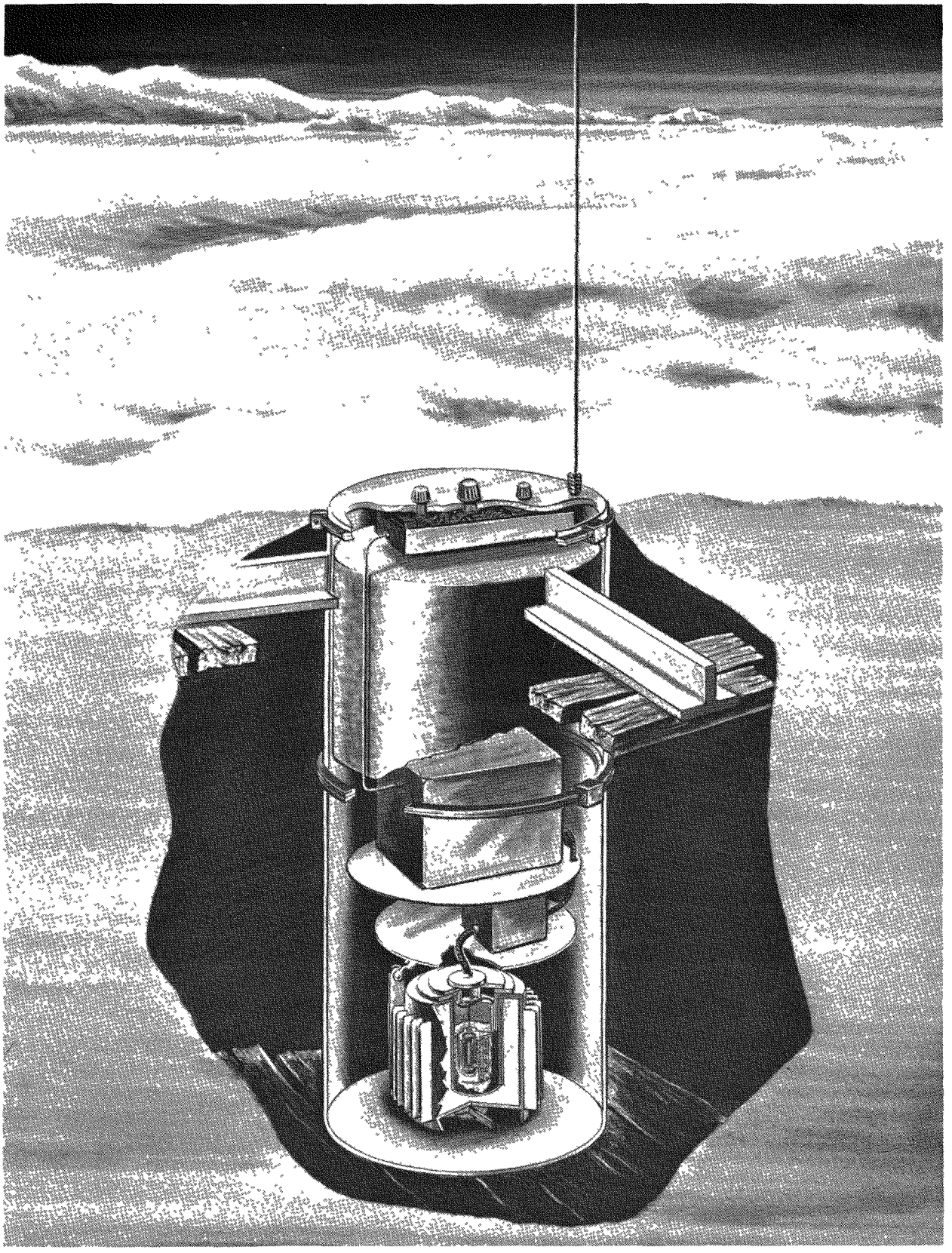

Artist's Concept of SNAP 7C

DISTRIBUTION LIST

	No. of Copies
1. Atomic Energy Commission	
a. Washington	
For: Mr. G. M. Anderson, DRD	10
Lt. Col. C. M. Barnes, DRD	1
Capt. T. L. Jackson, DRD	1
R. G. Oehl, DRD	1
E. F. Miller, Jr., Prod	1
R. A. Anderson, Patents	1
Technical Library	1
Lt. Cdr. J. P. Culwell	1
Capt. R. Carpenter	1
b. Canoga Park Area Office	
For: J. V. Levy, Area Manager	1
c. Chicago Operations Office	
For: T. A. Kemmek	2
d. New York Operations Office	
For: J. Cline	2
J. E. McLaughlin	1
e. Hanford Operations Office	
For: J. T. Christie	1
f. Division of Technical Information Extension	35
2. Convair, San Diego	
For: K. G. Blair	1
3. Defense Atomic Support Agency, Sandia	1
4. Department of the Air Force	
a. Space Systems Division	
For: Capt. W. W. Hoover	1
b. Aeronautical Systems Division	3

DISTRIBUTION LIST (continued)

	No. of Copies
c. Special Weapons Center (SWOI)	2
d. Rome Air Development Center	
For: RCSG, J. L. Briggs	1
e. School of Aviation Medicine	1
f. Air University Library, Maxwell AFB	
For: Maj. L. C. Free	1
g. Advanced Research Projects Agency	
For: F. A. Koether	1
Dr. J. Huth	1
h. Air Technical Intelligence Center	1
5. Deparment of the Army	
a. Atomic Division	1
b. Diamond Ordnance Fuze Laboratories Office of the Chief of Ordnance	
For: ORDTL 0/2	2
Mrs. E. W. Channel	1
c. Ballistic Missile Agency	
For: ORDAB-RSI	2
6. Department of the Navy	
a. Bureau of Naval Weapons	
For: Code RR-12	2
Code RA-8	1
R. W. Pinnes, RR-24	1
b. Bureau of Ships	
For: Lt. Cdr. F. W. Anders, Code 353	1
c. Chief of Naval Operations	1

DISTRIBUTION LIST (continued)

		No. of Copies
	d. Naval Ordnance Laboratory	1
	e. Naval Research Laboratory	1
	f. Office of Naval Research	
	For: Code 429	1
	g. Naval Radiological Defense Laboratory	1
7.	Lawrence Radiation Laboratory	
	For: T. C. Merkle	1
	Dr. R. W. Hoff	1
8.	Los Alamos Scientific Laboratory	
	For: Dr. R. D. Baker	1
	Dr. W. Maraman	1
9.	Rand Corporation	1
10.	Oak Ridge National Laboratory	
	For: E. Lamb	1
	Dr. K. Z. Morgan	1
11.	University of Pennsylvania	
	For: Dr. D. S. Murray	1
12.	University of Washington, APL	1

FOREWORD

This is the final report on the five-watt system for the U.S. Navy Weather Station. It has been prepared for the U.S. Atomic Energy Commission in compliance with Contract AT(30-3)217. The work was completed by the Martin Marietta Corporation.

CONTENTS

CONTENTS (continued)

SUMMARY

The objectives of the SNAP 7C program were to design, manufacture, test, and deliver a five-watt electric generating system for a U.S. Navy Weather Station in Antarctica. This report describes the 10-watt Sr-90 thermoelectric generator, the dc-dc converter, batteries and weather station housing that were delivered to Antarctica in December 1961. Subsequent checkout tests at McMurdo Sound in January 1962 indicated satisfactory performance of the weather station power supply.

In addition to delivering the power supply, many tests were required for the SNAP 7C system to demonstrate its qualifications for conformance to the contract statement of work. Such tests as electrical performance, shock and vibration, environmental temperature extremes and many others are explained in detail. This program was initiated in October 1960, and delivery of the complete SNAP 7C system was made to Davisville, Rhode Island for overseas shipment in October 1961.

NOMENCLATURE

Chapter III

A_n	cross-sectional area of N element (cm^2)
A_p	cross-sectional area of P element (cm^2)
C	contact resistivity (μ-ohm-cm^2)
D_n	N element diameter (cm)
D_p	P element diameter (cm)
e	open circuit voltage (volts)
K	thermal conductivity of element pair (watts/°C)
k_n	thermal conductivity of N element (watts/cm/°C)
k_p	thermal conductivity of P element (watts/cm/°C)
l	thermoelement length
N	number of thermoelements
R_c	hot junction contact resistance (ohms)
R_i	thermoelement internal resistance (ohms)
R_l	load resistance (ohms)
α_n	N element Seebeck coefficient (μvolts/°C)
α_p	P element Seebeck coefficient (μvolts/°C)
T_I	hot junction temperature (°K)
ΔT_t	thermoelement temperature difference (°K)
v	voltage
Z	Figure of Merit ($°C^{-1}$)
α	total Seebeck coefficient for element pair (μvolts/°C)
η	thermoelectric conversion efficiency

μ	Prefix meaning 10^{-6}

Chapter IV

A_c	area available for heat transfer by convection (ft^2)
A_r	area available for heat transfer by radiation (ft^2)
A	profile area of fin (ft^2)
e_s	fin efficiency
h_c	heat transfer coefficient for convection (Btu/hr-ft^2-°F)
h_r	heat transfer coefficient for radiation (Btu/hr-ft^2-°F)
k	thermal conductivity (Btu/hr-ft-°F)
N	number of fins on generator shield surface
r_1	inner radius of insulation (ft)
r_2	outer radius of insulation (ft)
q	rate of heat flow (Btu/hr-watts)
q_{conv}	rate of heat flow by convection (Btu/hr-watts)
q_{rad}	rate of heat flow by radiation (Btu/hr-watts)
ΔT_i	temperature difference between inner and outer insulation surfaces
W	fin length (ft)
W_c	fin length plus one-half fin thickness (ft)
δ	one-half fin thickness (ft)
ϵ	variable used in calculation of fin efficiency (dimensionless)
ϵ_s	surface emissivity (dimensionless)

Chapter IX

a	amperes
cps	cycles per second

DA	double amplitude displacement
MS	millisecond
Tc	thermocouple
v	volts
W	watts

I. INTRODUCTION

A radioisotope fueled thermoelectric generator system has been developed by the Martin Marietta Corporation for the Atomic Energy Commission/U. S. Navy (Contract AT(30-3)-217, SNAP 7 Program). This system will provide electrical power for a five-watt remote weather station which will automatically broadcast local weather conditions at regular intervals from Little America V, Antarctica.

The system was designed to operate in the environmental extremes of the Antarctic Continent without attendance or maintenance for periods of two years, and to have a useful life of 10 years when maintained in accordance with Contractor Instructions (Ref. 4). It will transmit weather data to the base at McMurdo Sound.

The SNAP 7C System consists of a thermoelectric generator, a dc-dc voltage converter, and a battery pack to serve as a reservoir for the storage of electrical energy.

II. PHYSICAL DESCRIPTION

The generator, battery-converter package, and U.S. Navy weather station acquisition and radio transmission equipment are enclosed in a water tight, two-piece cylindrical container 36 inches in diameter and 96 inches high. The system is installed as shown in Figs. II-1 and II-2.

A. SYSTEM INSTALLATION

The system enclosure container is buried in the ice so only the antenna-instrument mast and its bushing are exposed. This arrangement allows the waste heat from the generator to be used to protect the converter battery package and weather station equipment from the environmental temperature extremes. The container air temperature ranges between ~20° and 60° F during the year. In addition, the dampening of the generator external temperature fluctuations yields more uniform generator output.

The container rests on a wooden platform of 2 by 8-inch planks buried in the ice. Additional planks are employed to support the outriggers at the top of the container. The two sets of planks will keep the container from sinking into or tipping on the ice.

The thermoelectric generator is located at the bottom of the system container. The watertight battery-converter enclosure is mounted on a removable panel immediately above the generator. Weather station equipment is mounted on a separate panel above the battery-converter pack. A styrofoam thermal insulation plug fills the top of the container.

B. THERMOELECTRIC GENERATOR

The SNAP 7C thermoelectric generator consists of a Sr-90 heat source, a thermoelectric conversion circuit, a heat rejection system and a biological shield. Figures II-3 and II-4 show the configuration of the generator.

The Sr-90 heat source, 250 watts thermal at start of life, will power the generator for 10 years. The isotope fuel is formed into flat disks and sealed within Hastelloy C cylindrical containers. Four fuel containers are installed in a Hastelloy C fuel block which is used to conduct the heat energy to the thermoelement hot junctions. The flat surfaces of the fuel block that contact the thermoelements are coated with aluminum oxide to electrically insulate the thermoelements and allow the heat to be transferred.

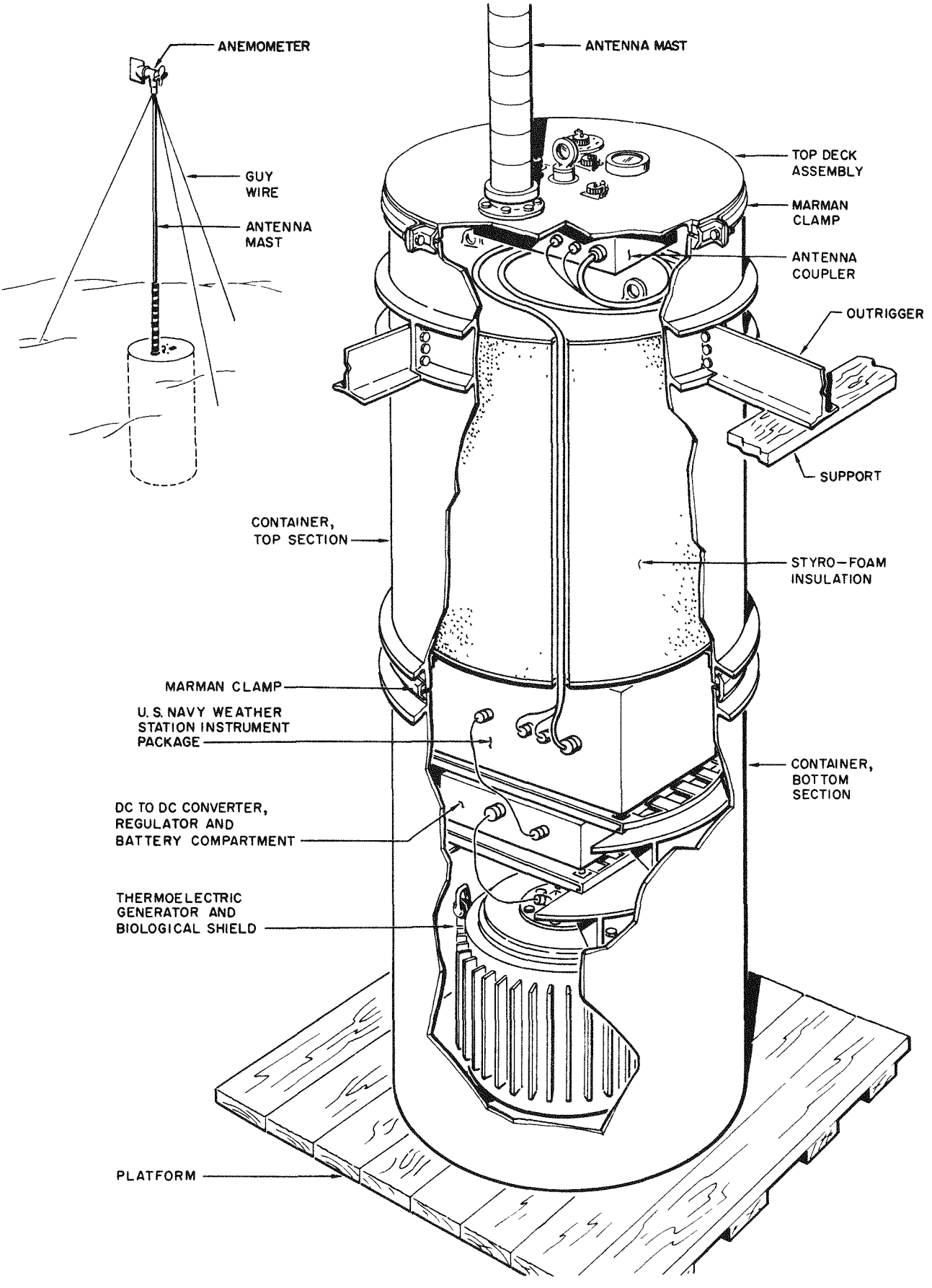

Fig. II-1. SNAP-7C Electric Generation System Installation

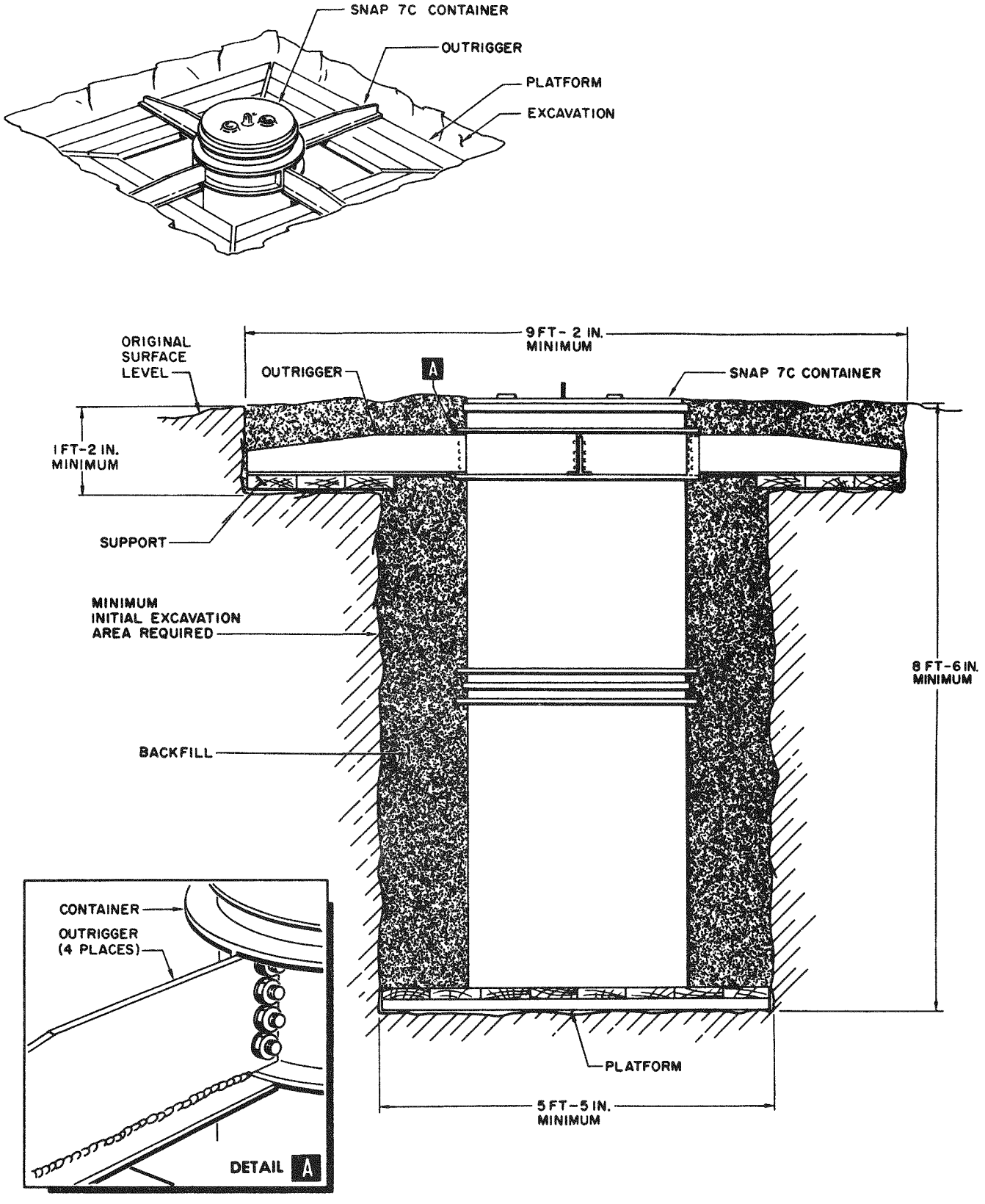

Fig. II-2. Installed Container and Platforms

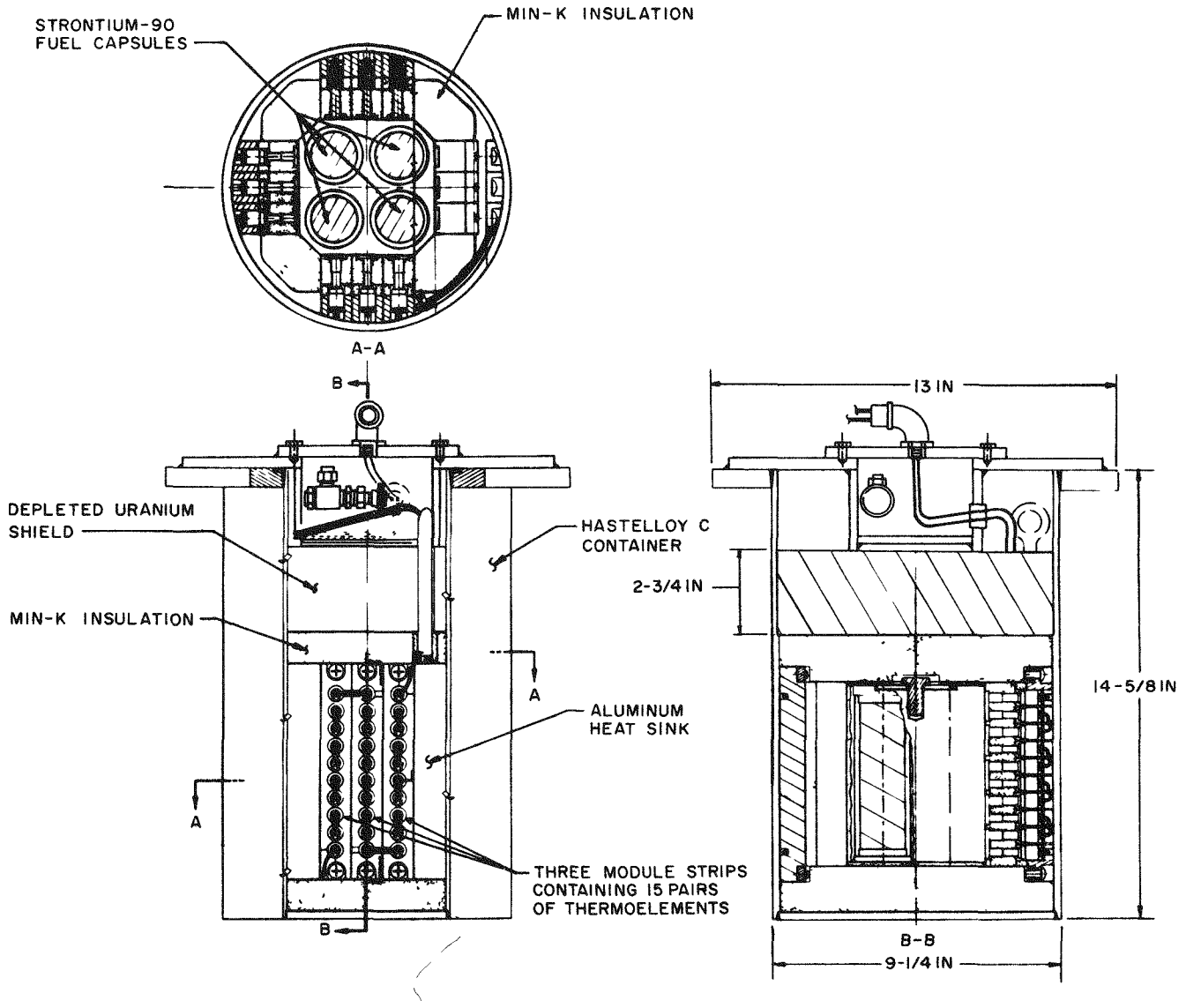

TOTAL WEIGHT OF GENERATOR ASSEMBLY = 235 LB
INCLUDING 114 LB OF DEPLETED URANIUM

Fig. II-3. Generator Details

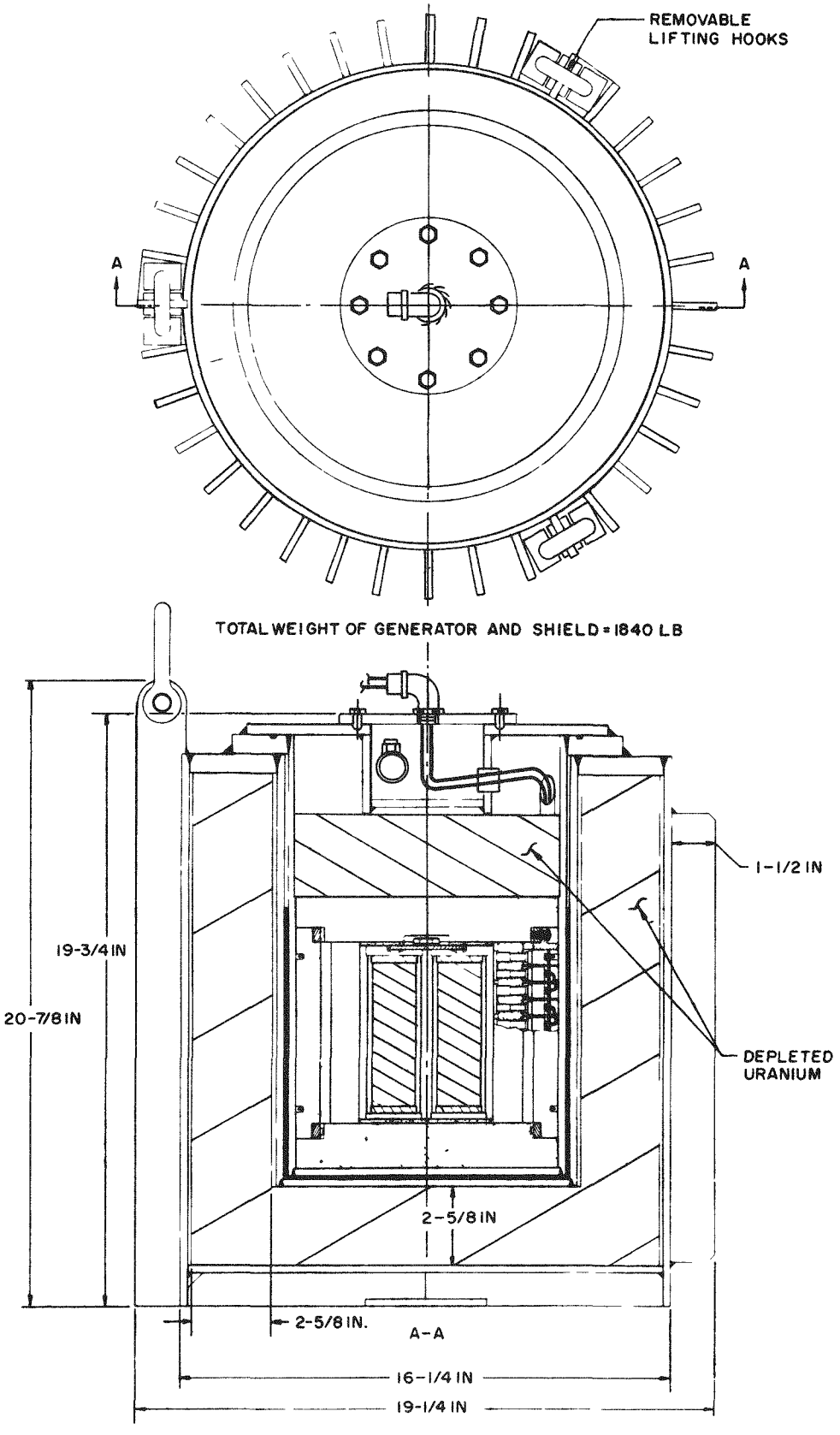

Fig. II-4. Biological Shield

A pair of thermoelements are attached to an iron shoe that serves as a hot junction connection and transfers heat from the fuel block to the lead telluride thermoelectric elements (see Figs. II-5 and II-6). A copper cap is soldered to the cold end of each element to conduct heat from the element and to serve as an electrical connection. Martin Hard Coat aluminum hardware is used to conduct heat from the copper cap to the heat sink. The hard coat serves as an electrical insulation.

Sixty pairs of lead telluride thermoelements are used to convert a part of the decay heat to 10 watts of electrical power.* Five pairs are assembled into module strips. Three module strips are assembled on each of the four sides of the fuel block. The remaining volume around the fuel block is filled with Johns-Manville Min-K insulation. The fuel, fuel block, thermoelectric elements and associated hardware are contained within a Hastelloy C can.

The generator housing is flushed and backfilled with one atmosphere of an inert gas. The flushing and backfilling removes the oxygen that acts as poison to the thermoelectric elements. By changing the gas at maintenance periods and replacing it with a gas that is a poorer thermal conductor, it is possible to obtain a stepwise power flattening method. This method alleviates the thermal output reduction from the isotope as it decays and allows the generator to meet design power requirements for a 10-year period.

When the generator is operating in a 70° F ambient environment, the hot junction temperature at the beginning of life is approximately 920° F. At the end of service life, this will decrease to about 820° F under the same ambient conditions.

The generator container is installed in the biological shield container. Mercury between the containers serves as a heat conducting medium. The heat rejected at the cold junction is then conducted through the biological shield to the 36 fins mounted on the outside of the shield container. This rejected heat is utilized to maintain a temperature of 20° to 60° F in the system container enclosure.

Depleted uranium metal is used for radiation shielding. The top portion of the shield is contained in the same can as the generator. The shielding on the sides and bottom consists of a separate assembly contained in a Hastelloy C shell. The shielding thickness is sufficient to safely meet Interstate Commerce Commission (ICC) shipping and handling requirements.

---

*Five watts are lost in the converter and battery resulting in five watts total system output.

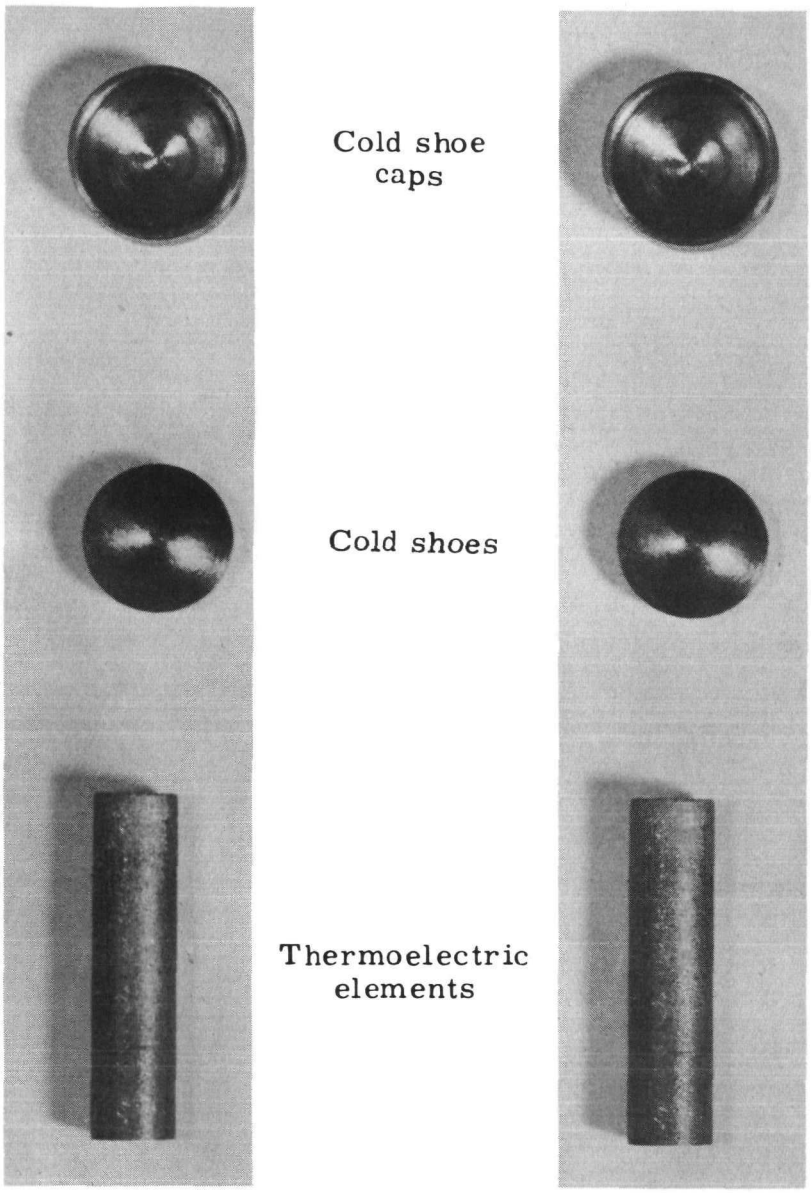

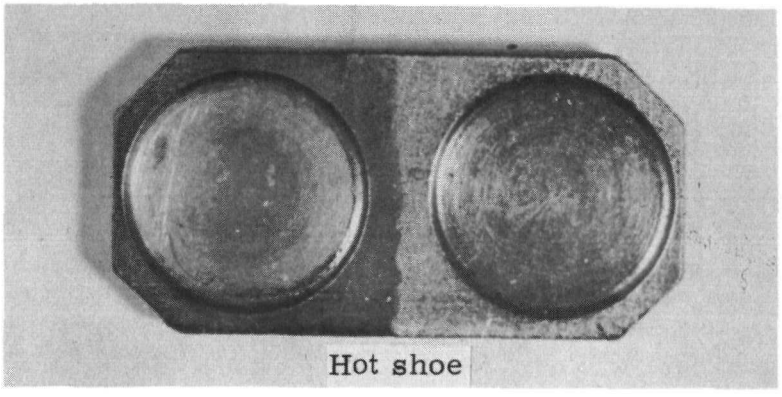

Fig. II-5. Components of Thermoelectric Couple

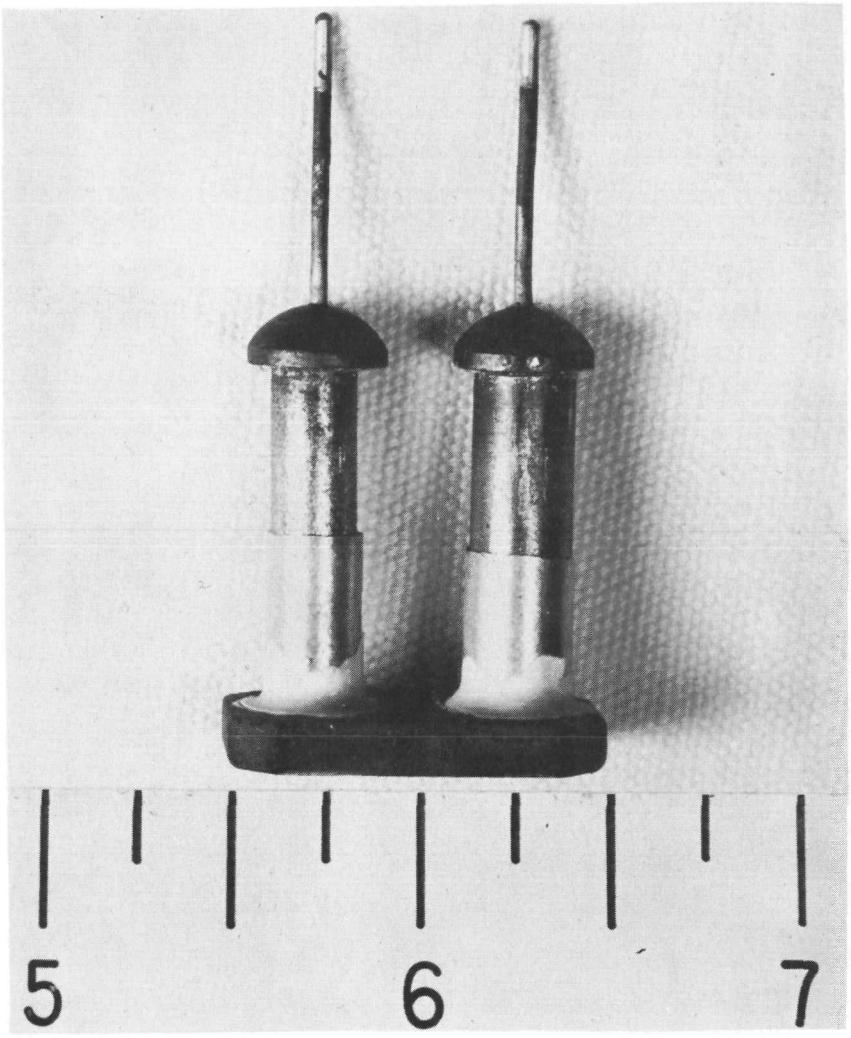

Fig. II-6. SNAP 7C Thermoelectric Couple

Due to the possible hazards associated with the use of a radioisotope, very stringent requirements were placed on isotope containment. The Sr-90 isotope, used in the titanate form, is virtually insoluble. Disks of the compacted and sintered isotope were sealed in Hastelloy C containers. This material was chosen because of its very good structural qualities and its excellent corrosion resistance. It was calculated that the fuel container would retain the Sr-90 titanate for over 1000 years if submerged in sea water. This would be true even if the corrosion rate was double that found through tests at the Wrightsville Beach Corrosion Center, N.C. The Hastelloy C fuel container, in conjunction with the generator housing and the system container, provides triple containment for the radioisotope.

C. BATTERY AND CONVERTER COMPARTMENT (see Fig. II-7)

The battery and converter compartment is a steel container that houses the battery and converter. It contains the input and output electrical connectors in addition to the interconnecting wiring and test circuits as illustrated in Fig. II-8. A pressure relief valve prevents pressure buildup due to possible battery gassing. A calorimeter is installed to monitor the generator output voltage and transmit the data to the remote receiving station.

1. Battery

The battery is a 10-ampere-hour, sintered plate, nickel-cadmium type (Sonotone 24-1-H120) which provides high current service and cold temperature operation to -65° F. The battery is made up of 22 cells which are connected in electrical series and tapped to provide -4, -8, -12, and -28 volts.

All cells have plastic cases and are housed together in a steel battery case. The assembly of the cells within the steel case is such that a cell may be removed and replaced if it is accidentally damaged during assembly. The cells contain a built-in venting system that prevents spilling when the battery is operated in any position, but permits the escape of the small amount of gas that may form while the battery is being charged. The battery does not form gas during discharge.

2. DC-to-DC Converter

The dc-to-dc converter is an epoxy resin potted unit with two input terminals and eight output terminals. The low voltage d-c output from the thermoelectric generator is connected to the converter which changes the direct current to an alternating voltage and then by means

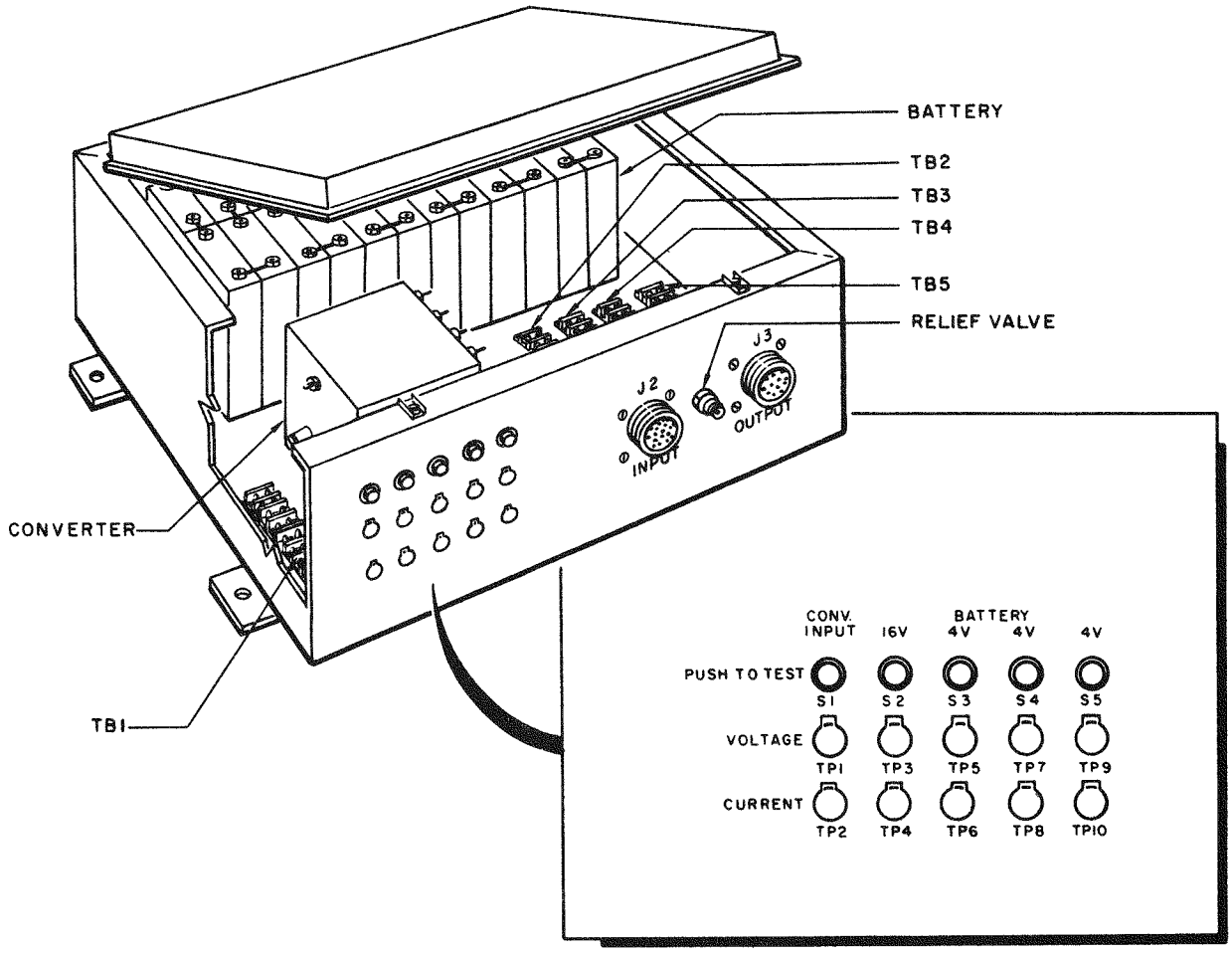

Fig. II-7. Battery and Converter Compartment

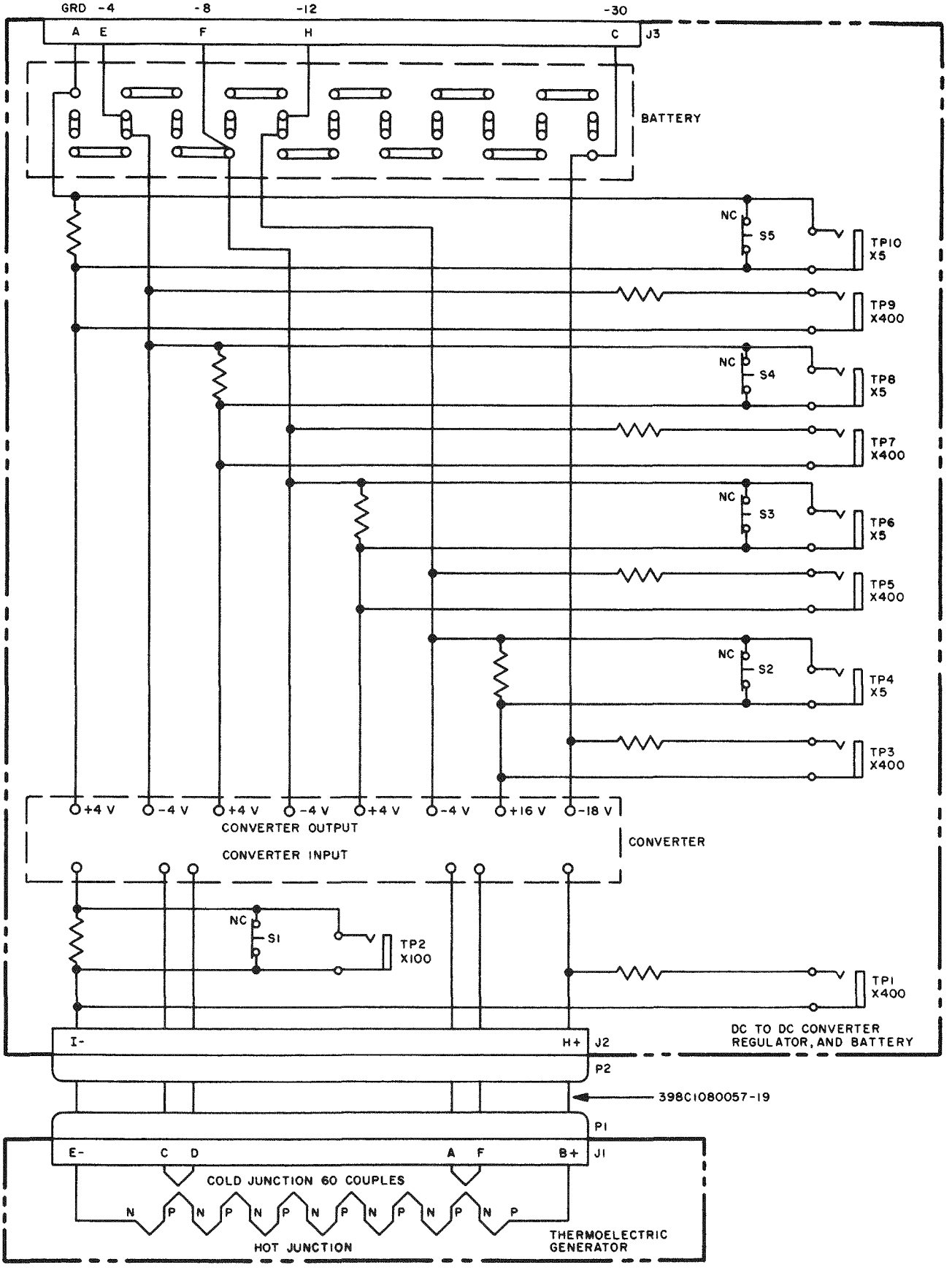

Fig. II-8. Battery and Converter Compartment Schematic

of a transformer, steps up the voltage. There are three 4-volt output sections and one 18-volt output section, each output being rectified and independently applied to cells of the battery. The voltage of each output circuit is closely regulated to provide a fixed potential charging system for each section of the battery. The converter provides a fixed load on the thermoelectric generator, regardless of output load, to maintain stable operation.

III. THERMOELECTRIC ANALYSIS

A. MATERIAL SELECTION

The basic parameter involved in the choice of a thermoelectric material to operate over a given temperature range is the figure of merit, Z. Materials exhibiting high figures of merit will give higher heat to electrical conversion efficiencies than those with low values. This is especially important in radioisotope fueled thermoelectric generators because of the high cost of the isotope. The figure of merit is defined by:

$$Z = \frac{\alpha^2}{k\rho}$$

where

α = Seebeck coefficient

k = thermal conductivity

ρ = electrical resistivity.

The figure of merit, however, is not the sole basis for thermoelectric material selection. Other factors which must be taken into consideration are the structural stability and bonding characteristics of the material. If a thermoelement is brittle and should happen to crack while within the generator, an open circuit will result. Or, if low electrical resistance bonds cannot be made between the thermoelement and its hot and cold shoes, large electrical losses will occur at these junctions, thus resulting in lowered heat to electricity conversion efficiencies.

Lead telluride is the thermoelectric material which has the highest figure of merit over the temperature range considered for this generator. Even though it is a brittle material, it still possesses enough structural stability to be usable in a properly designed generator and relatively low junction resistances can be obtained. Further, this material is readily available from several manufacturers.

The lead telluride that is used as a thermoelectric material is a semiconductor that is doped with carefully controlled, minute concentrations of impurities in much the same manner as a transistor. Also, like a transistor, the properties of lead telluride thermoelectric material will vary radially with the type and concentration of doping and the method of manufacture. Therefore, a further choice of the type

of lead telluride material to be used must also be made. This choice is based on the same considerations that were given previously in the basic selection of a material.

Samples of lead telluride materials were obtained from Transitron, Incorporated, located in Wakefield, Massachusetts, for comparison with the Martin Marietta produced material. These samples were bonded to simulate the hot and cold shoe installation in the generator (Figs. II-5 and II-6) and operated over the anticipated temperature differential expected to be the end of life condition (700° to 320° K). Measurements made during these tests were used to calculate the Seebeck coefficient, electrical resistivity and electrical contact resistivity of the element. The properties of the test samples were statistically averaged and are shown with independently measured values of thermal conductivity in Table III-1.

TABLE III-1

Summary of Module Test Thermoelectric Properties*

	Average Properties			
	Martin N	Transitron N	Martin P	Transitron P
Seebeck voltage (μv/°C)	204	257	177	213
Resistivity (μohm-cm)	1310	2870	2675	4300
Contact resistivity (μohm-cm^2)	386	575	830	760
Thermal conductivity (watts/cm-°C)	0.0199	0.0180	0.0208	0.0196
Figure of merit (°C^{-1})	1.585 x 10^{-3}	1.325 x 10^{-3}	0.564 x 10^{-3}	0.538 x 10^{-3}

*Based on a hot end temperature of 700° K and a cold end of 320° K.

The N and P designations given in Table III-1 simply represent the two legs of materials used in a thermoelectric couple. The N

material develops a plus to minus potential in going from the hot to cold end, while P material develops a minus to plus potential. In this manner, N and P materials may be connected in series to form a couple, and an additive rather than a bucking voltage output is obtained.

Based on the figures of merit determined from the measured properties, the best combination of thermoelements would be the Martin Marietta N and P types. Operation over long periods of time showed these materials to be durable and to experience only slight degradation in performance.

B. THERMOELECTRIC EFFICIENCY AND ELEMENT SIZING

Once a thermoelectric material has been selected, based on a specified temperature range, the number and size of the thermoelements and their conversion efficiency must be determined. These values may be obtained from the desired voltage and power output of the generator to be produced. The thermoelement properties listed in Table III-1 were used in these determinations.

The maximum heat to electricity conversion efficiency of a thermoelement operating over a specified temperature range is given by:

$$\eta = \frac{\Delta T_t}{T_I} \cdot \frac{\left(\frac{R_1}{R_i + R_c}\right)}{\left(\frac{R_1}{R_i + R_c} + 1\right) + \frac{K(R_c + R_i)\left(\frac{R_1}{R_i + R_c} + 1\right)^2}{\alpha^2 T_I} - \frac{\Delta T_t\left(\frac{R_i}{2} + R_c\right)}{T_I (R_i + R_c)}}$$

where

$\alpha = \alpha_n + \alpha_p$ = combined Seebeck coefficient (v/°C)

α_n = Seebeck coefficient of N element (v/°C)

α_p = Seebeck coefficient of P element (v/°C)

R_1 = load resistance

$R_i = \frac{\rho l}{A}$ = thermoelement resistance (ohms)

ρ = thermoelement resistivity (ohm-cm)

l = thermoelement length (cm)

A = thermoelement cross sectional area (cm^2)

$R_c = \frac{C}{A}$ = contact resistance (ohms)

C = contact resistivity ($ohm\text{-}cm^2$)

ΔT_t = thermoelement temperature difference (°K)

T_I = thermoelement hot junction temperature (°K)

$K = \frac{kA}{l}$ = thermal conductance (watts/°C)

k = thermoelement thermal conductivity (watts/cm-°C).

The origin of this expression will not be clarified in this report. For the means of deriving this equation and a complete explanation of thermoelectric theory, reference is made to "Semiconductor Thermoelements and Thermoelectric Cooling," by Ioffe.

Other expressions required for the optimum sizing of the thermoelements are:

$$e = N\alpha\Delta T_t$$

and

$$\frac{R_l}{R_i + R_c} = \left[1 + \frac{\alpha^2 T_I}{K(R_c + R_i)} - \frac{\alpha^2 \Delta T_t \left(\frac{R_i}{2} + R_c \right)}{K(R_c + R_i)^2} \right]^{1/2}$$

where

e = open circuit voltage of the generator (volts)

N = thermoelement pairs (No.)

An iterative balance may now be performed between the previous three equations and the insulation losses, given in Chapter IV, and all the thermal and electrical characteristics of the generator may be determined. In this procedure the generator system is treated as though it is a simple d-c electrical circuit. Either the thermoelement length or diameter must be arbitrarily specified. The thermoelement length was chosen to be 2.54 centimeters for the design of this particular generator and the material properties used were those listed in Table III-1 for the Martin N and P thermoelements. Based on these inputs, the generator characteristics listed in Table III-2 were determined.

TABLE III-2

Generator Physical and Operational Characteristics

	N-Type	P-Type
Thermoelement		
Length (cm)	2.54	2.54
Diameter (cm)	0.585	0.705
End of life thermal power (watts)	200 (based on initial fuel loading)	
Insulation losses (see Chapter IV) (watts)	50.75	
Thermoelement efficiency (%)	6.23 (end of life)	
Generator efficiency (%)	4.65 (end of life)	
Power output (watts(e))	9.3 (end of life)	
Element pairs (No.)	60	
Open circuit voltage (volts)	8.70 (end of life)	
Load voltage (volts)	4.71 (end of life)	

It may be noted that the end of life power output is given as 9.3 watts(e) which is slightly lower than the design goal of 10 watts(e). The design goal will be achieved by altering the thermal losses through the generator insulation. This will be accomplished by changing the insulation gas fill at each maintenance period with successively poorer conducting gases. The range of gases to be used will vary from

highly conductive helium at the beginning of life when excess thermal power is available to a poorer conductor such as xenon at the end of life. A thorough discussion of this method of varying the thermal conductivity of Johns-Manville Min-K insulation may be found in Chapter IV.

IV. THERMAL ANALYSIS

The analysis of heat flow and temperatures within the SNAP 7C system was divided into two general areas: thermal analysis of the outer shell of the generator and thermal analysis of the SNAP 7C system with the generator as a heat source. The outer shell analysis was necessary to determine the temperature difference between the thermoelement hot and cold junctions and the heat losses through the Min-K 1301 thermal insulation. The thermal analysis of the system with the generator as a heat source was required to determine the actual operating temperature of the generator and other temperature-sensitive system components.

The most critical temperature in the thermal analysis is the hot junction temperature. Lead telluride thermoelectric elements deteriorate rapidly by sublimation at temperatures greater than 1000° F. For an extended period of life such as is desired in the SNAP 7C generator, the maximum tolerable hot junction temperature was chosen as 980° F. This fixes the maximum beginning of life temperature and, assuming no change in the thermal properties of the generator, enables calculation of the end of life hot junction temperature as 800° F.

The initial step in the thermal analysis of the generator was to determine the ambient conditions in which the generator will operate. Given a rough configuration of the generator, the outer heat rejecting surface can be designed to maintain the inner temperatures at desired levels. The outer shell of the generator acts as the heat rejection surface. The design of the fuel block, thermoelements, inner container shield and outer container fixes the minimum dimensions of the outer generator silhouette. Additional surface in the form of thermal fins could be added if they are required for an additional heat rejection capability.

A thermal study was made to determine the best location for the generator radiation shielding. The choice of location included either completely enclosing the heat source, thus requiring a shield of smaller volume, or completely enclosing the generator. The study indicated that the shield should be located on the outside of the generator. The increase in the fuel block surface area, resulting from incorporation of the shield into the fuel block, results in lower hot junction temperatures and higher insulation heat losses, thus reducing generator efficiency.

The generator must be adaptable to operation in two different environments:

(1) During shipment, when the air temperature may go as high as 125° F in an enclosed space. (However, the generator

terminals may be short-circuited during shipment producing lower hot junction temperatures due to the Peltier effect.)

(2) Installed in its container that is buried in the ice in the Antarctic.

Condition (2) poses no problem to cooling the generator surface. The generator design point is for operation in the temperature range resulting from this condition.

Since there is a possibility of high ambient temperature and lack of circulating air during shipment, the surface of the generator had to be designed so that it operated at temperatures no higher than 175° F to prevent the excessively high temperatures damaging the thermoelements. This was accomplished in the following manner.

The maximum heat input to the generator was anticipated to be 256.5 watts. The heat lost from the generator surface is given by:

$$q_{total} = q_{conv} + q_{rad} = 256.5 \text{ watts} \quad (1)$$

where

$$q_{conv} = h_c A_c \Delta T \text{ (heat rejected by convection)} \quad (2)$$

$$q_{rad} = h_r A_r \Delta T \text{ (heat rejected by radiation)} \quad (3)$$

The generator surface was considered to consist of a cylinder 16.25 inches in diameter and 17 inches high with a number of 1.5-inch long fins running longitudinally along the cylindrical surface. The 1.5-inch fin length represents an optimum for Hastelloy C, a poor conductor of heat, but which is desirable for its corrosion resistance. The number of fins required was determined as follows.

The surface area available for radiant heat transfer is approximately the area of the cylinder taken over the edge of the fins, including the top of the cylinder, but excluding the bottom (refer to "Heat Transmission," McAdams).

$$A_r = 8.59 \text{ ft}^2$$

The convective heat transfer area is approximately the area of the cylinder excluding the bottom plus the effective fin area. The effective fin area is the total fin surface area multiplied by the fin efficiency. The fin efficiency accounts for the reduced heat rejection capability of the fin that results from the temperature gradient along its length. The fin efficiency is given by (Ref. 3, p 72):

$$e_s = \left(\frac{1}{\sqrt{2\epsilon}}\right) (\tanh \sqrt{2\epsilon}) \quad (4)$$

where

$$\epsilon = W_c^{3/2} \sqrt{h_c / kA} \quad (5)$$

W = fin length

$W_c = W + \delta$

δ = one-half of fin thickness (0.125 inch)

$h_c = 0.27 (\Delta T)^{0.25}$ (Ref. 3, p 474) (6)

The resulting fin efficiency is then:

$e_s = 0.826$

Therefore:

$A_c = 7.46 + 0.291 \text{ N ft}^2$

where

N = number of fins required

The radiant heat transfer coefficient was determined by:

$$h_r = \sigma \epsilon_s \frac{\left[(T_s/100)^4 - (T_r/100)^4\right]}{T_s - T_r} \quad (7)$$

where

ϵ_s = surface emissivity = 0.50

σ = Stefan-Boltzmann constant = 0.173 (Btu/ft^2-hr-°R^4)

T_s = generator surface temperature (°R)

T_r = ambient temperature (°R)

The heat rejected by the outer surface is thus given by (Eqs (1), (2) and (3)):

$$q_{total} = (0.718)\,(7.46 + 0.291N)\,(50) + (0.692)\,(8.59)\,(50)$$

which must equal the total design input of 877 Btu/hr. From this consideration

$$N = 29.9 \text{ fins.}$$

It was thus shown that a minimum of 30 fins was required on the outer surface. To supply a margin of safety to the calculation, the number of fins actually used was 36.

A. INSULATION HEAT LOSSES

A limited test program was conducted to determine the thermal conductivity of the Min-K insulation filled with various gases. The gas serves a twofold purpose, preventing sublimation of the thermoelements and changing the thermal conductivity of the insulation to reduce heat losses as the heat input to the generator is reduced by isotopic decay. (A less conductive gas is used to fill the generator at each biennial maintenance.)

The following values of insulation thermal conductivity were obtained for various gas fills at a pressure of one atmosphere.

Gas Fill	Thermal Conductivity (Btu-in./hr-ft^2-°F)
Air	0.2865
Argon	0.2285
Hydrogen	0.597
Vacuum	0.118

The fuel block is separated from the cold portions of the generator by a layer of Min-K 1301 insulation chosen for its low thermal conductivity, good structural qualities and machinability. The insulation fits between the fuel block and cold junction heat sink snugly enough to provide support for the block. Powdered Min-K is packed around the thermoelements to further reduce heat losses. The mean insulation thickness is 1.38 inches.

For the generator design calculation, a nominal value of thermal conductivity of 0.0175 Btu/hr-ft-°F was selected. This corresponds roughly to a mixture of approximately 90% argon, 10% hydrogen in the Min-K insulation.

Heat losses through the insulation were calculated by the following relationship which holds for cylinders with a length-to-diameter ratio of one, surrounded by a constant thickness of insulation.

$$q = \frac{6\pi r_1 r_2 k \Delta T_i}{r_2 - r_1}$$

where:

q = insulation heat loss (Btu/hr)

r_1 = inner radius of insulation (ft)

r_2 = outer radius of insulation (ft)

k = thermal conductivity of insulation (Btu/ft-hr-°F)

ΔT_i = temperature drop across insulation (°F)

The total heat loss at the end of life was calculated as 50.75 watts including an estimated 2.75 watts lost through the mica sleeves surrounding the thermoelements. The mica insulator loss was estimated by treating it and the thermoelement heat flow by analogy with current flow through resistors connected in parallel.

B. EXCESSIVE THERMAL POWER IN FUEL

In the fission product waste obtained by processing spent reactor fuel elements, Strontium-90 is accompanied by the shorter lived Strontium-89 which may produce as much as 80 times the heat of the heavier isotope when discharged from the reactor. Although the half life of Strontium-89 is only 51 days, production schedules indicate that appreciable quantities could be present when the generator was loaded, causing temporary overheating and consequent damage to the thermoelectric elements. However, because of its short duration, the heat supplied by the absorption of Strontium-89 beta emissions cannot be considered part of the thermal power requirement.

Figure IV-1 illustrates the combined thermal output of the two strontium isotopes for 47 kilocuries of the heavier isotope as a function of months after discharge from the reactor. Atomic ratios of Sr-89 to

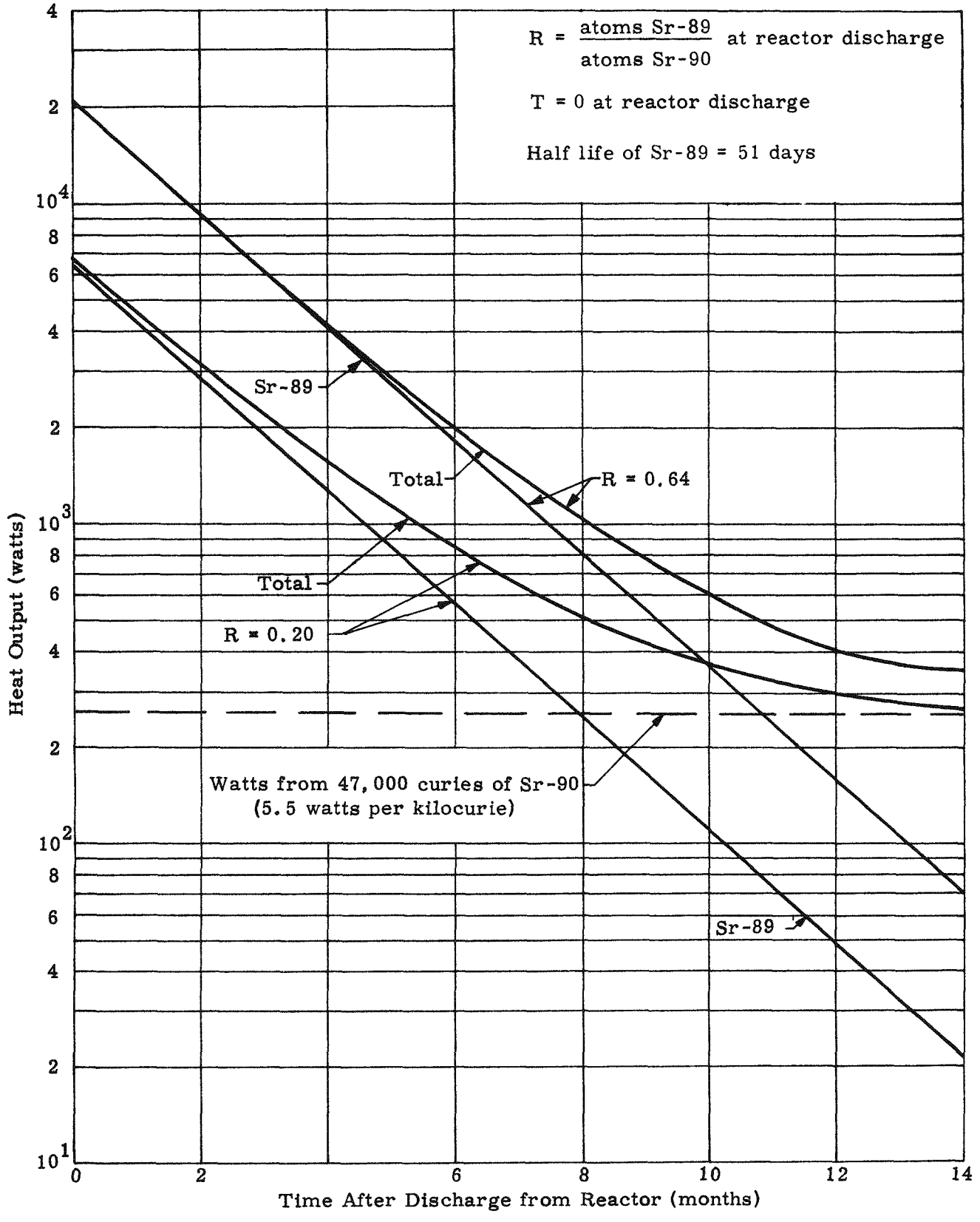

Fig. IV-1. Effect of Strontium-89 on Heat Output of SNAP 7C 10-Watt Generator

SR-90 were estimated to be 0.20 and 0.64. Analysis showed that with the proper conducting gas in the insulation, the excess heat can be accommodated without seriously affecting generator performance over its design lifetime.

This analysis takes into account the SNAP 7C fuel specification permitting a thermal overload of 40 watts due to Sr-89 content.

C. ANALYSIS OF BURIED SYSTEM

A temperature analysis of the SNAP 7C power supply as installed was performed to determine the wall temperature of the U.S. Navy weather station housing during its operation in Antarctica.

Basically, it is undesirable to expose the generator to the Antarctic environmental temperature variations because of the effect on generator performance. Further, the weather station batteries and electronic gear are not designed to withstand the Antarctic environment. A suitable environment for the batteries and electronic gear can be provided and temperature excursions minimized by packing all weather station components, including the generator system, within a single container and burying it in permanent ice.

At depths below approximately four feet, the ice temperature responds slowly to variations in local air temperature. The maximum variation in ice temperature at a depth below four feet has been measured to be about 50° F when the local air temperature variation is in excess of 100° F.

The generator and equipment are located at the bottom of a cylindrical container and covered with a plug of styrofoam insulation which completely fills the upper end of the cylinder (see Fig. II-1). An exact thermal analysis of this container is difficult because of the geometry and temperature gradient in the ice itself. An approximate analysis was performed to determine roughly the temperature which may be expected within the buried container. The results of this analysis indicate that the air temperature within the steel container housing will range from a maximum of 60° F to a minimum of 20° F, under the extremes of a yearly temperature cycle.

This analysis is described in detail in Appendix A.

V. FUEL FORM AND SHIELDING REQUIREMENTS

A. FUEL FORM

Strontium-90, with its relatively long half life (27.7 year) was selected as the radioisotope to provide the thermal energy for the SNAP 7C system. The form selected was the titanate ($SrTiO_3$), a stable ceramic compound with extremely low solubility in sea water. In the original design of the generator the specific thermal power of the prepared fuel form was estimated at 0.5 watt/cm^3.

Because of the long lead time required for chemical processing of the fuel, it was necessary to fix the fuel volume prior to the detailed design of the generator. Assuming a 5% overall conversion efficiency, producing 10 watts after 10 years, the end of life thermal power was 200 watts. From the decay rate of the isotope, an initial requirement of 256.5 watts was calculated. This resulted in a design volume of 513 cm^3.

The fuel is distributed into four capsules as shown in Figs. II-3 and II-4. The total loading was estimated as 47 kilocuries of Sr-90 based on a conservative estimate of 0.0055 watt per curie. Considerations in the fuel capsule design were minimum heat loss, i.e., maximum heat flow to thermoelectric elements, ceramic fuel pellet diameter of two inches or less and the use of an existing remote control welder at Oak Ridge National Laboratory for capsule sealing.

Each fuel capsule (see Fig. V-1) has a button protruding from its top surface to facilitate remote handling in the hot cells and loading into the fuel block. The fuel container is made of Hastelloy C, chosen for its excellent structural properties and high resistance to corrosion. Results of a 10-year corrosion test in sea water at Wrightsville Beach, N. C., show that Hastelloy C has an average corrosion rate of 0.1 mil/yr with no tendency toward pitting. This ensures safe cladding for over 1000 years, even if the corrosion rate is double that experienced in the test.

The Sr-90 titanate received from Oak Ridge National Laboratory produced a higher specific power than the 0.5 watt/cm^3 anticipated in the design. The pellets received for loading had specific powers of 0.7 to 0.9 watt/cm^3 so that excess volume was available. The total thermal output of the four capsules was 250 watts from the Sr-90 at the time of installation as compared to the design input of 256.5 watts. The actual amount of isotope fuel was 40,000 curies at about 6.25

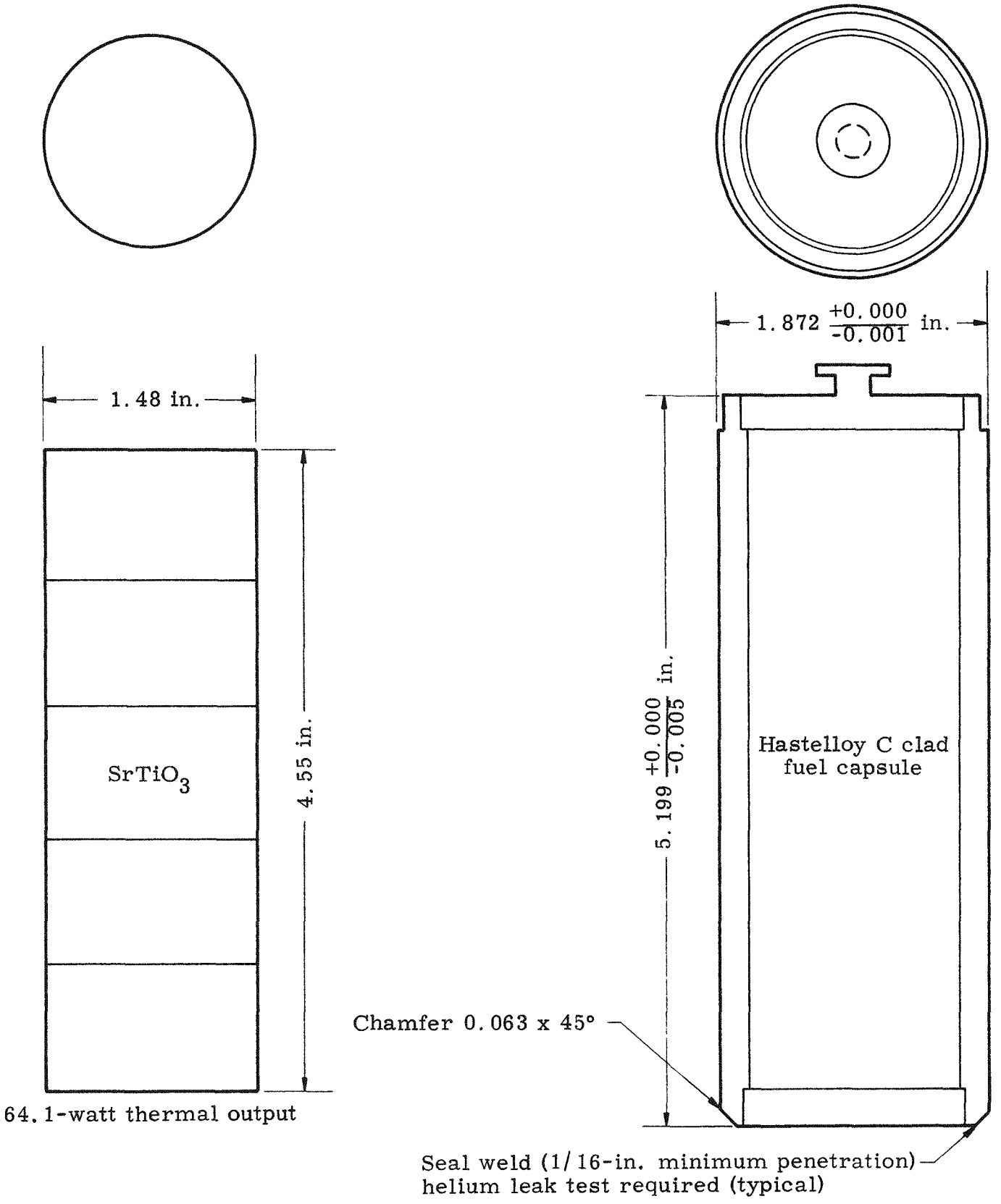

Fig. V-1. Fuel Capsule Assembly of Strontium-90 Generator

watts/kc. The excess capsule volume was filled with Hastelloy C spacers by Oak Ridge National Laboratory.

B. SHIELDING REQUIREMENTS

Radiation dose rates from the unshielded capsules of the 10-watt thermoelectric generator were calculated by means of an IBM 709 digital computer. Each capsule was assumed to contain one-fourth of the total 47,000 curies of Sr-90 in the geometrical configuration of the fuel block. On this basis the dose from one bare capsule was as follows.

	Dose at Side (r/hr)	Dose at Top and Bottom (r/hr)
At surface	89,000	62,000
At one meter from surface	136	59

From the four capsules loaded into the fuel block without shielding, the total dose rate was calculated as follows.

At one meter from surface of fuel block	500 r/hr at side	235 r/hr at top and bottom

Shielding values were computed for depleted uranium to reduce the dose rate from 47 kilocuries of Sr-90 to 100 mr/hr at one meter from the center of the generator, in accordance with the specifications established at the inception of the program. Uranium is employed as the shield material because its use results in a generator of smaller size and weight. The minimum thicknesses of uranium required are as follows.

Shield	Thickness (in.)
Top	1.87
Side	1.54
Bottom	1.67

However, the biological shield for the 10-watt generator was designed with a thickness greater than the minimum to permit the use of

the shield as a shipping container for transportation by common carriers in interstate commerce. The designed thicknesses and the resulting dose rates are as follows.

Shield	Thickness (in.)	Dose Rate at One Meter (mr/hr)
Top	2.75	1.92
Side	2.625	3.61
Bottom	2.625	2.88

A comparison of calculated and measured dose rates was made for the SNAP 7A and SNAP 7C generator and is shown in Table V-1.

TABLE V-1

		SNAP 7A 40,800 Curies		SNAP 7C 40,000 Curies	
		Calculated	Measured*	Calculated	Measured**
At one meter	Top	1.89	2.5	1.86	3
	Side	1.87	1.0	1.84	1.5
At surface	Top	29.9	30	29.4	50
	Side	31.3	15	30.8	20

*Letter dated November 28, 1961 (Ref. No. p 1404) to Commander Culwell from J. J. Keenan.
**Letter dated September 19, 1961 (Ref. No. p 1313) to Commander Culwell from J. J. Keenan.

The shielding is adequate to meet ICC regulations for unescorted shipments (10 mr/hr maximum at one meter and 200 mr/hr maximum at the surface).

Calculated dose rates were originally based upon 47,000 curies of Sr-90 and have been adjusted to conform to the estimated curie loading of the generators.

The measured and calculated dose rates agree within a factor of about two, which is considered good in shielding.

Note that the measured dose rates are higher for the SNAP 7C generator even though this generator contains less curies.

This is possibly due to the differences in instruments used for measuring, uncertainty in the location at which readings were taken, differences between design and actual generator construction or by a combination of several of these items. It is concluded that the shielding for the 10-watt generator is conservative.

A complete safety analysis report concerning the use of strontium-fueled thermoelectric generators has been prepared and is given in Ref. 5.

Subsequent to the original calculation of the shield thickness, it was found that the strontium isotope produced by spent element processing at Hanford would contain 2.5 millicuries of Ce-144 per curie of Sr-90. Cerium-144 is a beta emitter which also emits a hard gamma photon at each disintegration. Examination of the results reveals that even with the additional radiation contributed by the cerium, the total dose rate is still well below the 10 mr/hr at one meter that is the ICC shipping requirement.

Power (thermal watts)	250
Sr-90 (curies)	4.0×10^4
Ce-144 (curies)	100
Dose rate for Ce-144 at one meter (mr/hr)	1.7
Dose rate for Sr-90 at one meter (mr/hr)	2.5
Total dose rate at one meter (mr/hr)	4.2

The calculations and comparison of the calculated values with experimental results were carried out as described in Appendix B.

VI. GENERATOR ASSEMBLY

The SNAP 7C generator was custom assembled with special precautionary measures to ensure integrity, reliability and nonhazardous conditions.

Thermoelectric couples were assembled by bonding lead telluride elements (one N type and one P type) to a common iron shoe as shown in Fig. VI-1. Five couples, a block of Min-K insulation and copper caps (one soldered to each element) were assembled to form a module as depicted in Fig. VI-2.

The Hastelloy C fuel block was centrally located within the aluminum heat sink frame and held in position by corner blocks of Min-K insulation. A base plate of Min-K insulation supports the aluminum heat sink and provides vertical positioning of the fuel block.

Twelve thermoelectric modules, positioned in groups of three against each of the four flat surfaces of the fuel block, were held in position by means of Min-K filler strips and aluminum heat sink bars. Each bar was attached to the aluminum frame with screws as shown in Fig. VI-5.

The thermoelectric module components (see Fig. VI-4) were inserted through each heat sink bar after individual module installations.

Couples and modules were electrically interconnected with copper straps and each group of three modules interconnected to the next with Ceramatemp wire (Fig. VI-5). This series-type connection terminated in a single output lead.

Instrumentation at two locations within the generator provides measurement of hot junction temperature. Thermocouples were attached at the center of the hot shoe on the upper and lower couple of a particular module.

The assembled generator was then inserted in a Hastelloy C container and subjected to test to provide verification of the thermal and electrical characteristics. Electrical heaters were substituted for the isotope heat source.

Upon completion of the tests, the Hastelloy C shell containing the assembled generator was inserted into the biological shield that contained 18 pounds of mercury. After positioning, the generator container was welded in place. The mercury level was at a position above the top of the heat sink as shown in Fig. II-4. The generator-biological shield assembly was then placed in the hot cell at the Quehanna Facility.

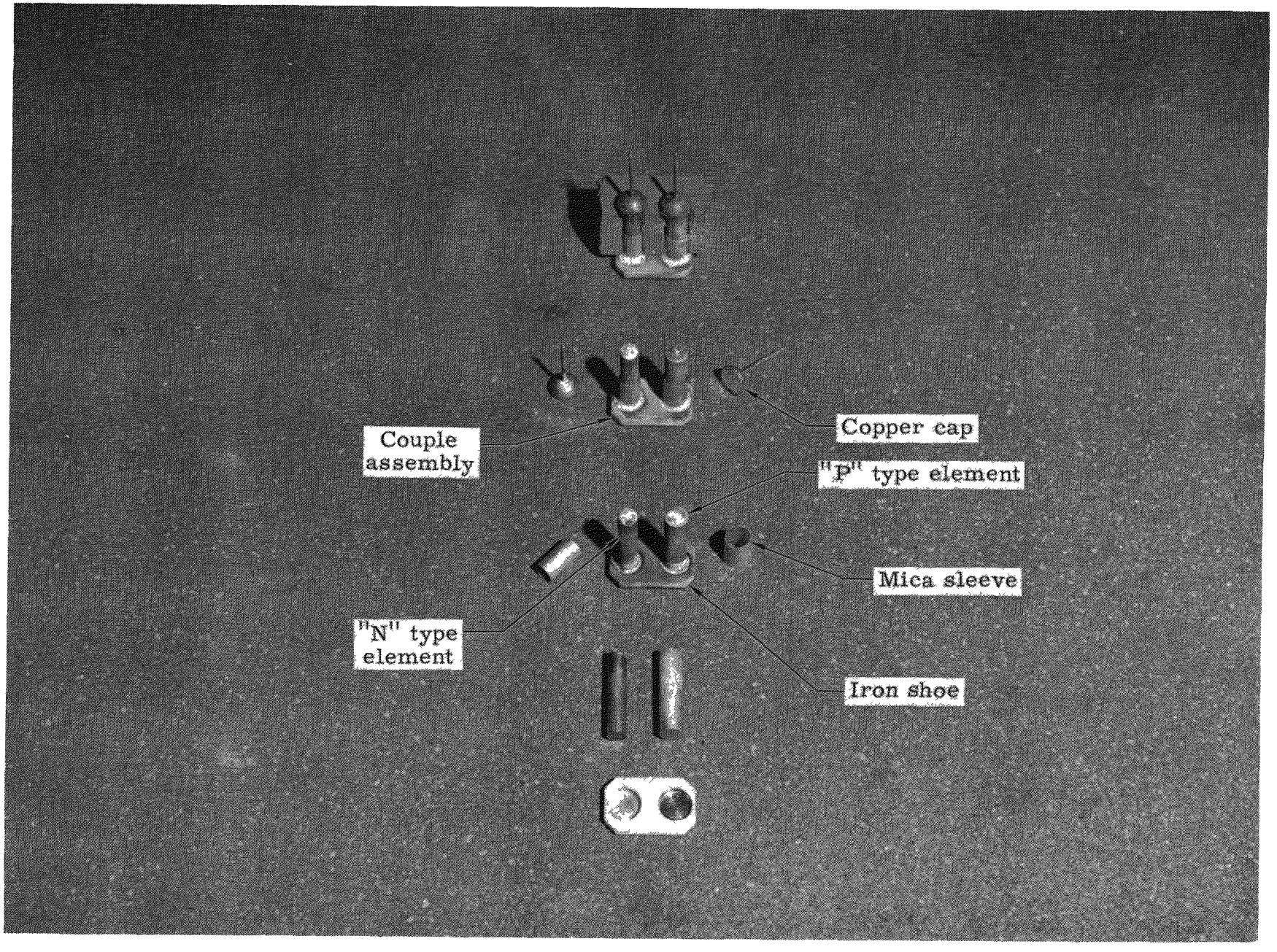

Fig. VI-1. Thermoelectric Couple

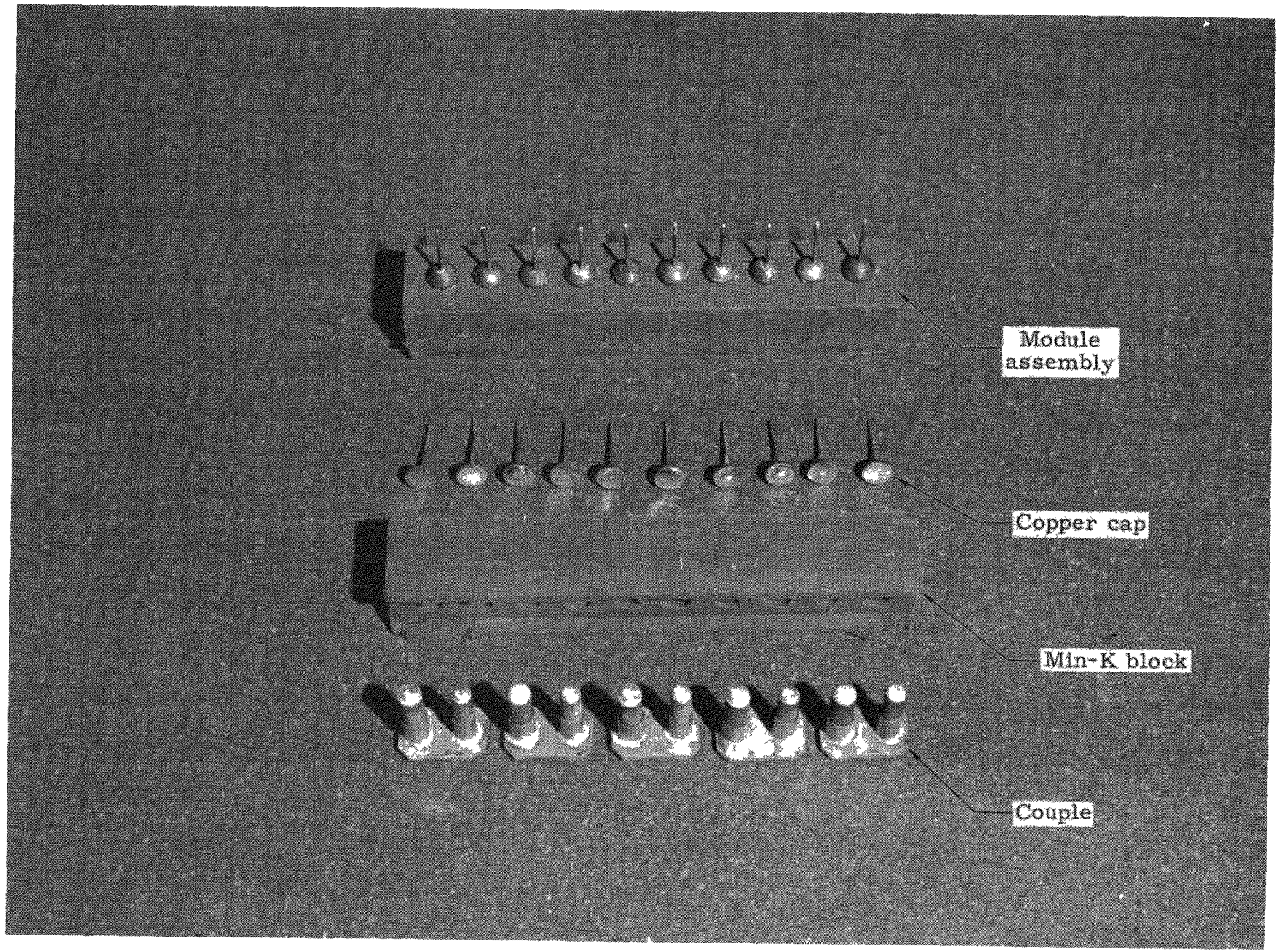

Fig. VI-2. Thermoelectric Module

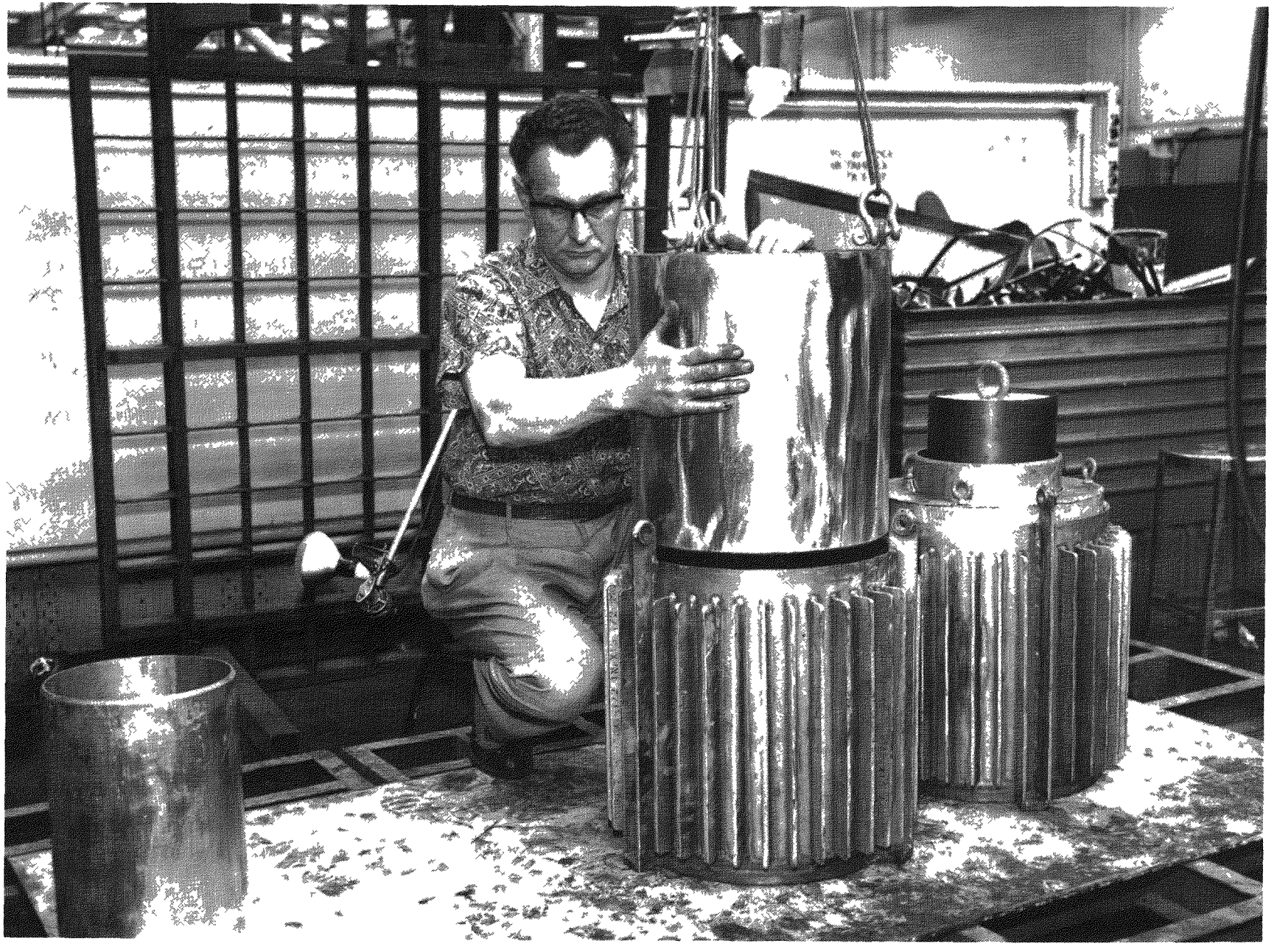

Fig. VI-3. Depleted-Uranium Shield Being Positioned for Insertion into Outer Hastelloy-C Shell

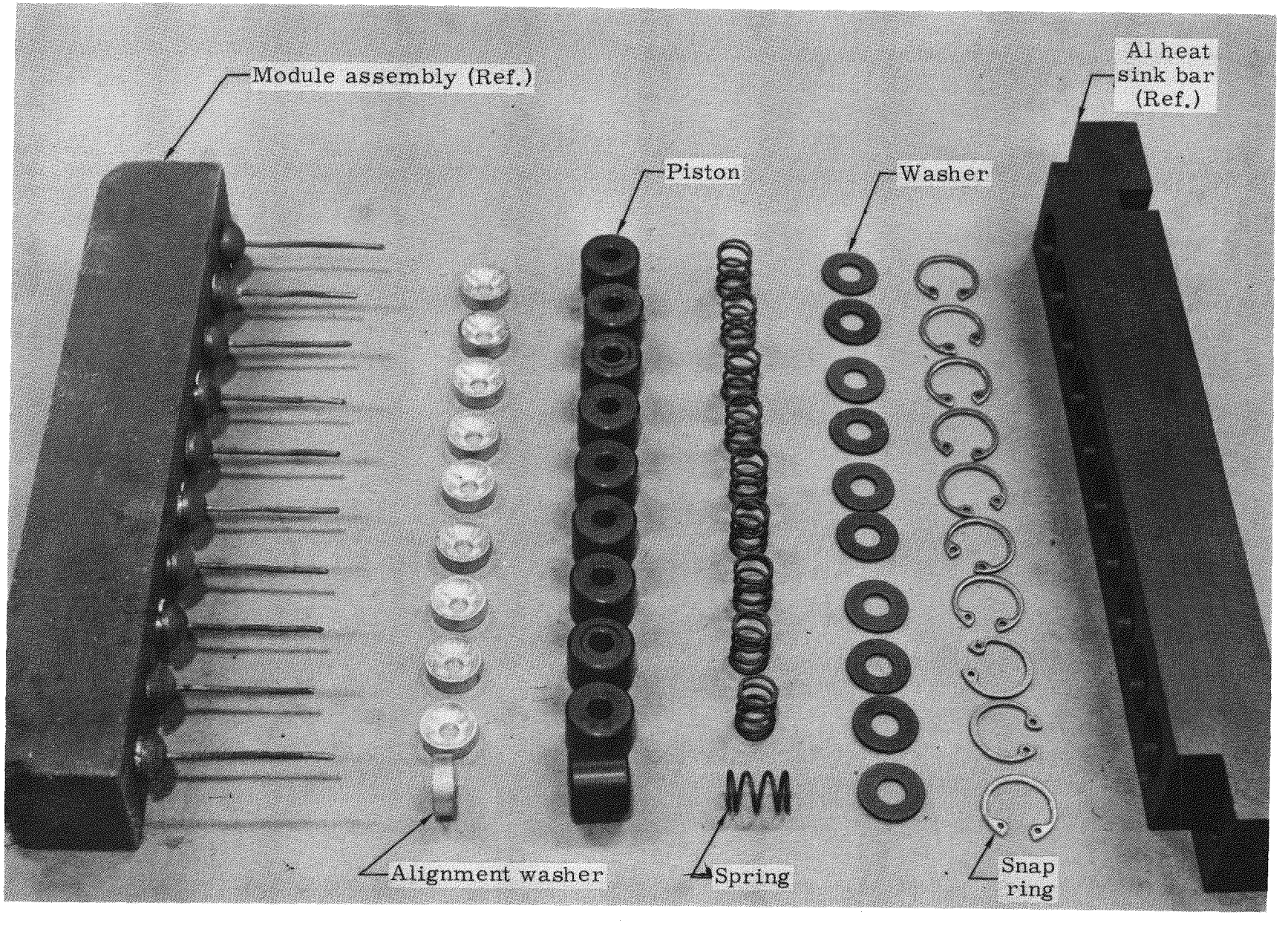

Fig. VI-4. Thermoelectric Module Components

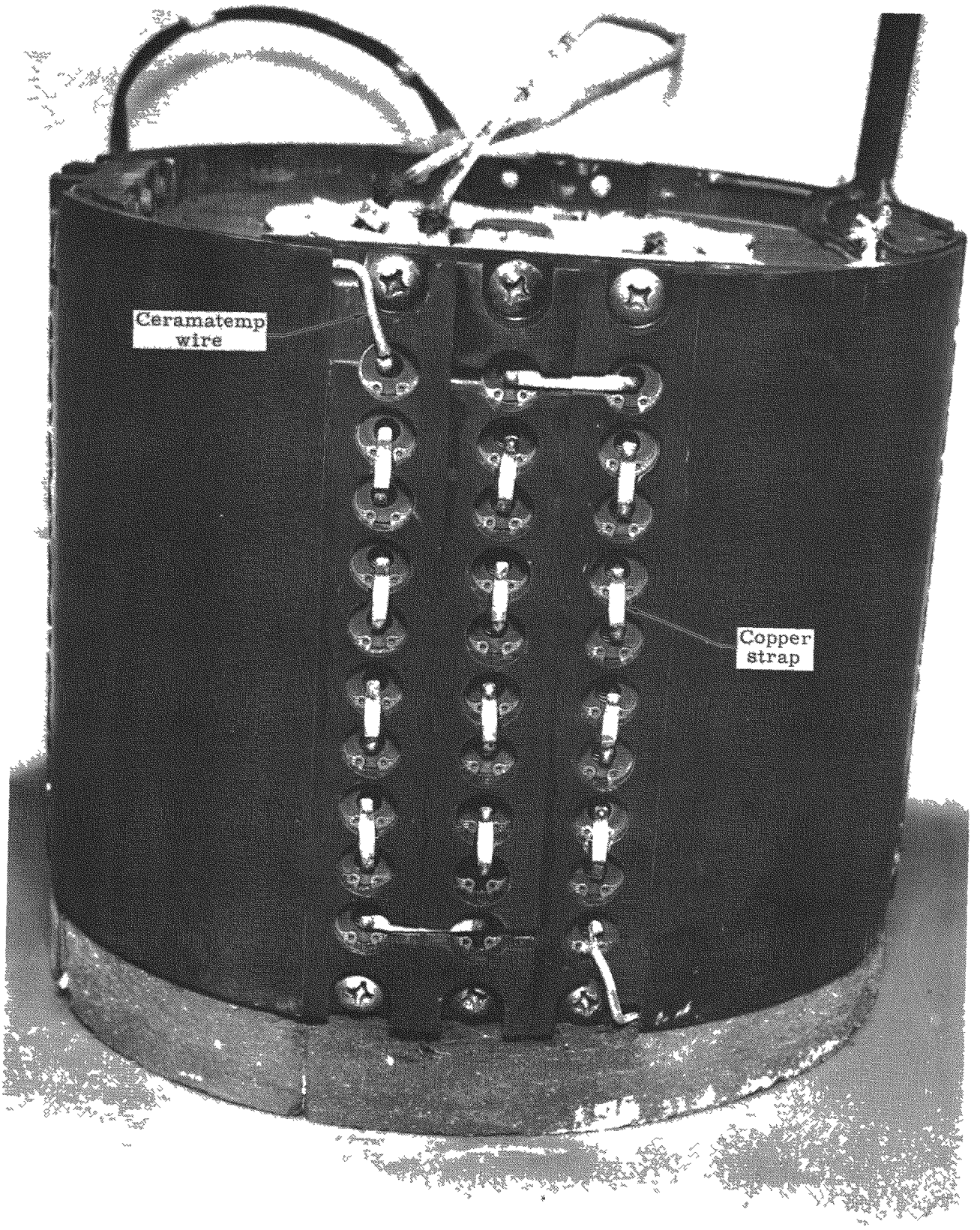

Fig. VI-5. Thermocouples and Modules

Generator fueling included the installation of four fuel capsules in their respective holes located in the fuel block, installation of the fuel block cover plate, Min-K insulation plate and uranium shield block and attachment of generator closure. Figure VI-6. illustrates this. The generator electrical output leads and hot junction thermocouples were terminated at the hermetically sealed electrical connector located in the generator closure (Fig. II-4).

After the electrical test to verify generator operation was completed, the closure was welded in place and the generator delivered for operation. This is shown in Fig. VI-7.

Fig. VI-6. SNAP 7C Generator and Accessories Used in Remote Fueling Operations (photo taken looking through three-foot thick leaded glass window)

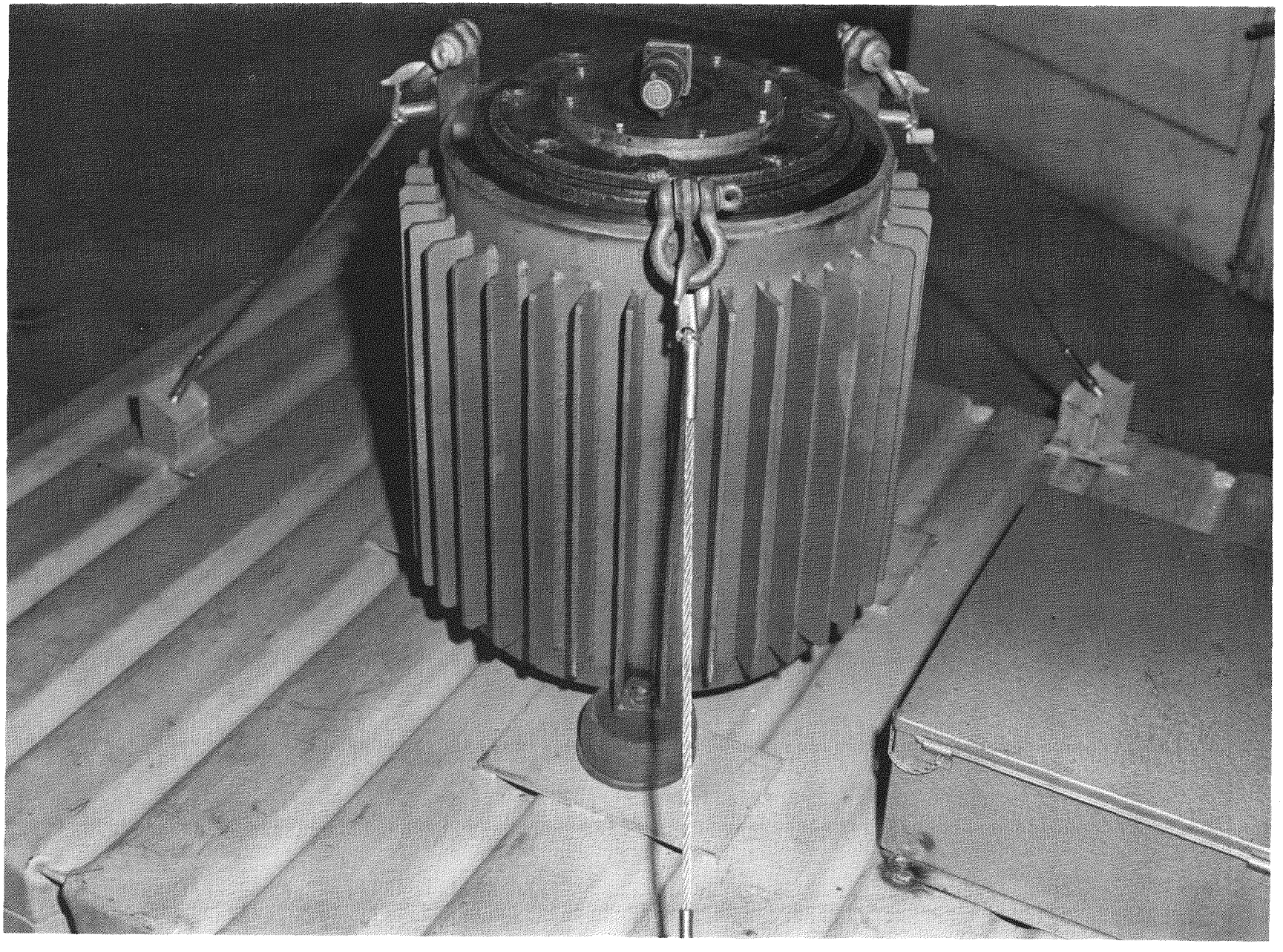

Fig. VI-7. Operational SNAP 7C Thermoelectric Generator

VII. ELECTRICAL SYSTEM

The SNAP 7C electrical system is designed to convert the electrical energy supplied by the nuclear powered thermoelectric generator into the proper operating voltages required by the weather station. The thermoelectric generator supplies a nominal 10 watts of electrical power. This power is converted by a dc-to-dc converter to the voltages used by the weather station. Since the weather station power requirements are not all continuous, batteries store the excess energy supplied by the generator during minimum load conditions. This stored energy is used during the intermittent transmitting cycles of the weather station when the power demands are in excess of that delivered by the generator. Since the generator is designed for end of life operating conditions, the generator power output will always exceed the integrated power demands and will normally maintain the battery in a fully charged condition.

A. BATTERY

The electrical storage system is a nickel-cadmium, rechargable battery capable of supplying a high rate of discharge during short periods of time. The battery consists of 24 cells of which two are spares. The remaining 22 cells are divided into four sections to equalize the current drain from the various cells as much as possible and to supply the voltages used by the weather station as shown in Fig. VII-1.

The cell blocks are as follow:

(1) Cell Block A consists of 13 cells in series with a nominal voltage of 18 volts.

(2) Cell Block B consists of three cells in series with a nominal voltage of four volts.

(3) Cell Block C consists of three cells in series with a nominal voltage of four volts.

(4) Cell Block D consists of three cells in series and a nominal voltage of four volts.

The positive terminal of Cell D is grounded to form the system ground. All voltages supplied to the system are negative.

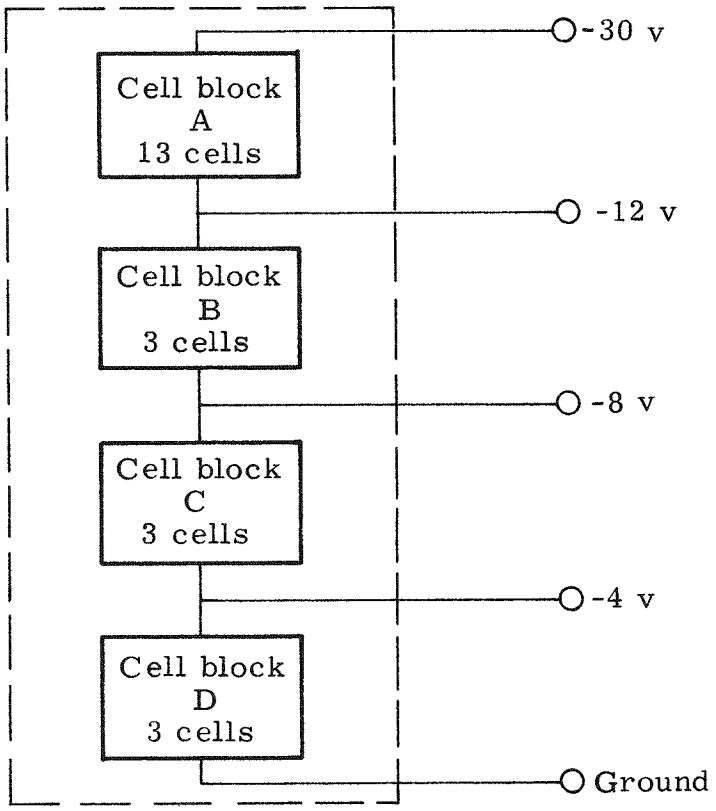

Fig. VII-1. Battery Block Diagram

B. DC-TO-DC CONVERTER

The SNAP 7C dc-to-dc converter is a transistorized electric component that converts the SNAP 7C generator voltage into the charging voltages required by the nickel-cadmium storage battery of the system. The power supplied to the converter by the generator is a function of the isotope life. The SNAP 7C generator was optimized to supply a nominal 10 watts of electrical power at the end of life with an operating voltage of approximately five volts (see Chapter III). The converter transforms this power into three voltage regulated output sections of 4.065 ± 0.075 volts and one voltage regulated output section of 17.615 ± 0.325 volts. The regulators are designed to function with a load current variation of 30 to 150 milliamperes and an ambient temperature range of 20° to 60° F.

The converter schematic is shown in Fig. VII-2. The first section of the converter operates as a voltage regulator and an over-driven, push-pull, transformer coupled oscillator. The voltage regulator consists of a Zener diode Z_1 and a variable resistor VR_1. The Zener diode was selected to maintain the converter input voltage at a maximum of 5.6 volts in the event the generator produced a higher operating voltage. If the output voltage is in excess of 5.6 volts at beginning of life, the Zener diode will break down and conduct a current. The additional current flow will reduce the generator output voltage and cause it to stabilize at the desired voltage. During the lifetime of the generator, the output voltage will normally decay to the 5.6-volt maximum value at which time the regulator circuit would cease to operate. The resistor R_1 serves as a current limiter for the Zener diode.

The over-driven, push-pull, transformer coupled oscillator consists of two transistors, Q_2 and Q_3, two resistors, R_2 and R_3 and a toroidal transformer. The transformer is wound and connected to provide a positive feedback from the collector to the emitter of each transistor. When Q_2 starts to conduct, a voltage is developed across the primary winding, inducing a voltage in the feedback windings that drives the emitter of Q_2 positive and causes increased conduction. The current increases rapidly until the collector of Q_2 is driven into the saturation region of its characteristics. When this occurs, the primary voltage can no longer increase and a condition of quasistable equilibrium is attained. During this equilibrium period, the voltage drop in the transistor from collector to emitter is very small, and essentially the full generator voltage appears across that half of the transformer primary.

With a constant voltage applied across the transformer primary, the magnetic flux begins to increase with time. Eventually the transformer core reaches saturation and the required exciting current

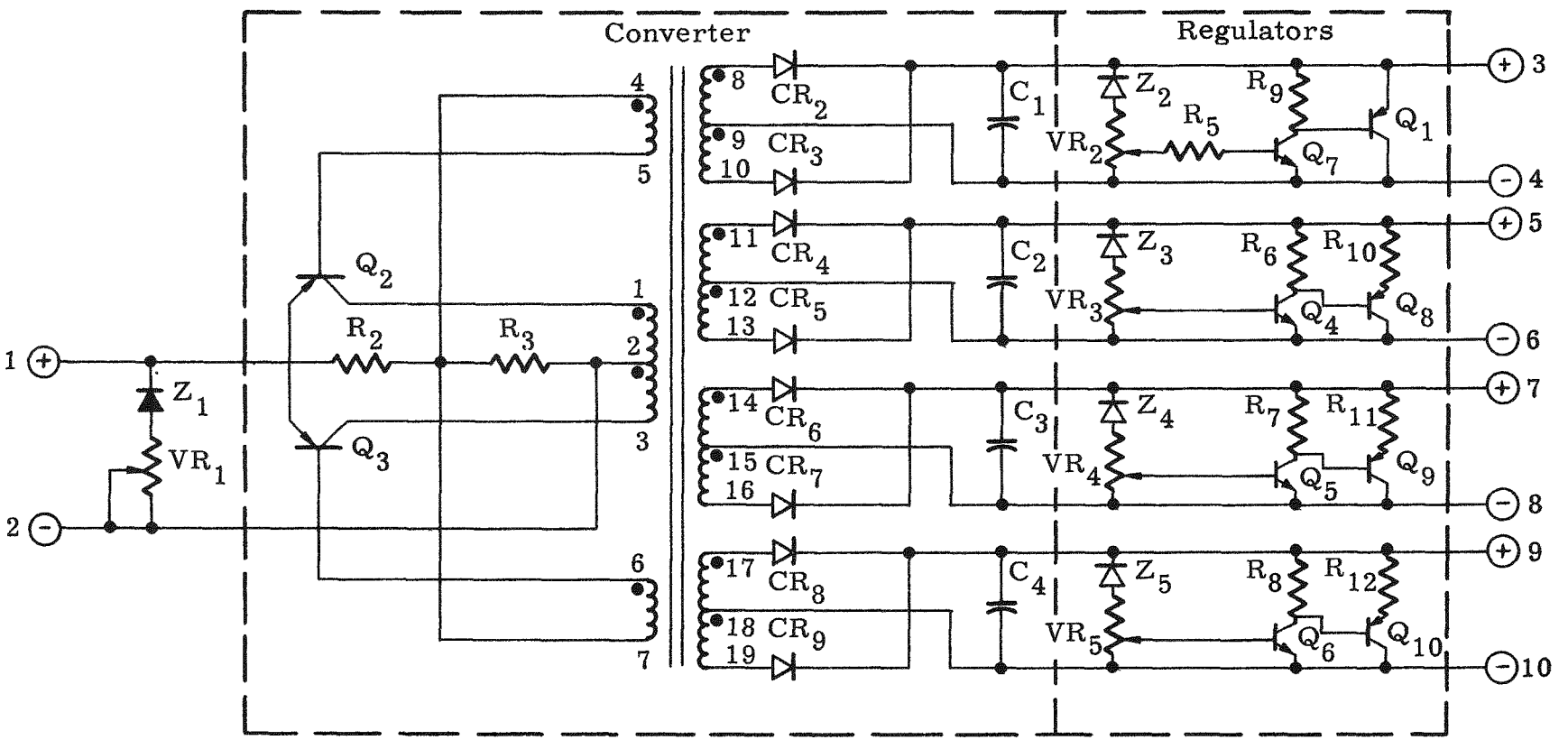

Fig. VII-2. SNAP 7C Schematic

increases rapidly to a value greater than can be supplied. As a result, the primary voltage decreases, reducing the emitter voltage and decreasing the collector current. Thus, transistor Q_2 turns off regeneratively, ending the half cycle. As the flux collapses, voltage is induced in the winding which biases transistor Q_3 to conduction, thereby initiating the next half cycle.

The operation of Q_3 during the next half cycle is identical with the operation of Q_2 during the first half cycle with the exception that Q_3 conducts until the core of the transformer is driven into negative saturation. After the core saturates, the flux collapses, and the cycle is complete. The starting circuit of the oscillator consists of two resistors which make up a low impedance bleeder circuit. This circuit will bias the transistors to conduction before oscillations start.

The second section consists of four separate full wave, center-tapped capacitor input filter circuits. They are coupled to the first section by the toroidal transformer. Since the operation of each of these circuits is identical, only the 18-volt output section will be functionally described. The full wave rectifier of the 18-volt section consists of two diodes, CR_2 and CR_3. When CR_2 is conducting current, CR_3 is biased negative and does not conduct. When the polarity of the transformer secondary changes, CR_3 will conduct current and CR_2 will be biased negative. The center tap of the secondary winding provides the ground for this circuit. The capacitor C_1 acts as a filter to any a-c component that is presented.

The last section of the converter consists of a voltage regulator attached to each of the input filter circuits. The operation of the regulators is identical and only the 18-volt section will be functionally described. The 18-volt regulator is a voltage dropping network consisting of a Zener diode Z_2 and a potentiometer VR_2. Parallel to this circuit are two transistors, a switching transistor, Q_7 and a current dumping transistor, Q_1. As the voltage across the Zener diode and potentiometer VR_2 increases due to a fully charged battery, it causes an increasing current to flow through the circuit. This current causes a higher voltage drop across VR_2 which biases the switching transistor Q_7 into high conduction. The switching transistor in turn biases the current dumping transistor Q_1 into high conduction. This increased current flow through transistor Q_1 loads the converter and slightly

reduces its output voltage. This action prevents the batteries from being overcharged and keeps a constant load on the generator. The output voltage regulation can be adjusted by varying the potentiometer VR_2. This changes the bias voltage swing on the switching transistor and determines its operational parameters.

Losses in the converter unit were minimized by component selection and design criteria. The 2N 1360 switching transistors used in the oscillator were chosen because of their low saturation voltage (typically 0.3 volt at two-ampere collector current). They have a typical current gain of 40 at a two-ampere collector current. The base drive voltage is typically 0.6 volt at a collector current of two amperes. A switching frequency of approximately 500 cycles per second was chosen to optimize the core and copper losses in the transformer.

The voltage regulators present the largest single power loss in the circuit. Since the thermoelectric generator supplies more power at the beginning of life than is required by the system, the regulator must detect and dump this excess energy to keep from overcharging the batteries. In addition, the regulator must present a constant load to the generator during the fully charged condition of the batteries. This requires complex circuitry which increases the power losses. As a result, the overall efficiency of the converter (including regulators) during normal operating conditions is approximately 54%.

Schematic representation of the converter enclosure is shown in Fig. VII-2 and the parts listed in Table VII-1. The complete unit was enclosed as a module with the variable resistors mounted for external adjustment. This permits final matching of the converter to the system during installation and subsequent servicing. Figure VII-3 shows the converter operating in the environmental test chamber.

TABLE VII-1

SNAP 7C Parts List

Schematic Part No.	Manufacturer's Part No.	Description	Manufacturer
Z_1	1N1600	Zener diode, 4.7 v	IRC
Z_2	1N2982B	Zener diode, 18 v	Motorola
Z_3, Z_4, Z_5	1N748A	Zener diode, 3.9 v	Motorola
CR_2 through CR_9	1N538	Rectifier diode	GE
Q_1, Q_2, Q_3	2N1360	Transistor, PNP	Motorola
Q_4, Q_5, Q_6	2N358	Transistor, NPN	GT
Q_7	2N697	Transistor, NPN	FC
Q_8, Q_9, Q_{10}	2N1039	Transistor, PNP	TI
VR_1		0-6Ω, 2-w WW potentiometer	Clarostat
VR_2 through VR_5		0-250Ω, 2-w carbon potentiometer	Ohmite
R_2		12.1Ω, 1/2-w resistor, 1%	Mepco
R_3		220Ω, 1/2-w resistor, 5%	Ohmite
R_5		820Ω, 1/2-w resistor, 5%	Ohmite
R_6, R_7, R_8		1200Ω, 1/2-w resistor, 5%	Ohmite
R_9		680Ω, 1/2-w resistor, 5%	Ohmite
R_{10}, R_{11}, R_{12}		22Ω, 1-w resistor, 5%	Ohmite

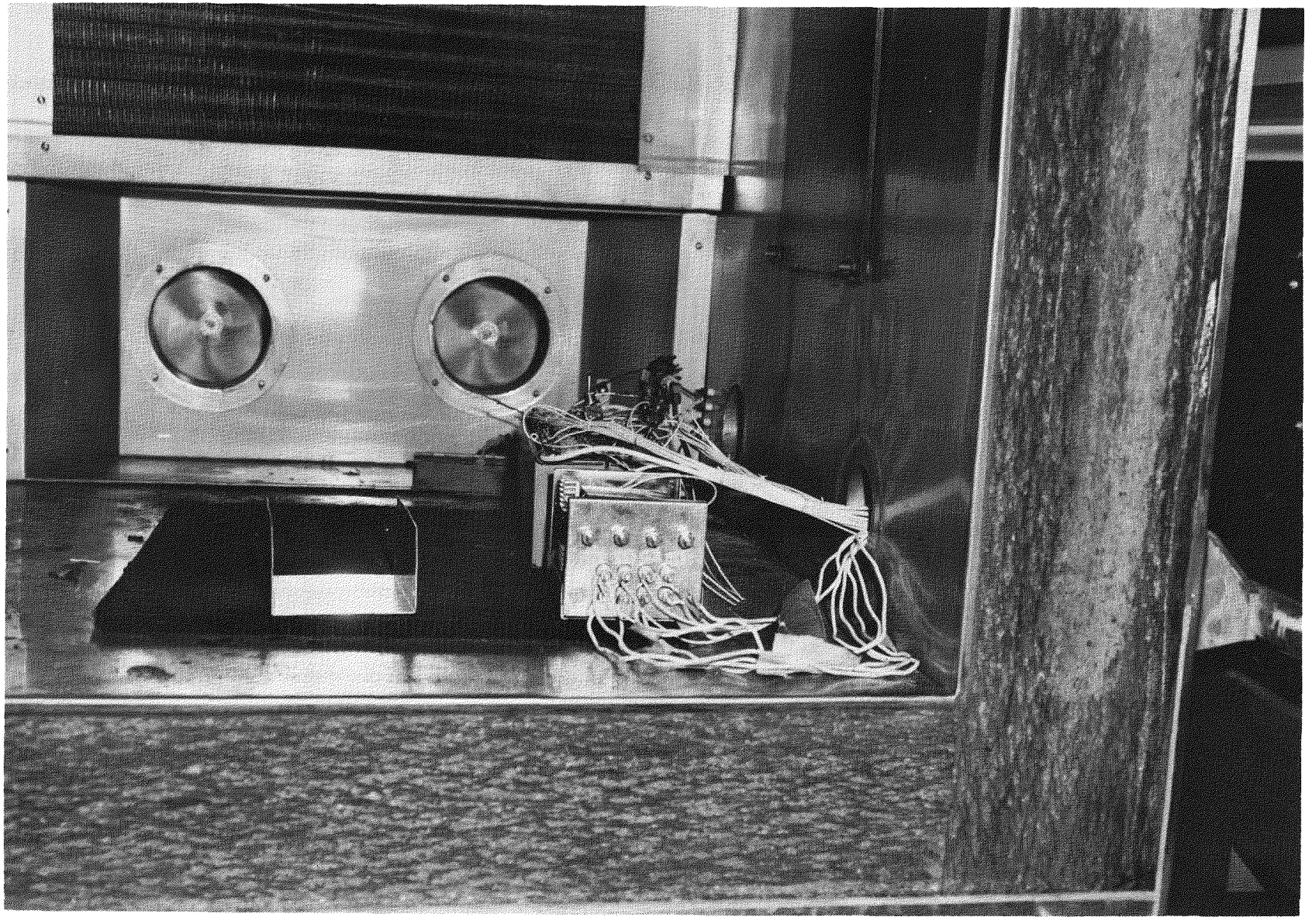

Fig. VII-3. Converter in Environmental Test Chamber

VIII. SNAP 7C OPERATIONAL TESTS

A. SNAP 7C GENERATOR

An initial series of high temperature tests, conducted using electrical heaters, was undertaken to determine beginning and end of life parametric data. The SNAP 7A-C test generator was then environmentally tested as described in Chapter IX. After environmental testing, a series of tests was performed to obtain the fill gas composition necessary to maintain the hot junction temperature within acceptable limits. These tests consisted of operating the generator with four different argon-hydrogen (A-H_2) gas mixtures. Several power inputs were used for each gas mixture.

The deliverable generator initially was filled with 25% A--75% H_2. After fueling, the hot junction temperature was 893° F which was below the desired initial value of 930° F. The fill gas was changed to 35% A--65% H_2 to increase the hot junction temperature. Twelve hours later the hot junction temperature was 921° F. Although it was anticipated that this would be a steady state value, the temperature continued to increase and 48 hours after changing the fill gas, it reached 963° F. The fill gas was then changed to the original composition. However, a continual increase in hot junction temperature was again observed.

Fill gas pressure was noted to be decreasing to negative values during this period. This was compensated for by adding pure H_2 to return the pressure to the design value. When this failed to correct the situation, the fill gas was replaced with 100% He. This gas fill stabilized the pressure and hot junction temperature.

It was concluded that the uranium metal shield on top of the generator was absorbing H_2 from the fill gases and causing a decrease in fill gas pressure. Initial operation with He as a fill gas and the use of other inert gases later in the generator life will provide the desired variation in the insulation thermal conductivity. Thus, the generator can be successfully operated for the 10-year lifetime.

When shipped, the fill gas composition was 1.6% H_2, the remainder He. No further variation in gas pressures is anticipated.

Since the fill gas composition no longer was consistent with the A-H_2 parametric study, several tests were repeated using fill gases

of He or A-He compositions. These data are presented in Figs. VIII-1 through VIII-6. Although some of the data were obtained using the SNAP 7A generator, it is applicable to the 7C program since the generators are identical. The generator labeled "SNAP 7A-C Operating Model" No. is the test generator used earlier for the electrically heated parametric studies.

B. CONVERTER AND BATTERY

The SNAP 7C converter and battery were tested to ensure the specifications outlined in the statement of work (Ref. 4) were met. Voltage requirements were 4, 8, 12 and 28 volts, each at a different power level. After some changes in the original design, the shunt-regulated converter with the manual voltage control as described in Chapter VII met all design requirements while operating with the actual generator, battery and weather station transmitter.

Testing of the battery showed three defective cells which were replaced prior to testing the complete SNAP 7C system.

C. SNAP 7C SYSTEM TESTS

A seven-day system test was initiated September 29, 1961 and utilized the SNAP 7C generator, converter, battery and simulated transmitter. A six-hour transmitter cycle was used instead of the three-hour cycle under which the system will actually operate. This was to evaluate the battery electrolyte loss. The six-hour cycle is more severe in this respect since the battery is in a fully charged condition for a greater percentage of the time. The average electrolyte loss for the seven-day period was 0.104 gram per cell. With a three-hour transmitter cycle, the estimated electrolyte loss for a two-year period will be 8.8 grams per cell. A loss of 13 grams per cell can occur before cell operation is affected.

Acceptance tests were successfully conducted for the generator-converter-battery system on October 18, 1961. The resistive loads specified in the statement of work were applied to the respective battery voltages and an oscilliscope was connected across the total battery output to verify that the ripple voltage was within limits. During acceptance tests, the transmitter was cycled three times in succession. The battery voltage dropped to 28.3 volts which compares favorably with the minimum acceptable battery voltage of 26.0 volts.

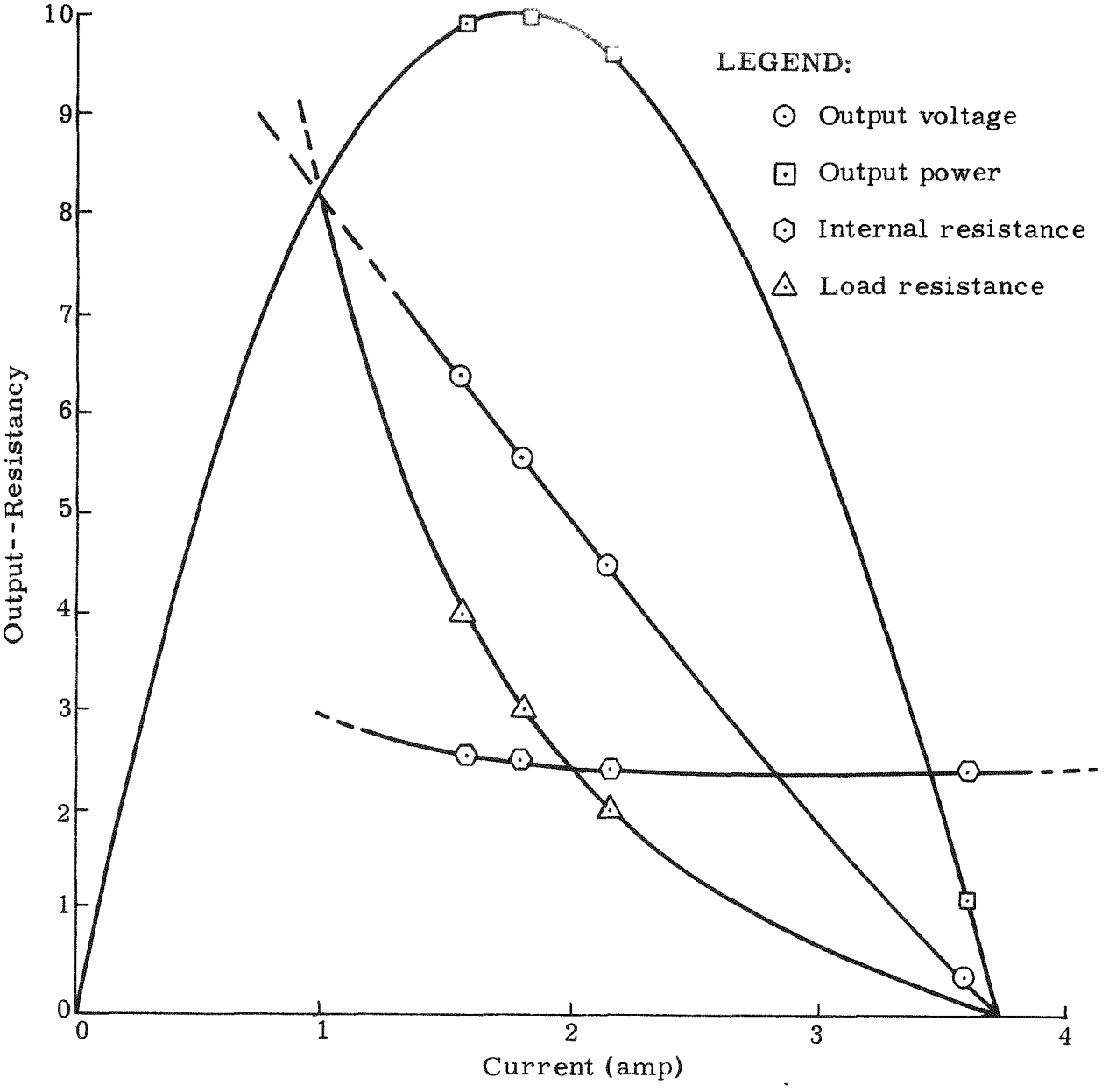

Fig. VIII-1. Plot of Parametric Data for SNAP 7 A-C Operating Model, Where Power Input Was 266. Electrical Watts and Internal Gas Composition Was 100% Helium (1.05 atm)

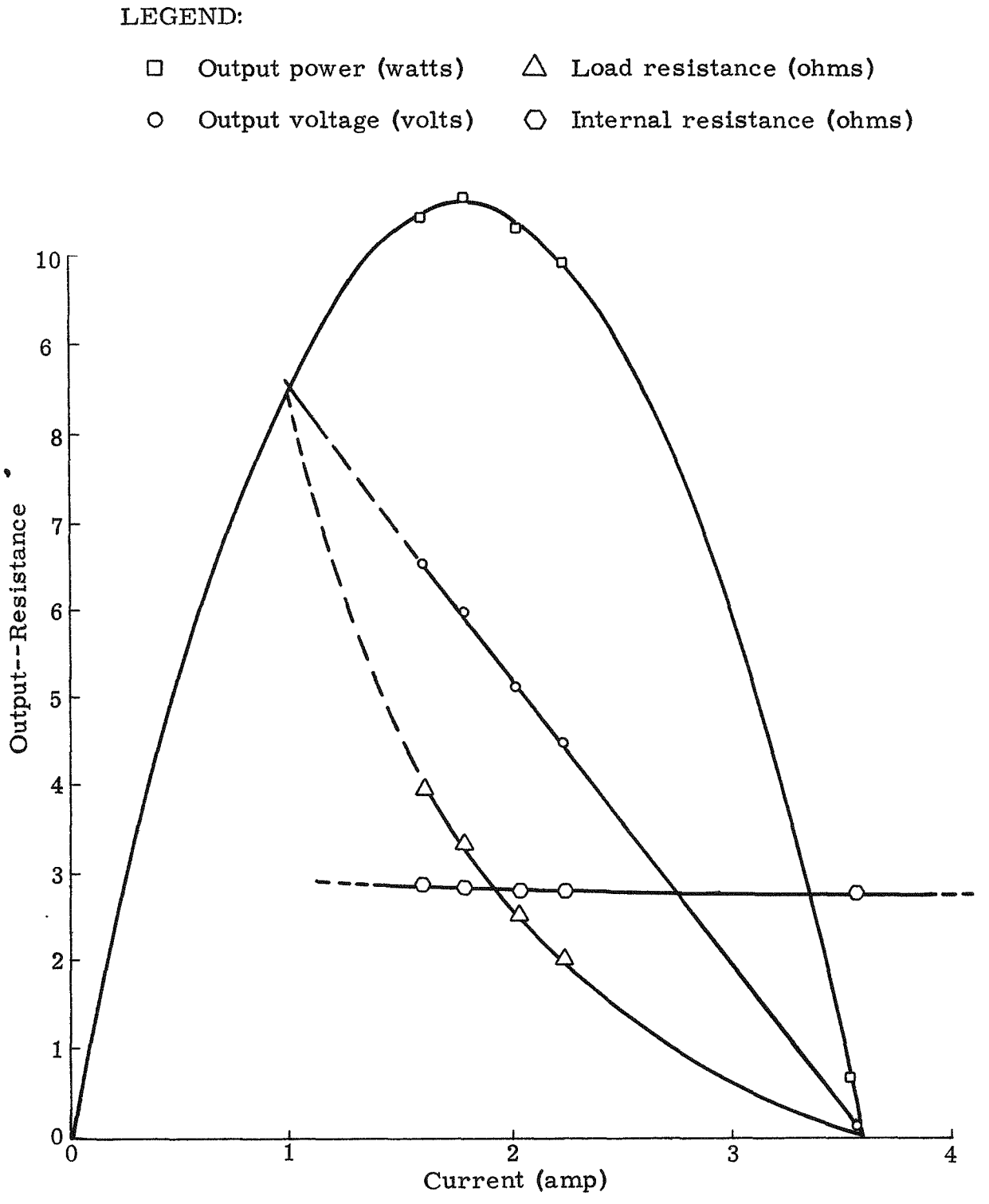

Fig. VIII-2. Plot of Parametric Data for SNAP 7A Generator, Where Power Input Was 266 Electrical Watts and Internal Gas Composition Was 100% Helium (1.05 atm)

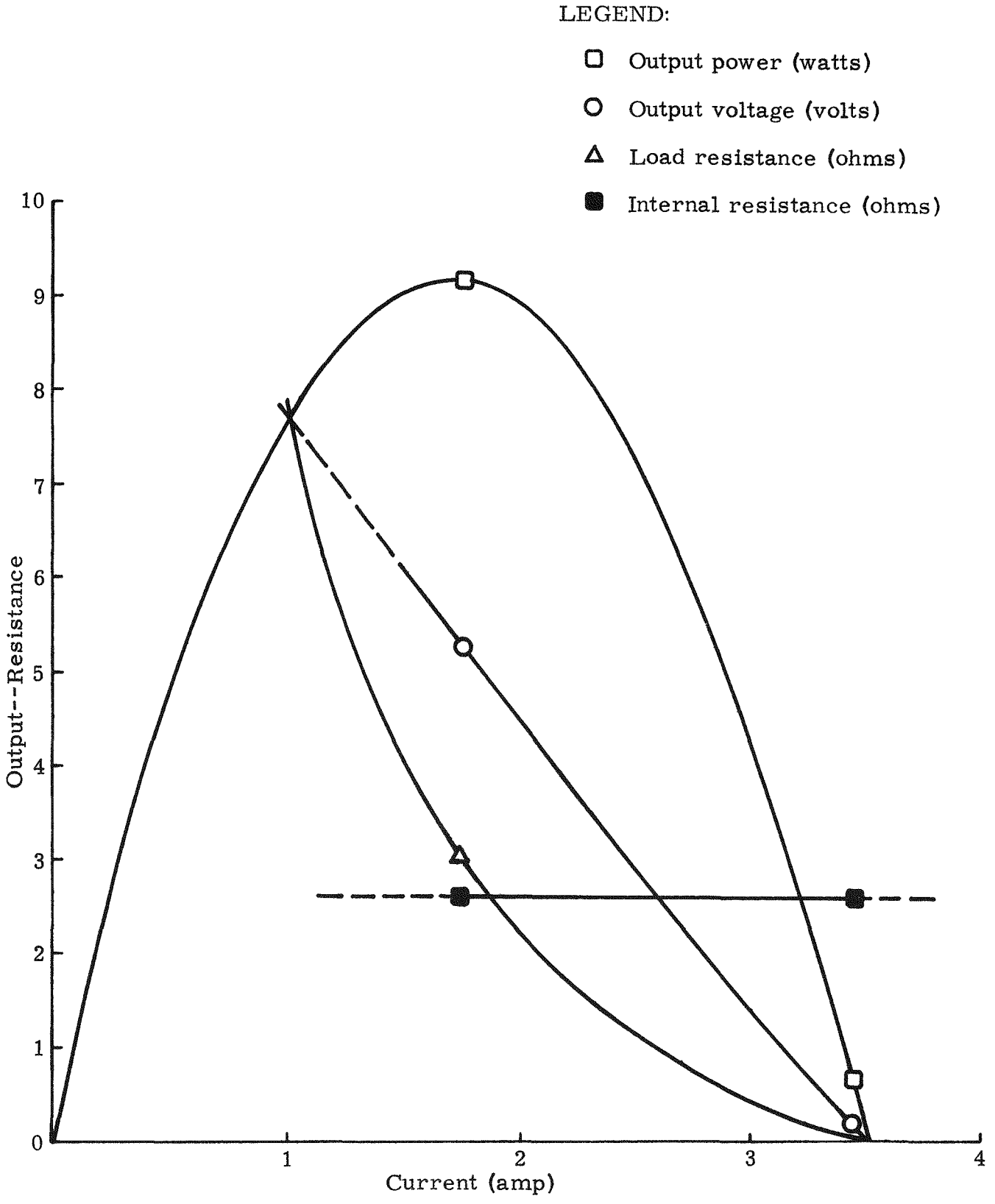

Fig. VIII-3. Plot of Parametric Data for SNAP 7A Generator, Where Power Input Was 248 Electrical Watts and Internal Gas Composition Was 100% Helium (1.05 atm)

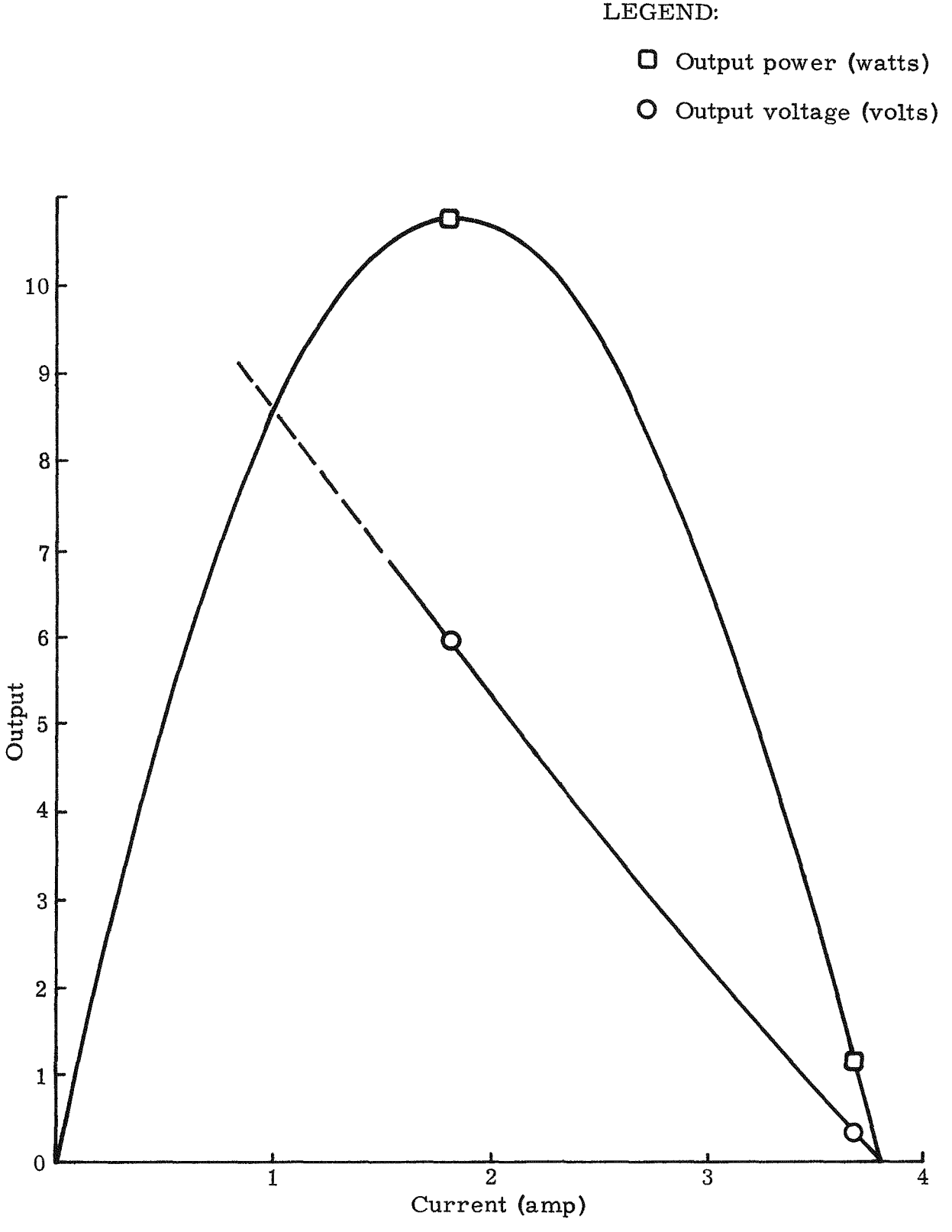

Fig. VIII-4. Plot of Parametric Data for SNAP 7A and SNAP 7C Test Generator (operating model), Where Power Input Was 278 Electrical Watts and Internal Gas Composition Was 100% Helium (1.05 atm)

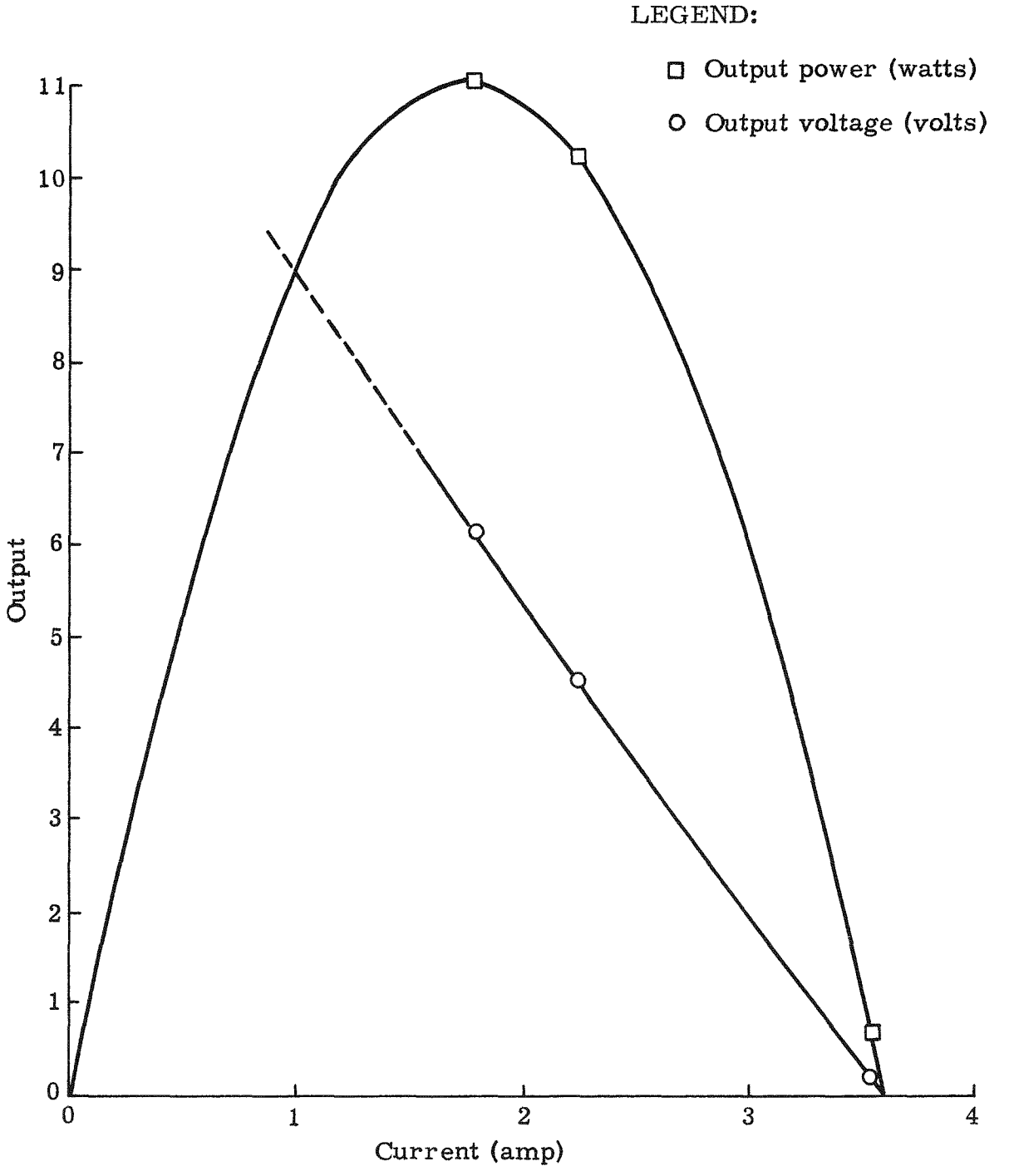

Fig. VIII-5. Plot of Parametric Data for SNAP 7A Generator, Where Power Input Was 240 Electrical Watts and Internal Gas Composition Was 75% Argon and 25% Helium (1.05 atm)

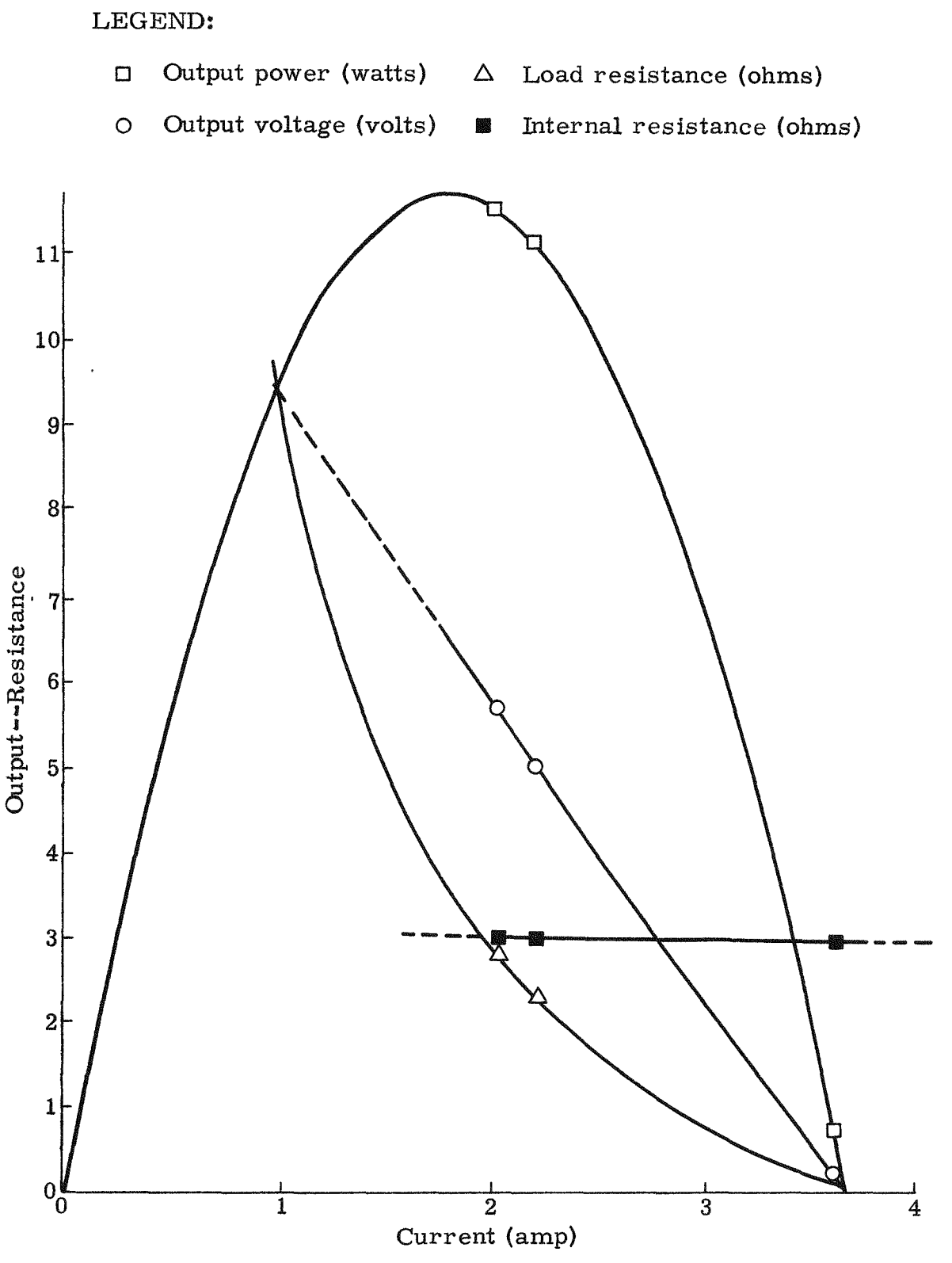

Fig. VIII-6. Plot of Parametric Data for SNAP 7A Generator, Where Power Input Was 252 Electrical Watts and Internal Gas Composition Was 75% Argon and 25% Helium (1.05 atm)

IX. ENVIRONMENTAL TESTING OF SNAP 7C ELECTRICAL GENERATING AND STORAGE SYSTEM

Environmental qualification of the major system components is necessary because:

(1) The equipment, after exposure to normal accelerations and vibrations, must be operable and must sustain no major damage from induced shock or vibration loads.

(2) The equipment must be capable of operating under the environmental conditions encountered at the installation site.

The tests were conducted under the conditions set forth in applicable portions of the statement of work (Ref. 4).

A. DESCRIPTION OF TEST SPECIMENS

The SNAP 7A-C test generator was used for the environmental tests. The biological shield was not used in the mechanical tests since it had no effect on the mechanical properties of the generator, and to include it would complicate the tests considerably. The simulated decay heat was removed by circulating water through an aluminum cooling jacket as shown in Fig. IX-1. The temperature tests, on the other hand, were conducted with the unit assembled in the biological shield so that the heat transfer properties were duplicated as indicated by Fig. IX-2. The battery and converter were tested at the same time as the generator Typical test configurations are shown in Figs. IX-3 and IX-4.

B. TEST CONDITIONS

The thermoelectric generator, converter and battery were subjected to vibration, shock and temperature tests as described in this subsection.

1. Vibration Tests

Since the SNAP 7A and 7C generators are identical, one model was subjected to a composite environment consisting of the following:

(1) Vertical plane.

(a) 5 to 33 cps in discrete frequency intervals of one cps, dwell for 3 minutes at each frequency, 3-g level or 0.060 ± 0.006-inch displacement, whichever is less.

(b) 5 to 300 to 5 cps sweep in 15 minutes at a 3-g level or 0.050 ± 0.006-inch displacement, whichever is less.

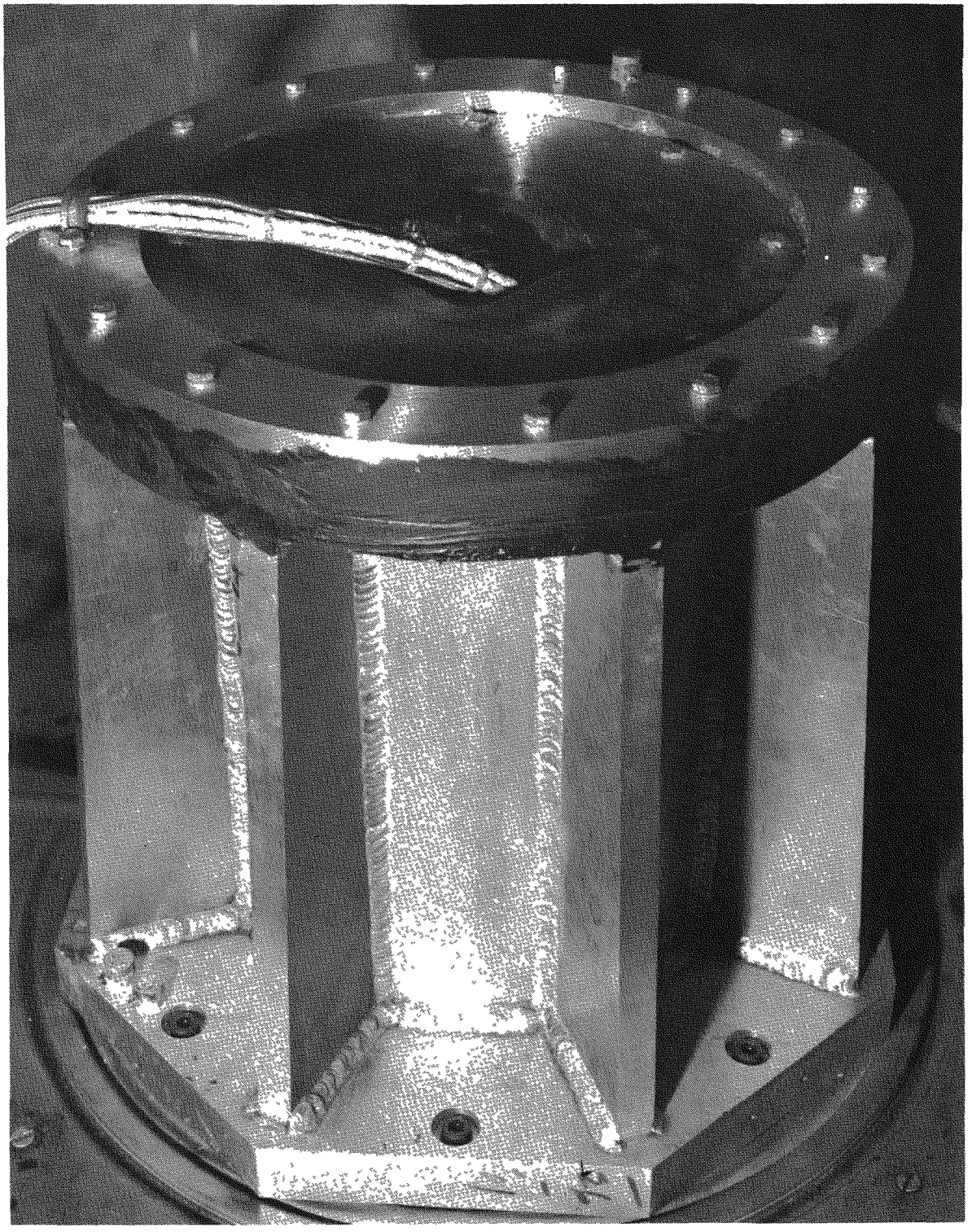

Fig. IX-1. SNAP 7A-7C Thermoelectric Generator and Test Fixture Positioned on MB-C25 Electrodynamic Shaker for Vertical Excitation

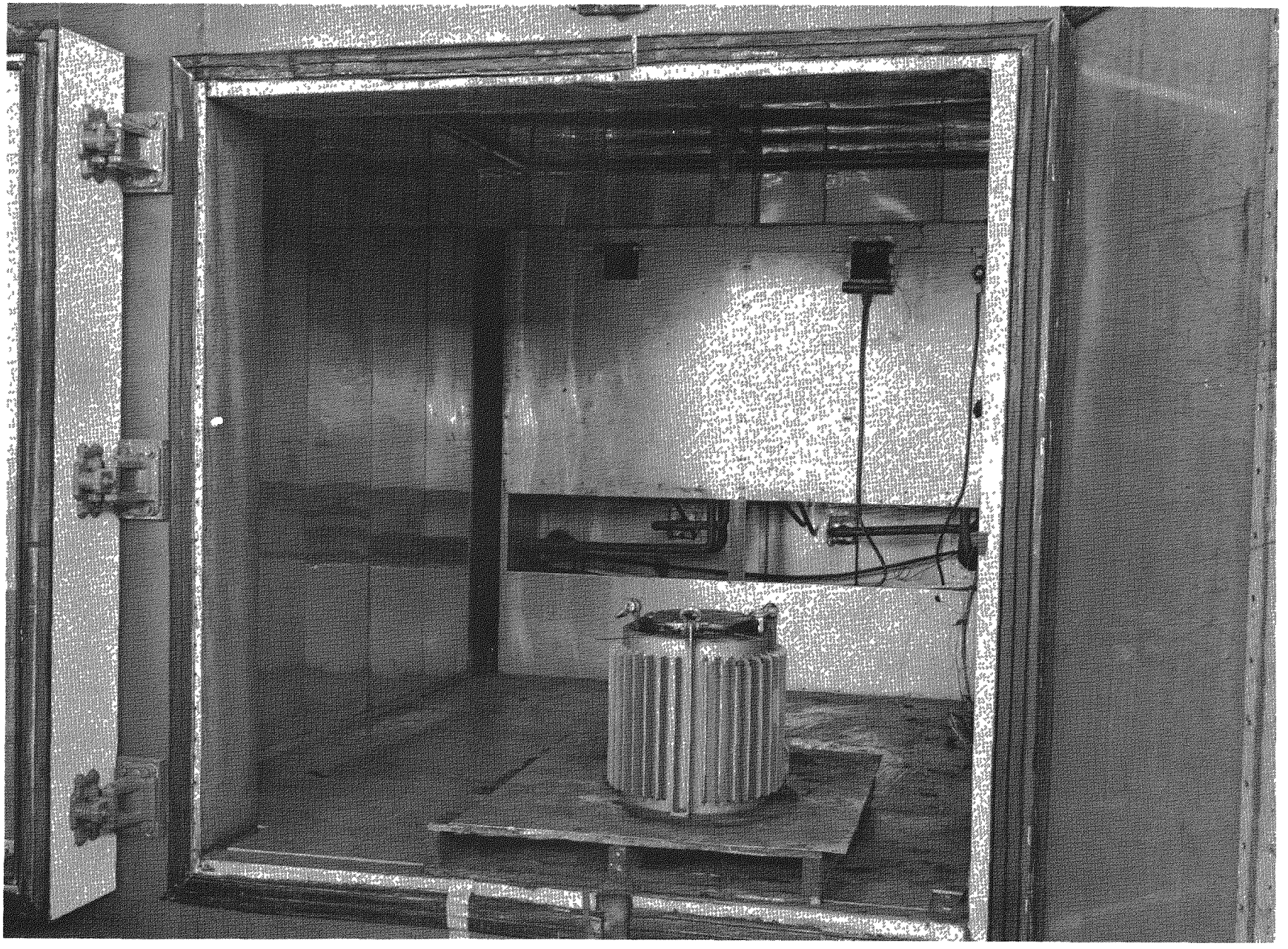

Fig. IX-2. SNAP 7A-7C Thermoelectric Generator with Biological Shield Positioned in Temperature Chamber for Temperature Output Tests

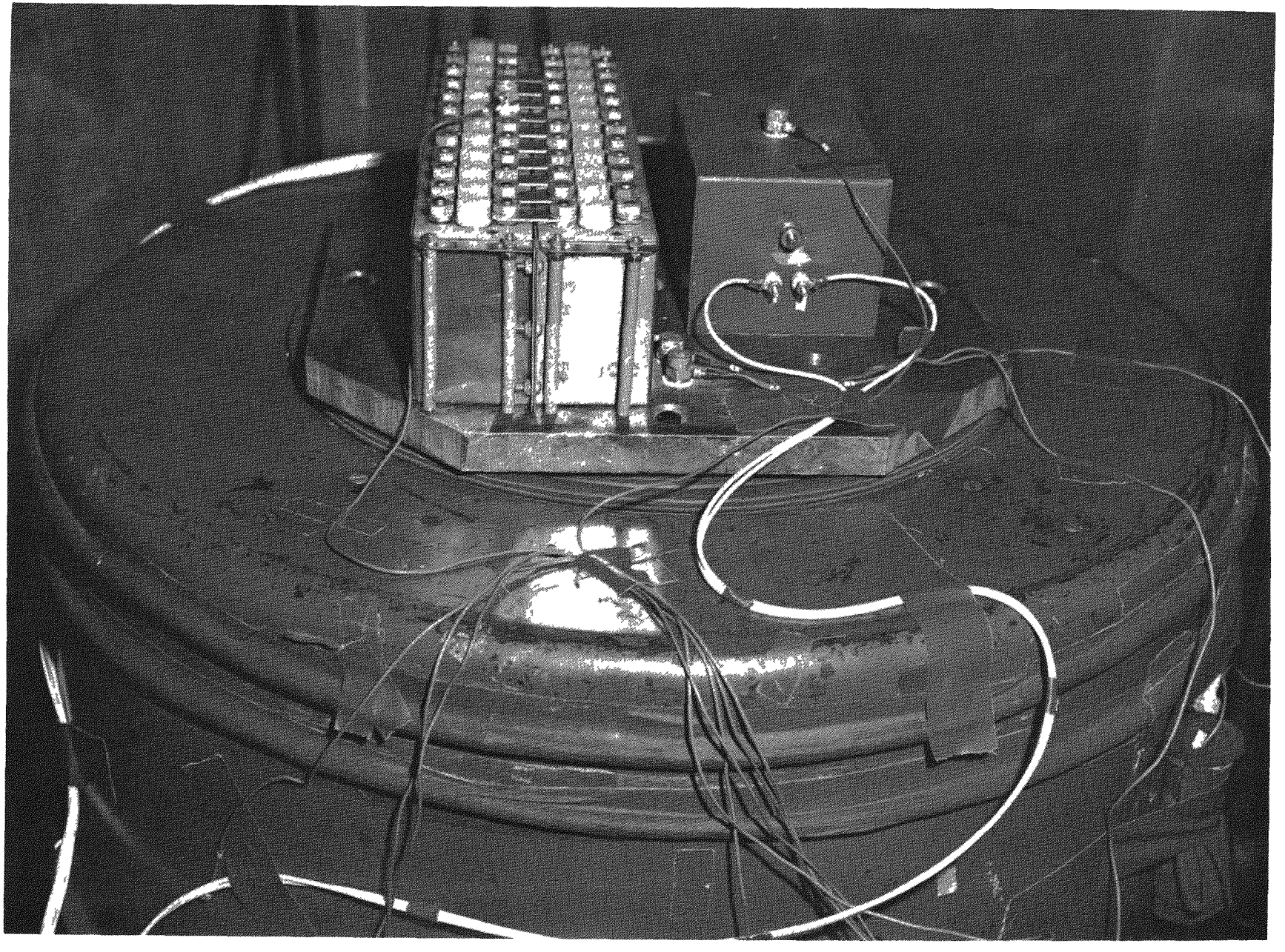

Fig. IX-3. SNAP 7C Battery and Converter Positioned on MB-C25 Electrodynamic Shaker for Vertical Excitation

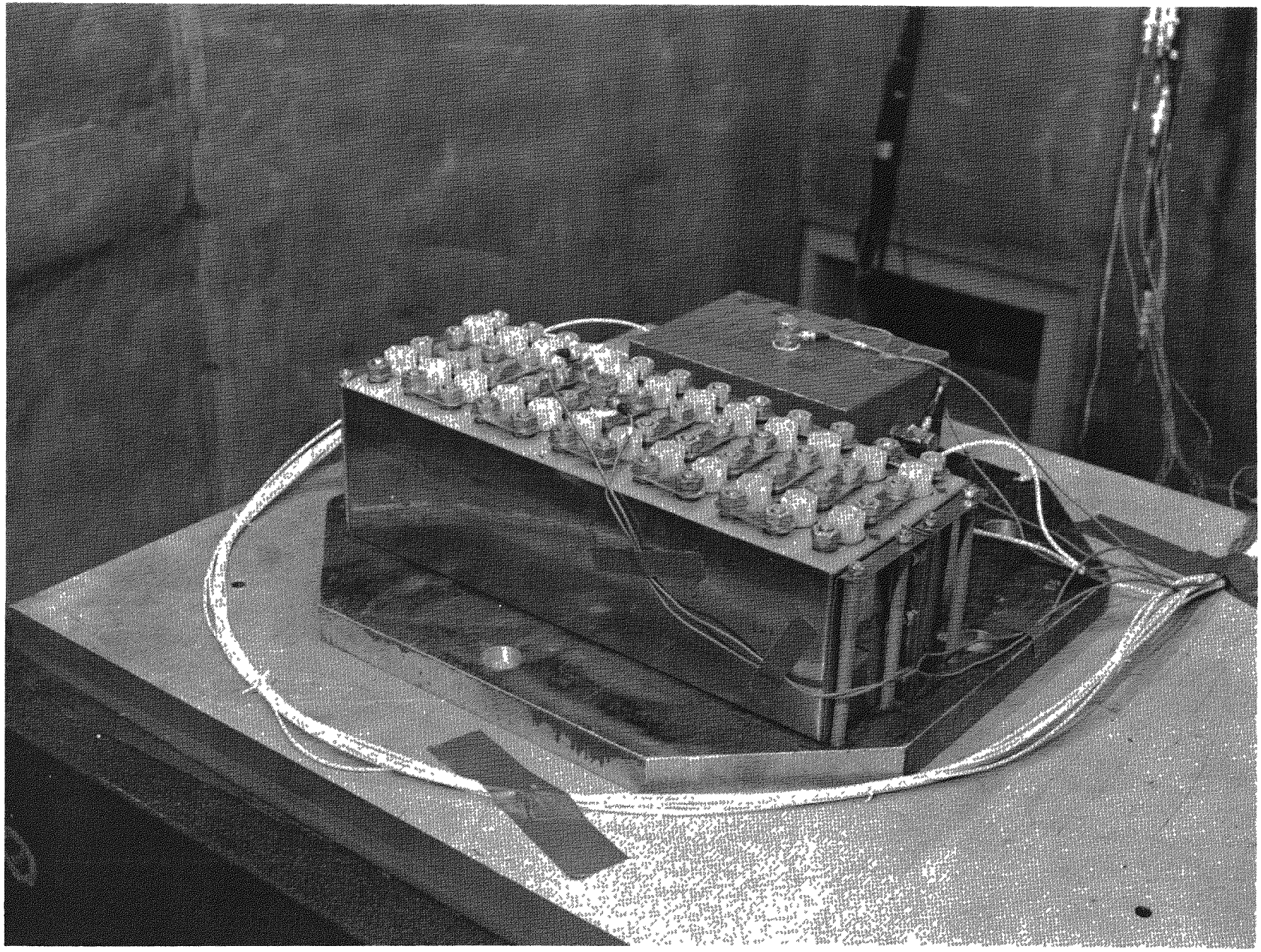

Fig. IX-4. SNAP 7C Battery and Converter Positioned on Vibration Slide Table for Excitation in Horizontal Axes

(2) Repeats (1) for the two remaining principal orthogonal axes.

(3) Dwell at the most severe resonant condition, at the input level consistent with the frequency, for a period of two hours.

The battery and converter were subjected to Parts (1)(a), (2) and (3) only, since this is the SNAP 7C requirement.

2. Shock Tests

The following requirement is identical for the SNAP 7A and 7C system:

(1) Subject the specimen to two 6-g shocks, having a 6-millisecond half sine wave pulse, in each of the three principal orthogonal axes.

3. Temperature

(1) Generator--Record performance and specimen temperature after stabilization at the following ambient conditions:

0° F--sea level pressure*

+28° F--sea level pressure

+70° F--sea level pressure*

+125° F--sea level pressure**

(2) Battery and converter--Record performance and specimen temperature after stabilization at the following ambient conditions:

+20° F--sea level pressure

+60° F--sea level pressure

C. TEST METHOD AND RESULTS

1. Generator Vibration

The thermoelectric generator was attached to a test fixture and positioned on an MB-C25 electrodynamic shaker for excitation in the vertical plane (Figs. IX-1 and IX-5).*** After testing, the generator and fixture

*Anticipated extremes of ambient temperature during operation--composite of SNAP 7A and 7C.

**Maximum anticipated ambient temperature during shipment with generator output short circuited to take advantage of the Peltier cooling effect.

***Circuitry for performance measurements was connected as shown in Fig. IX-6.

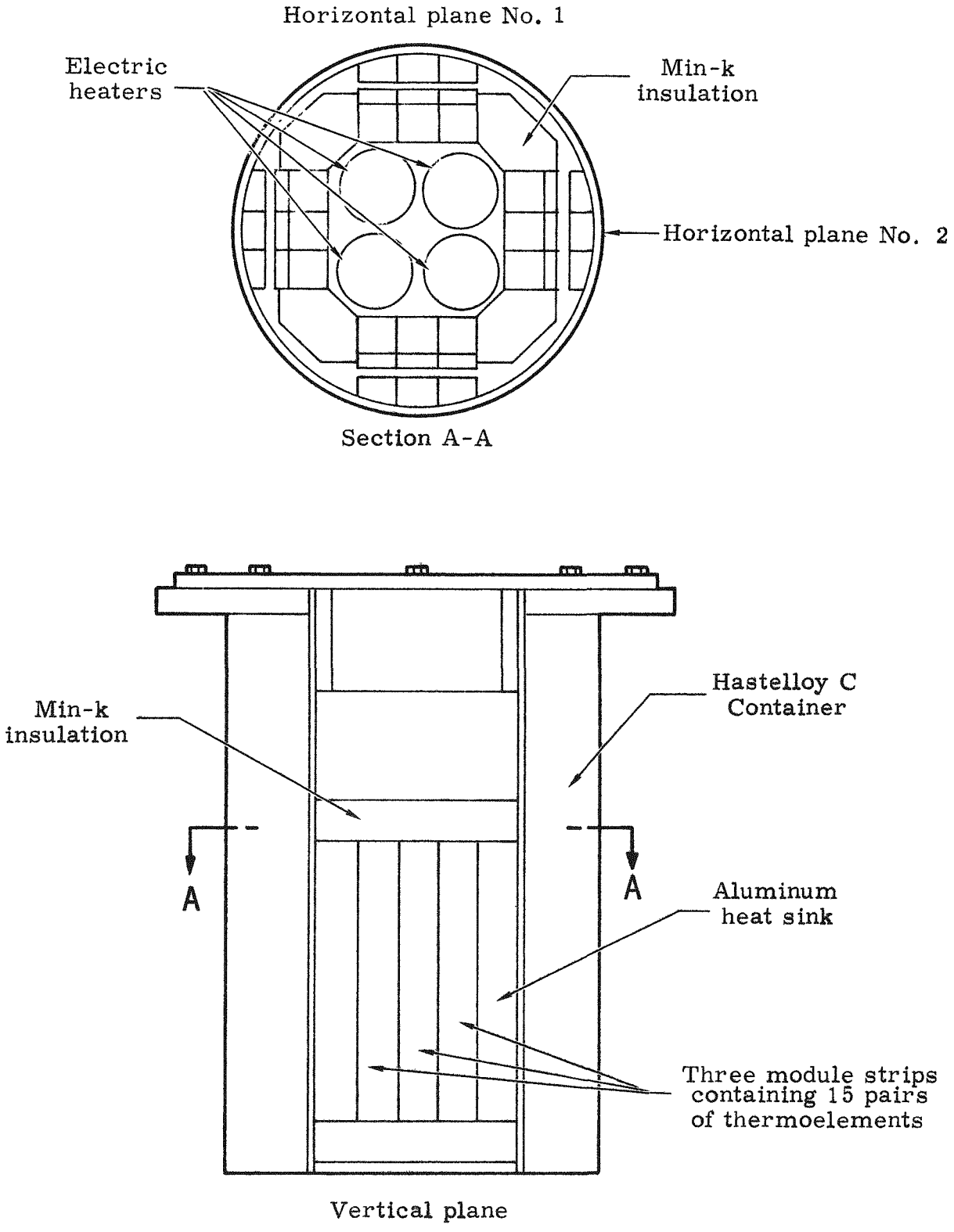

Fig. IX-5. Reference Axis for Vibration and Shock Testing

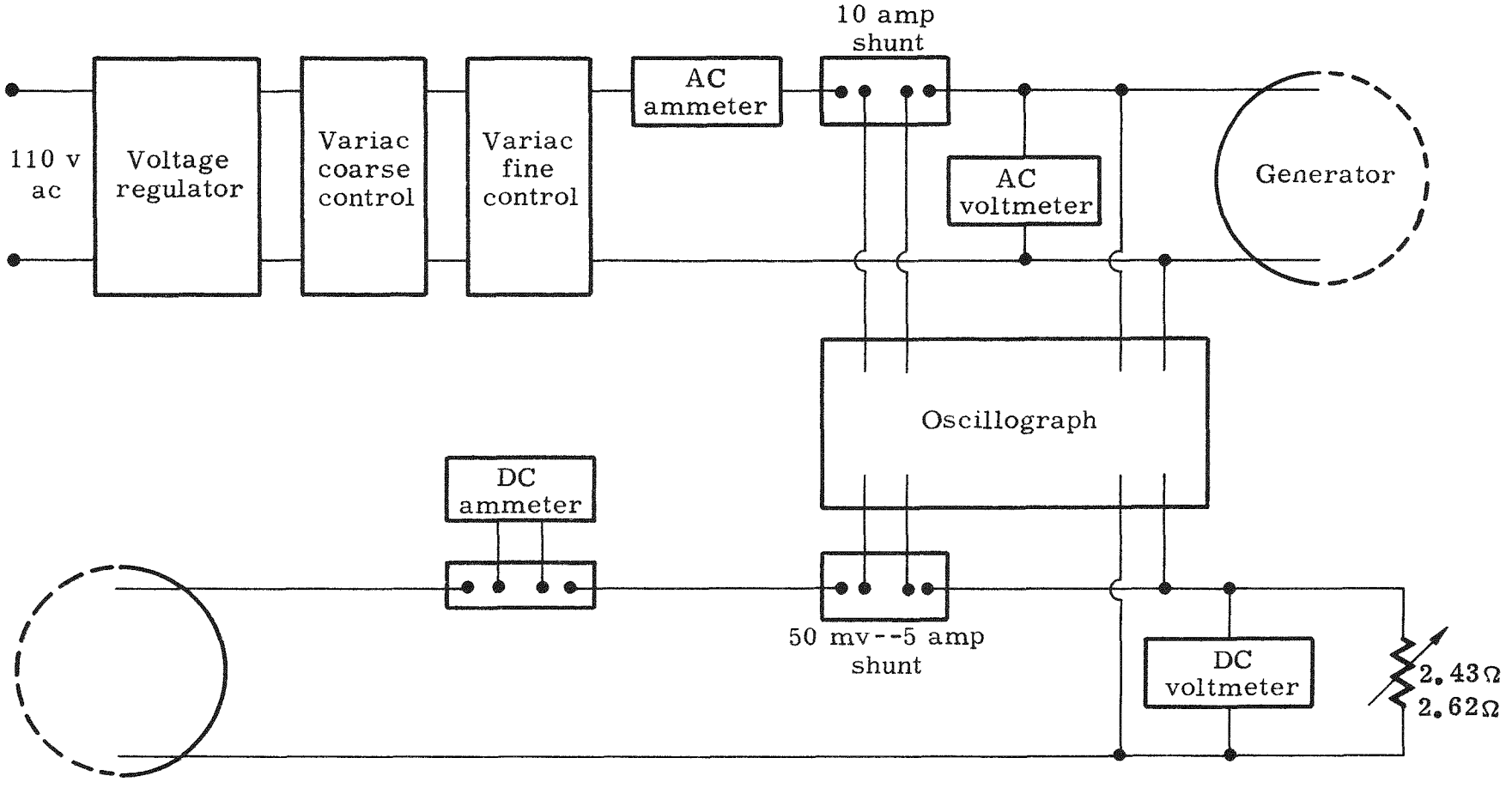

Fig. IX-6. Instrumentation Circuitry for Generator Test

were attached to a slide plate resting on an oil table for excitation in the horizontal planes as illustrated in Fig. IX-7.

The generator functioned properly throughout its exposure to vibration. During the test in horizontal plane No. 1, discontinuities in generator output occurred at approximately 90 and 250 cycles per second. This is shown in Figs. IX-8 through IX-11.

The 250-cycles per second frequency was selected for the vibration dwell in horizontal plane No. 1 because of the broad output response characteristic in that particular frequency range. The vibration dwell caused an increase in generator output, continuing for six hours after the dwell was completed. Table IX-1 summarizes the generator vibration data.

2. Battery and Converter Vibration

The battery and converter were attached to a flat fixture plate and tested simultaneously. Figure IX-12 illustrates the battery and converter positions for vertical and horizontal excitation. Figures IX-3 and IX-4 are pictures of the test apparatus. The converter and battery behavior were monitored throughout the test with the circuitry illustrated in Fig. IX-13.

Individual cell voltage checks and checks of converter output with simulated generator input prior to and after all vibration tests indicated satisfactory performance.

The major vibration resonance was detected at 284 cycles per second in the vertical plane at the top center of the converter. The specimens were subjected to the two-hour vibration dwell at this frequency with no adverse effects noted. Table IX-2 tabulates the functional data obtained for these tests.

3. Generator Shock

The generator and fixture were mounted on the table of the Barry Medium Impact Shock Machine (Fig. IX-14) for the 6-g, 6-millisecond impacts in the vertical plane. Generator functions were monitored in the same fashion as during vibration testing.

The generator was then repositioned as shown in Fig. IX-15 for shock impacts in the two horizontal planes.

The generator functioned properly throughout two drops in the vertical and horizontal axes. A typical effect on output is shown in Fig. IX-16 and a summary of the test results is given in Table IX-3.

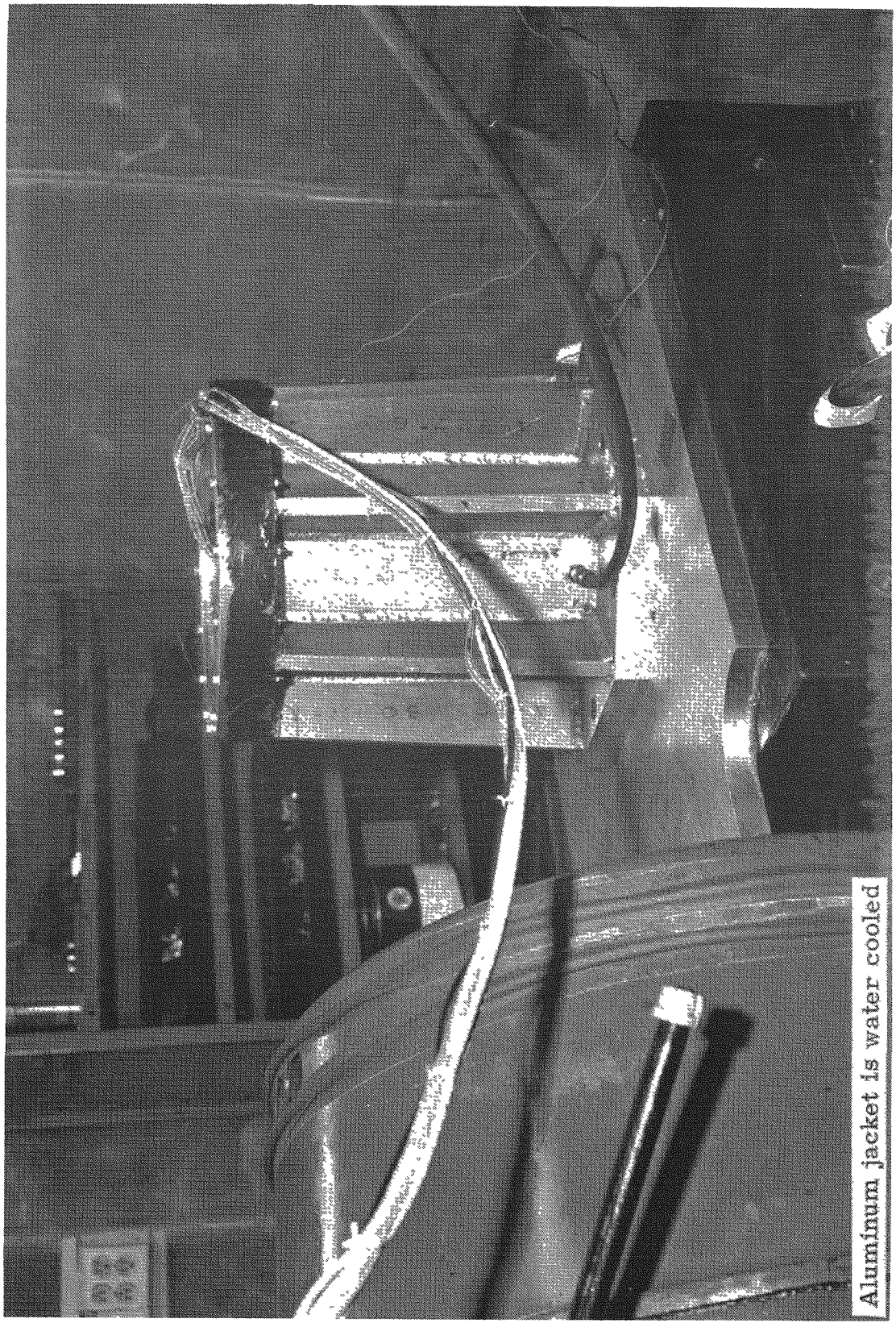

Fig. IX-7. SNAP 7A-7C Thermoelectric Generator and Test Fixture Positioned on Vibration Slide Table for Horizontal Excitation

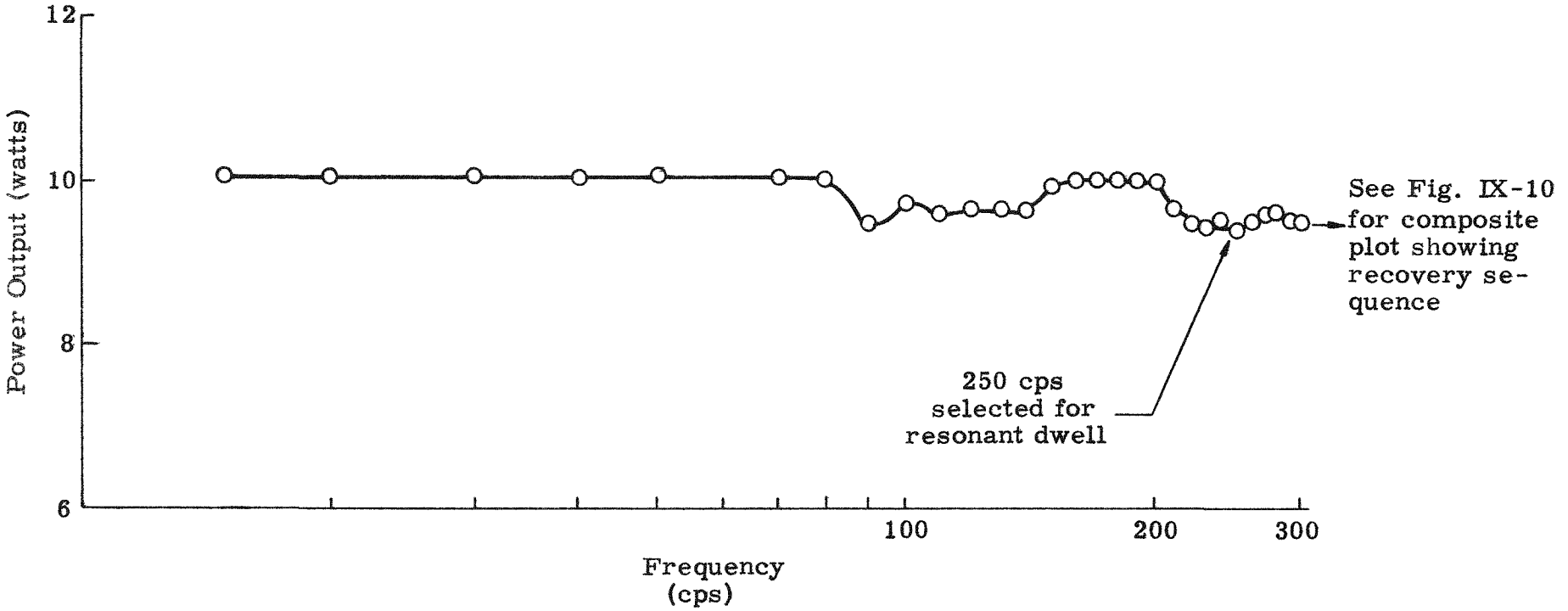

Fig. IX-8. Power Output Versus Frequency in Horizontal Plane No. 1

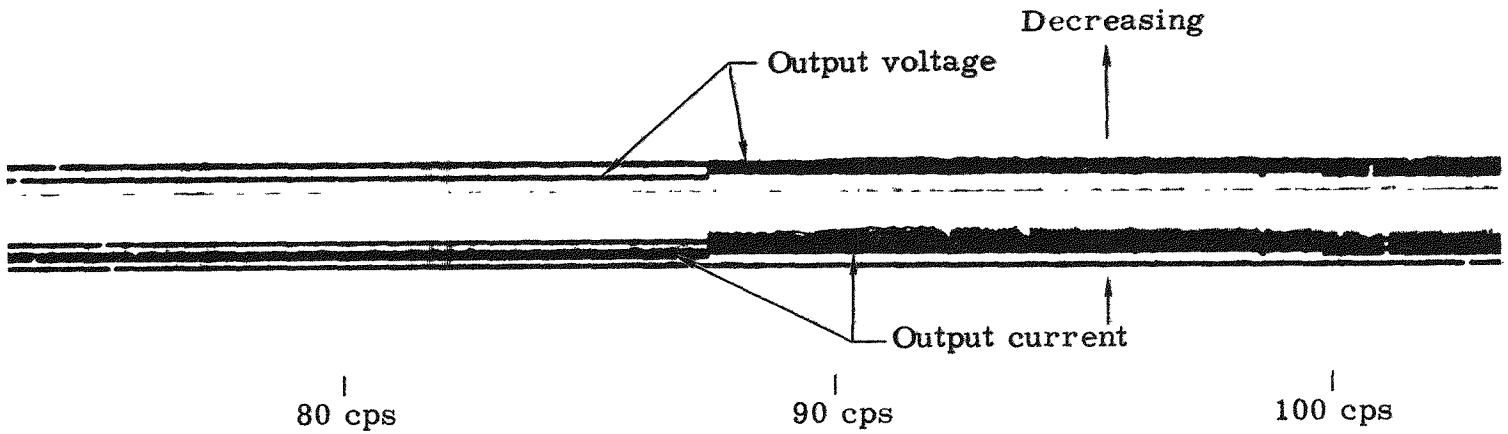

Fig. IX-9. Oscillograph Reproduction of Generator Output Response at 90 cps

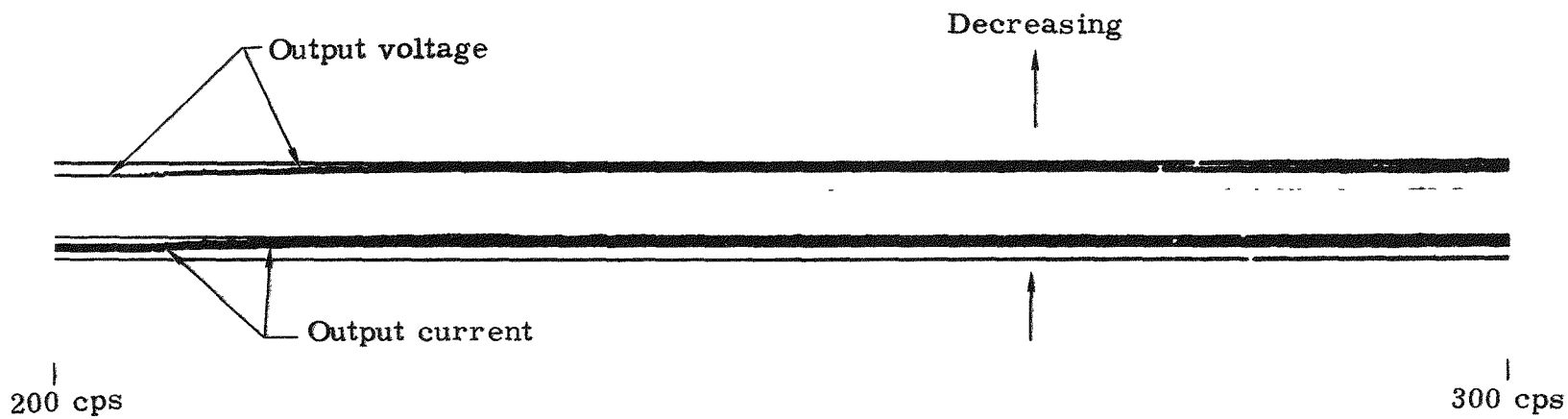

Fig. IX-10. Oscillograph Reproduction for Generator Output Response at 250 cps

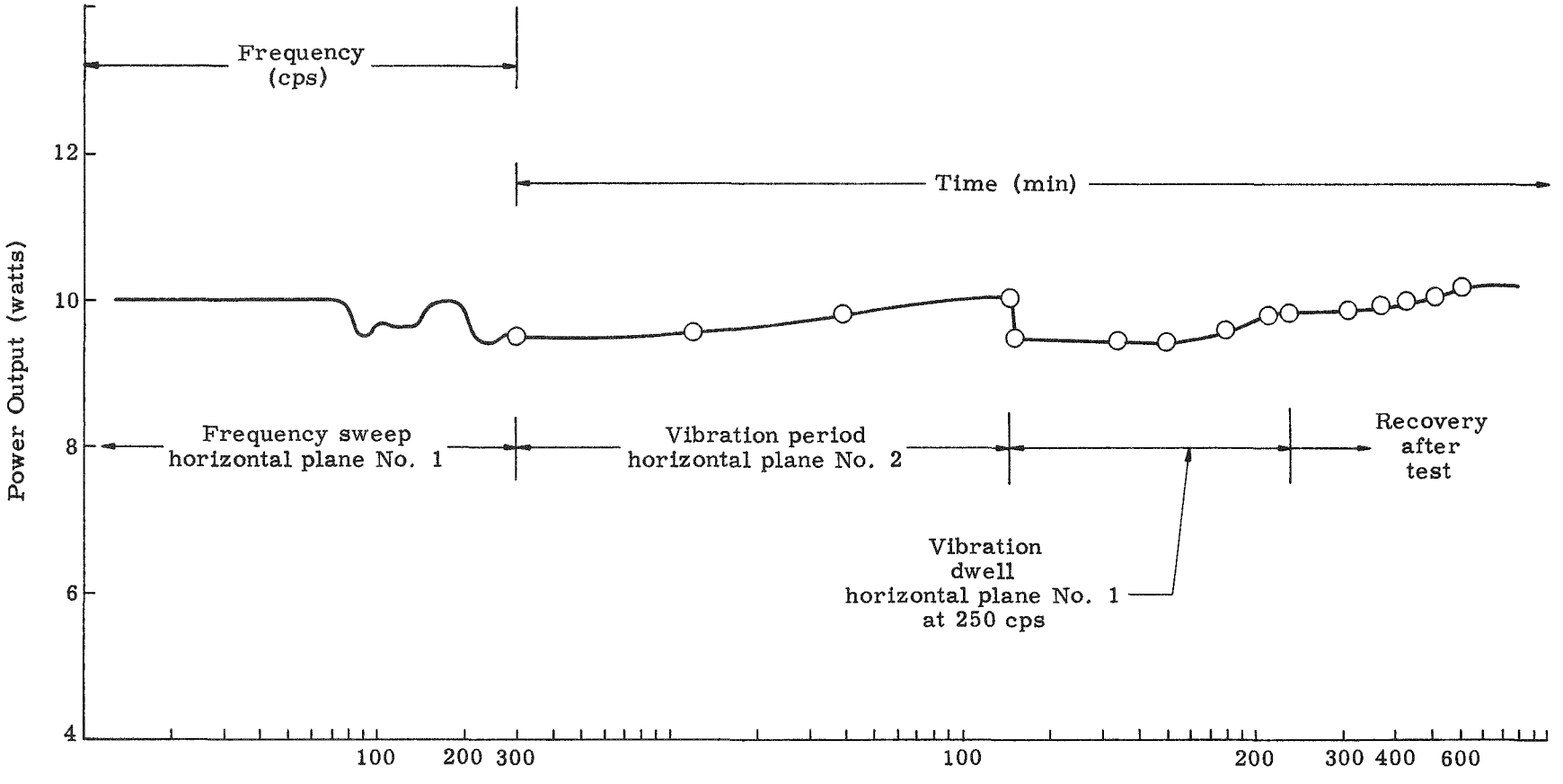

Fig. IX-11. Time History of Generator Output During and After Horizontal Vibration

TABLE IX-1

Snap 7A-7C Thermoelectric Generator Vibration Test Data

Reference Plane	Environment	Exposure Time (min)	Power Input (watts) Before	Power Input (watts) After	Power Output (watts) Before	Power Output (watts) After	Remarks
Vertical	5 to 300 cps at 0.06 DA & 1/2 g	7-1/2	240	240	10.05	10.05	Investigation for major resonant conditions--none noted
Vertical	5 to 33 cps at 0.06 DA & 3 g	87	240	240	10.05	10.05	Satisfactory
Vertical	5 to 300 to 5 cps at 0.06 DA & 3 g	15	240	240	10.05	10.05	Satisfactory
Horizontal 1	5 to 300 cps at 0.06 DA & 1/2 g	7-1/2	238	239	10.02	10.02	No resonances noted
Horizontal 1	5 to 33 cps at 0.06 DA & 3 g	87	238	238	10.02	10.02	Satisfactory
Horizontal 1	5 to 300 to 5 cps at 0.06 DA & 3 g	15	238	238	10.05	9.51	Discontinuity in output and ripple at 90 cps and decrease at 250 cps with ripple
Horizontal 2	5 to 300 cps at 0.06 DA & 1/2 g	7-1/2	238	238	9.51	9.82	No resonances noted
Horizontal 2	5 to 33 cps at 0.06 DA & 3 g	87	238	238	9.89	9.94	Satisfactory
Horizontal 2	5 to 300 to 5 cps at 0.06 DA & 3 g	15	238	238	9.94	10.05	Satisfactory
Horizontal 1	250 cps at 3 g dwell	120	238	238	10.05	9.80	At start of vibration output decreased to 9.43 watts. Ripple on output ceased after 90 min and output increased to 10.2 watts 6 hours after vibration was complete

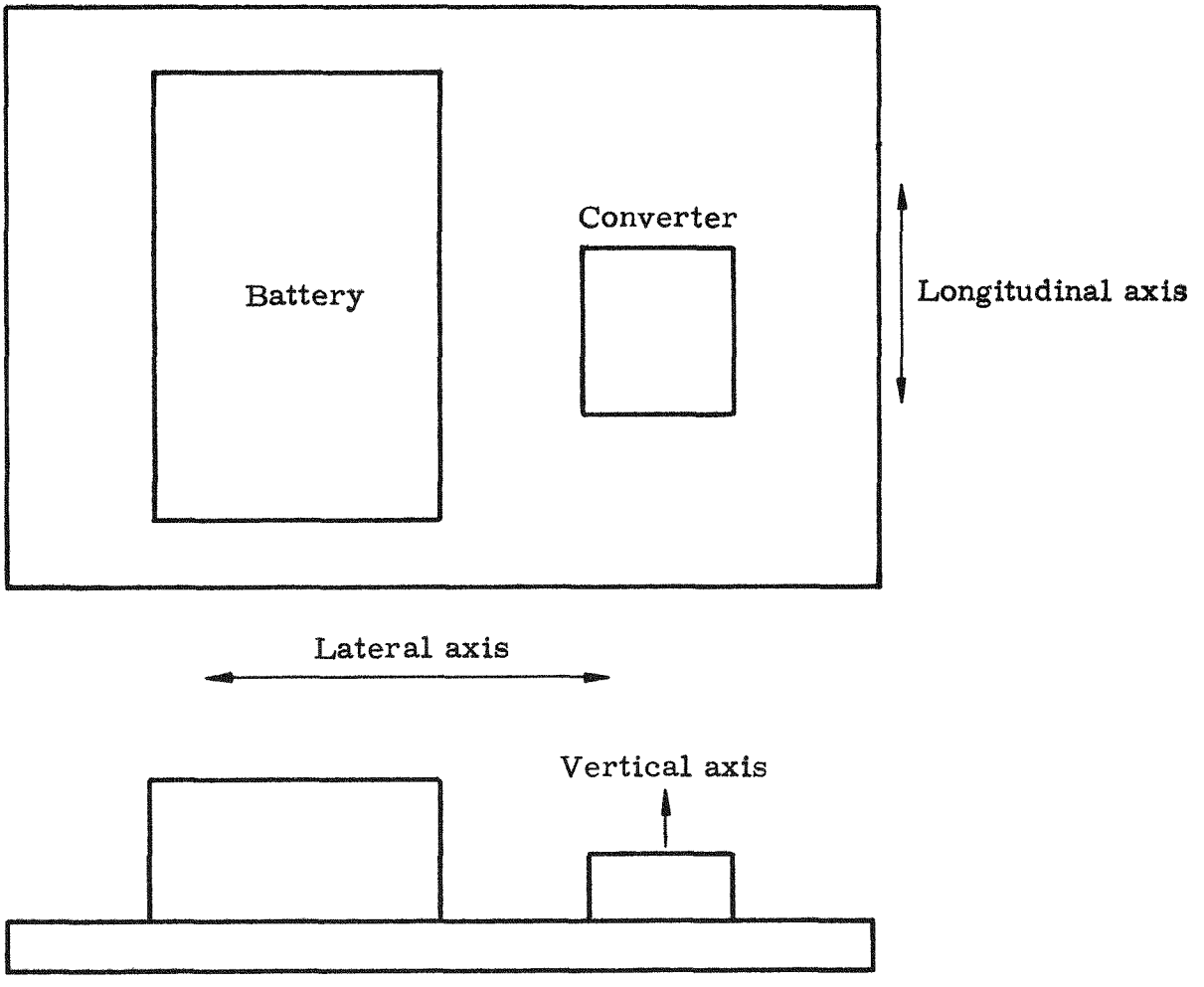

Fig. IX-12. Reference Axes for Vibration and Shock Testing of SNAP 7C Battery and Converter

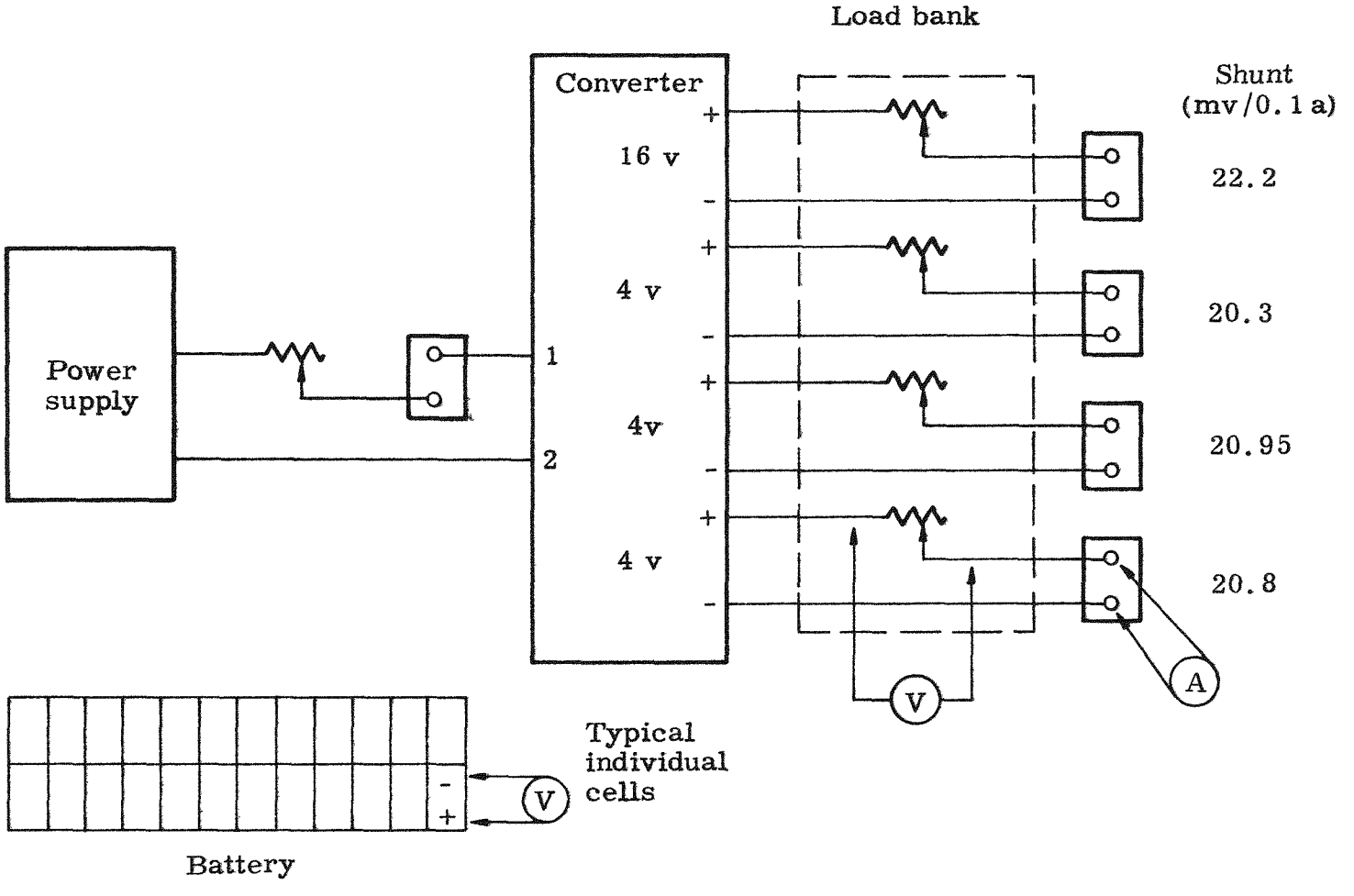

Fig. IX-13. Instrumentation Circuitry for SNAP 7C Battery and Converter Test

TABLE IX-2

Snap 7C Battery and Converter Vibration Test Data

Item	Vertical Vibrations Before	Vertical Vibrations After	Lateral Vibrations Before	Lateral Vibrations After	Longitudinal Vibration After	Vibration Dwell at 284 cps After
Battery cell voltages (volts)* Cells 1 through 22 (all identical)	1.28	1.28	1.28	1.28	1.28	1.28
Converter input						
Voltage (volts)	5.1	5.1	5.1	5.0	5.1	5.1
Current (amperes)	1.74	1.78	1.70	1.74	1.78	1.78
Converter output						
Section 1						
Voltage (volts)	16.0	16.0	16.0	16.1	16.3	16.3
Current (milliamperes)	99	99.3	98.6	99	99.3	100
Section 2						
Voltage (volts)	3.68	3.64	3.65	3.68	3.75	3.72
Current (milliamperes)	98.5	102	98.5	98.5	100	101
Section 3						
Voltage (volts)	3.35	3.35	3.30	3.32	3.38	3.37
Current (milliamperes)	100	103	99.5	100	101	102
Section 4						
Voltage (volts)	4.00	4.09	3.98	4.03	4.10	4.11
Current (milliamperes)	101	105	108	110	112	113

*Battery was not in fully charged condition.

Fig. IX-14. SNAP 7A-7C Thermoelectric Generator Positioned on Barry Medium Impact Shock Machine for Vertical Shock Tests

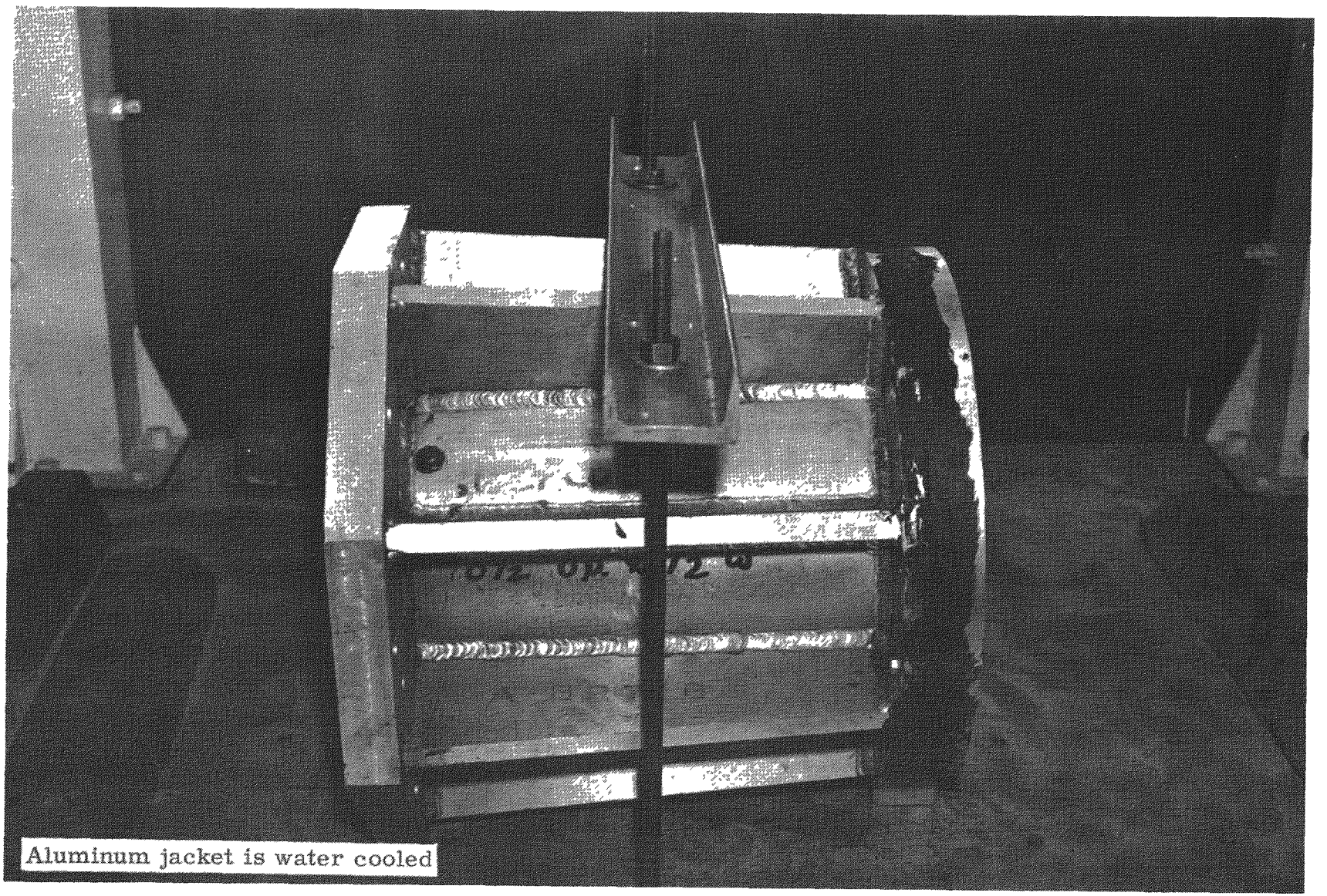

Fig. IX-15. SNAP 7A, 7C Thermoelectric Generator and Test Fixture Positioned on Barry Medium Impact Shock Machine for Horizontal Shock Tests

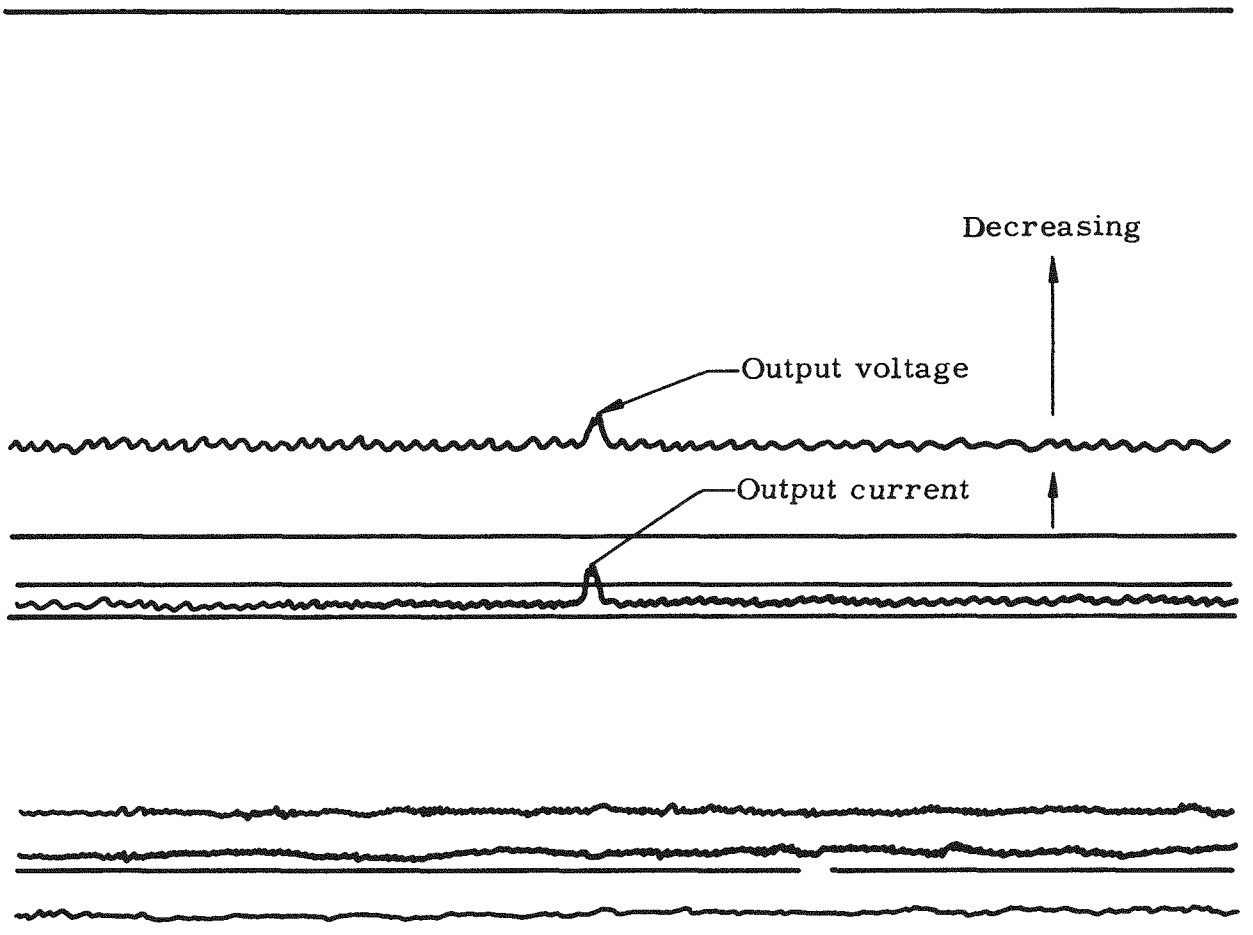

Fig. IX-16. Oscillograph Reproduction of Generator Output Effect of Horizontal Shock

TABLE IX-3

SNAP 7A-7C Thermoelectric Generator Shock Test Data

Reference Plane	Required Environment (g)	(**ms)	Power Input Before (watts)	Power Input After (watts)	Power Output Before (watts)	Power Output After (watts)	Results
Vertical No. 1	6 Half sine	6	238	238	9.92	9.92	Satisfactory.
Vertical No. 2	6 Half sine	6	238	238	9.92	9.92	Satisfactory.
Horizontal 1 No. 1	6 Half sine	6	238	238	9.92	9.92	Satisfactory.
Horizontal 1 No. 2	6 Half sine	6	238	238	9.92	9.92	Approximately 5 min after drop, output noted to have decreased to 8.3 watts.
Horizontal 2 No. 1	6 Half sine	6	238	238	8.3	8.3	Impulse caused momentary increase to normal output.
Horizontal 2 No. 2	6 Half sine	6	238	238	8.3	8.3	Impulse caused momentary increase to normal output.

**Actual shock environment was approximately 18-g, 6-ms half sine.

About five minutes after the second shock in horizontal plane No. 1, the output suddenly dropped approximately 15%. Testing was continued in horizontal plane No. 2. The output during both shock pulses momentarily returned to the maximum output as recorded in Fig. IX-17. After testing was complete, another slight shock in the vertical plane restored continuous, near maximum output (deficiency corrected). It was then noted that handling of the input-output plug on the generator produced the same 15% decrease in output. The decrease can be attributed to this plug and not the basic thermoelectric generator.

After the shock tests were completed, discrepancies in the shock machine were noted and a check was made of the actual shock loads. It was found that the generator had been subjected to 18-g, 6-millisecond, half-sine shock pulses. This represented a shock value three times greater than required by the statement of work.

4. Battery and Converter Shock

The battery and converter were secured to the table of the Barry Medium Impact Shock Machine shown in Fig. IX-18 for the 6-g, 6-millisecond impacts in the vertical plane. Battery and converter performance were monitored throughout the test.

The units were then positioned for shock impulses in the two remaining principal orthogonal axes shown in Fig. IX-19. The battery and converter functional checks made before and after each plane of shock show no structural damage or effects on the operation of the battery and converter. Table IX-4 tabulates the data obtained from the shock tests.

5. Temperature Tests

The generator assembly was placed in the finned biological shield using a glycol-water solution to conduct heat from the generator to the shield, and the complete unit was positioned in the Bowser temperature chamber shown in Fig. IX-2. Generator functions and temperatures were monitored throughout the temperature cycles and for a stabilization period at each temperature step. Figures IX-20 through IX-23 present the effect of ambient temperatures on the generator output. Tables IX-5 through IX-8 contain all data taken during the temperature - output tests.

The battery and converter positioned for the temperature test are shown in Fig. IX-24. The requirements for operation and performance of these components at temperatures of +20° and +60° F were substantiated.

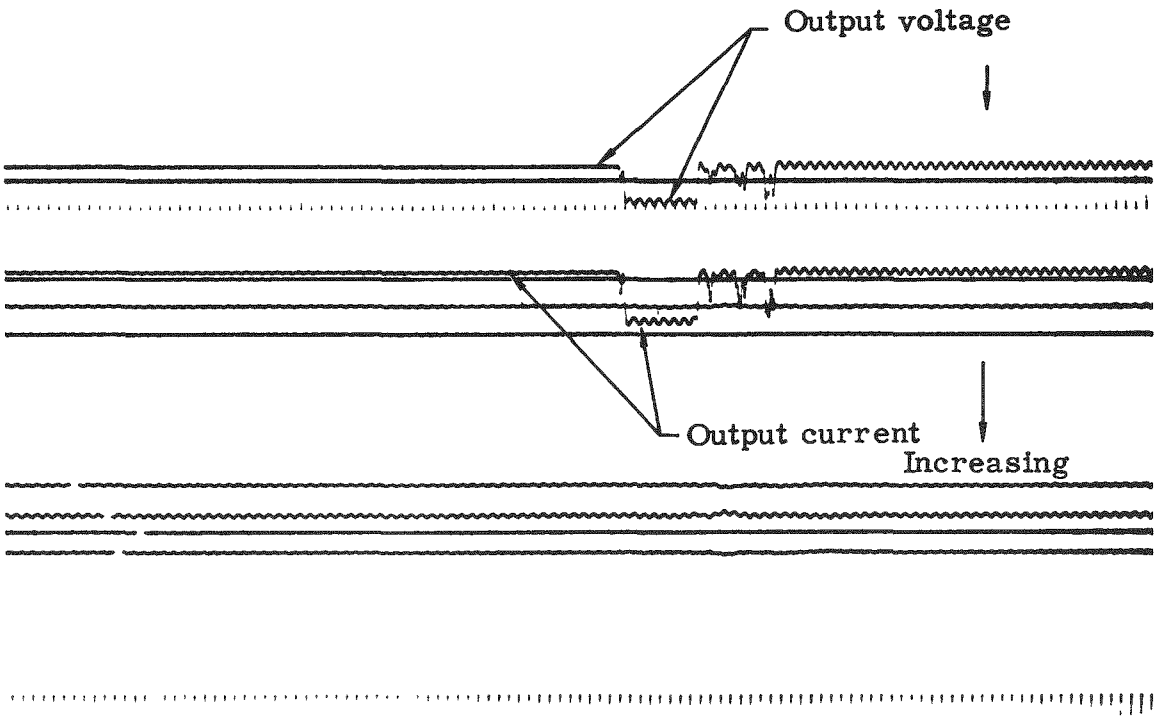

Fig. IX-17. Oscillograph Reproduction of Effect on Output from Horizontal Shock After Discrepancy in Output

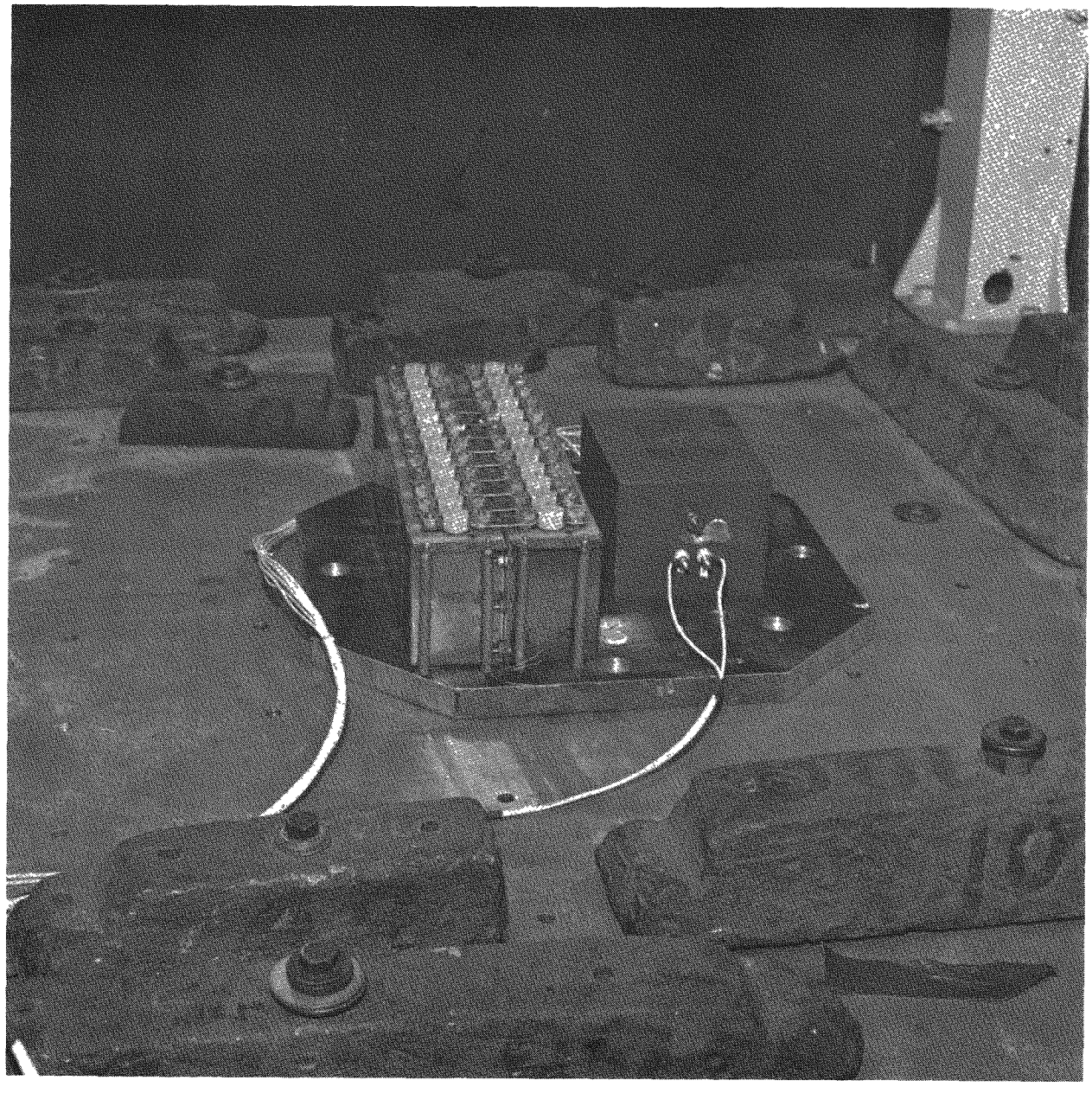

Fig. IX-18. Snap 7C Battery and Converter Positioned on Barry Medium Impact Shock Machine for Vertical Shock Tests

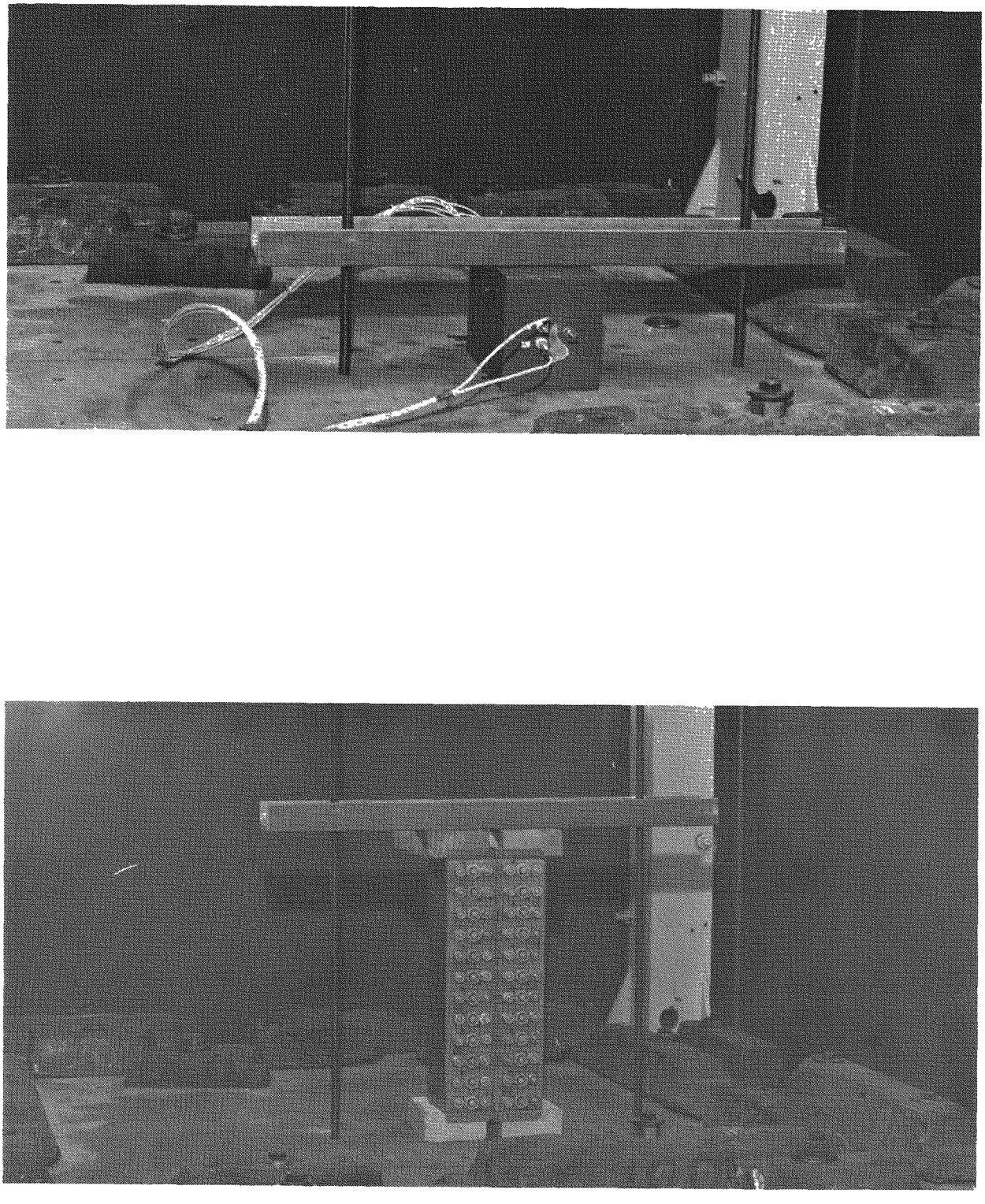

Fig. IX-19. SNAP 7C Battery and Converter Positioned on Barry Medium Impact Shock Machine for Horizontal Shock Tests

TABLE IX-4

SNAP 7C Battery and Converter Shock Test Data

Item	Vertical Shock Before	Vertical Shock After	Lateral Shock After	Longitudinal Shock After
Battery cell Voltages* (volts) Cell 1 through 22 (all identical)	1.28	1.28	1.28	1.28
Converter input				
Voltage (volts)	5.1	5.1	5.2	5.1
Current (amperes)	1.78	1.78	1.81	1.81
Converter output Section 1				
Voltage (volts)	16.3	16.3	16.5	16.5
Current (milliamperes)	101	103	103	103
Section 2				
Voltage (volts)	3.75	3.76	3.77	3.77
Current (milliamperes)	99	101	103	101
Section 3				
Voltage (volts)	3.37	3.37	3.37	3.38
Current (milliamperes)	101	101	101	101
Section 4				
Voltage (volts)	4.10	4.11	4.12	4.12
Current (milliamperes)	114	115	115	114

*Battery was not in fully charged condition.

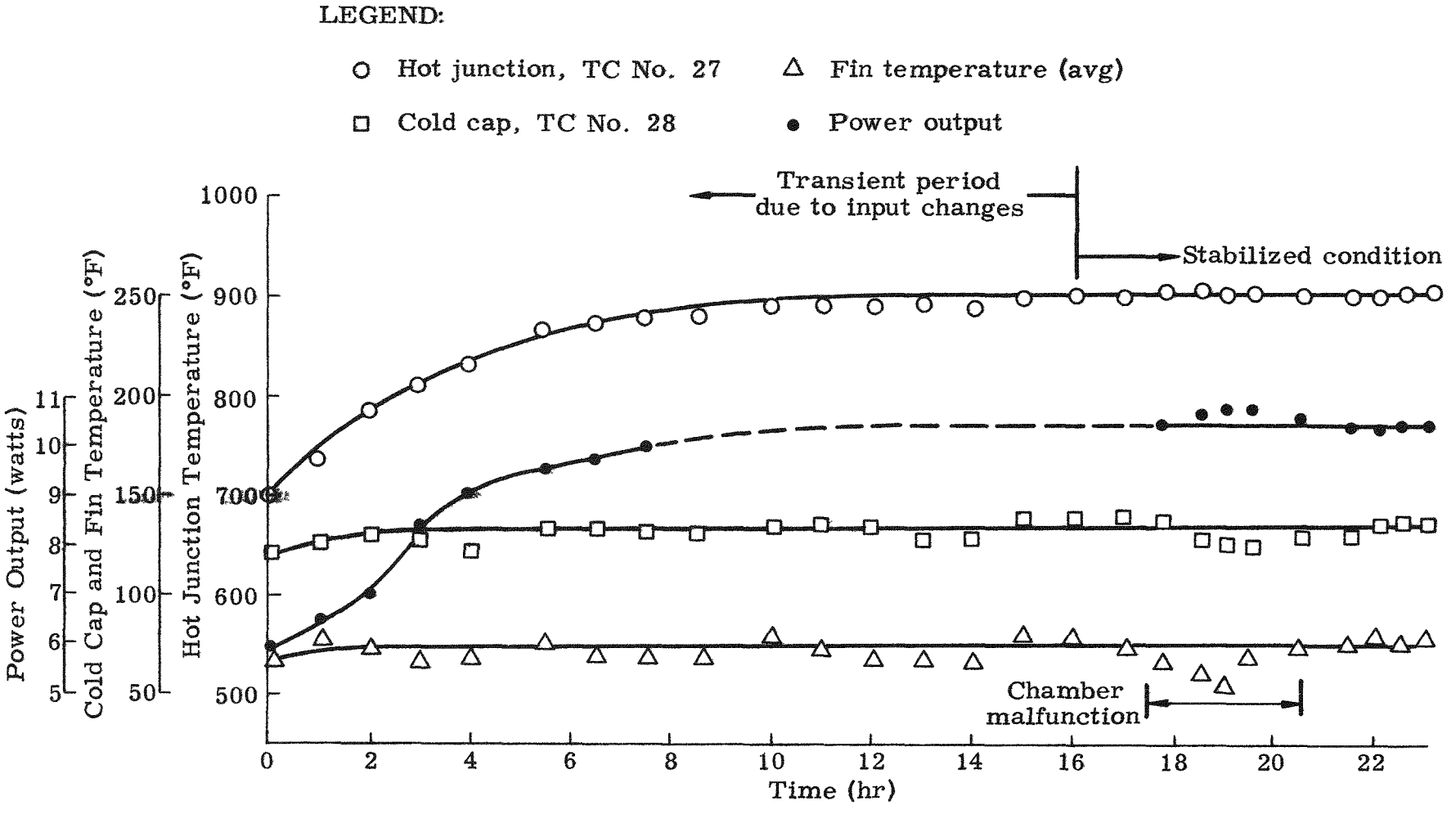

Fig. IX-20. Results of SNAP 7A and SNAP 7C Generator Temperature Chamber Tests, Where Nominal Power Input Was 257 Watts, Ambient Air Temperature Was 70° F, and Generator Atmosphere was 50% Argon and 50% Hydrogen

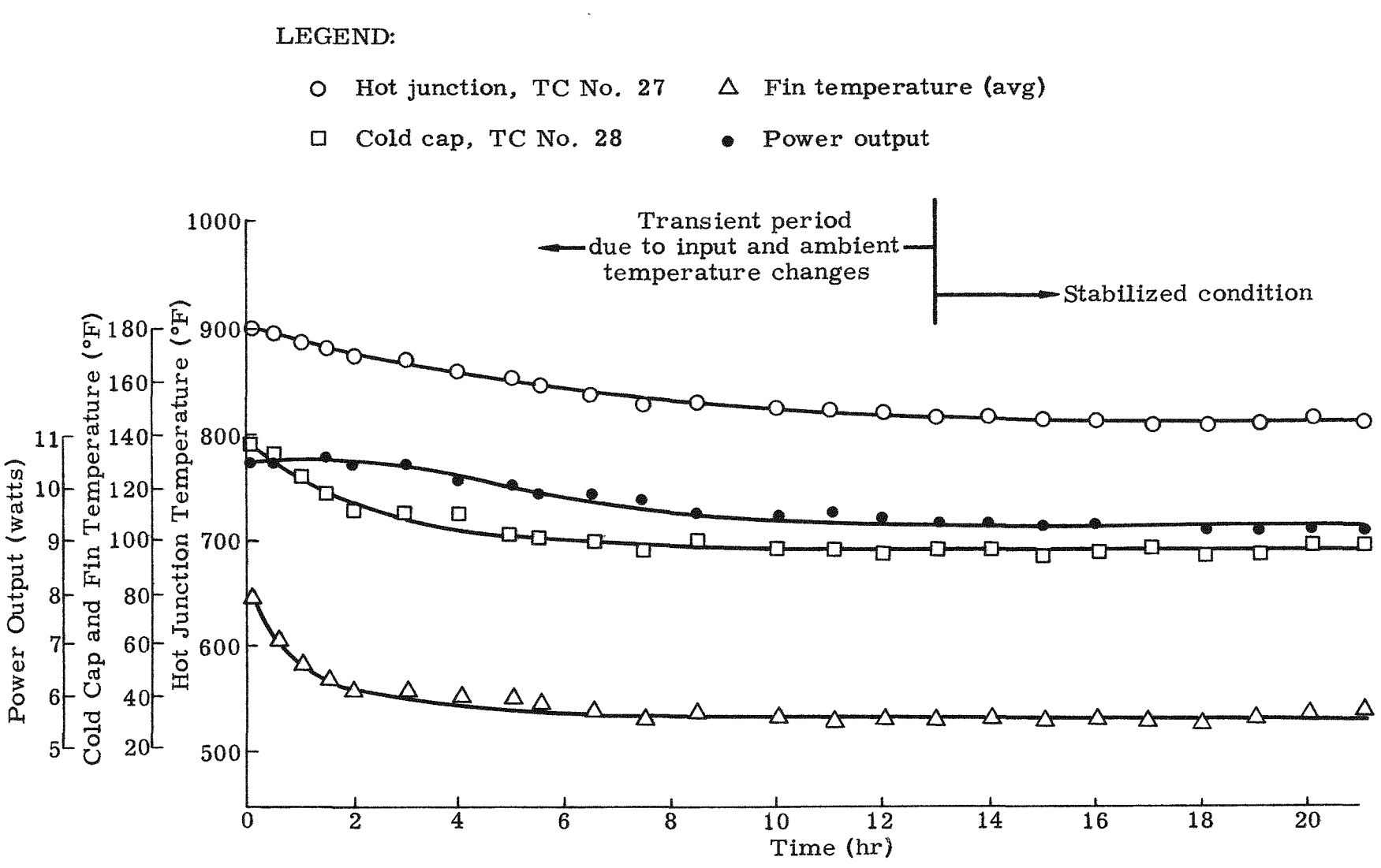

Fig. IX-21. Results of SNAP 7A and SNAP 7C Generator Temperature Chamber Tests, Where Nominal Power Input Was 247.5 Watts, Ambient Air Temperature Was 28° F, and Generator Atmosphere Was 50% Argon and 50% Hydrogen

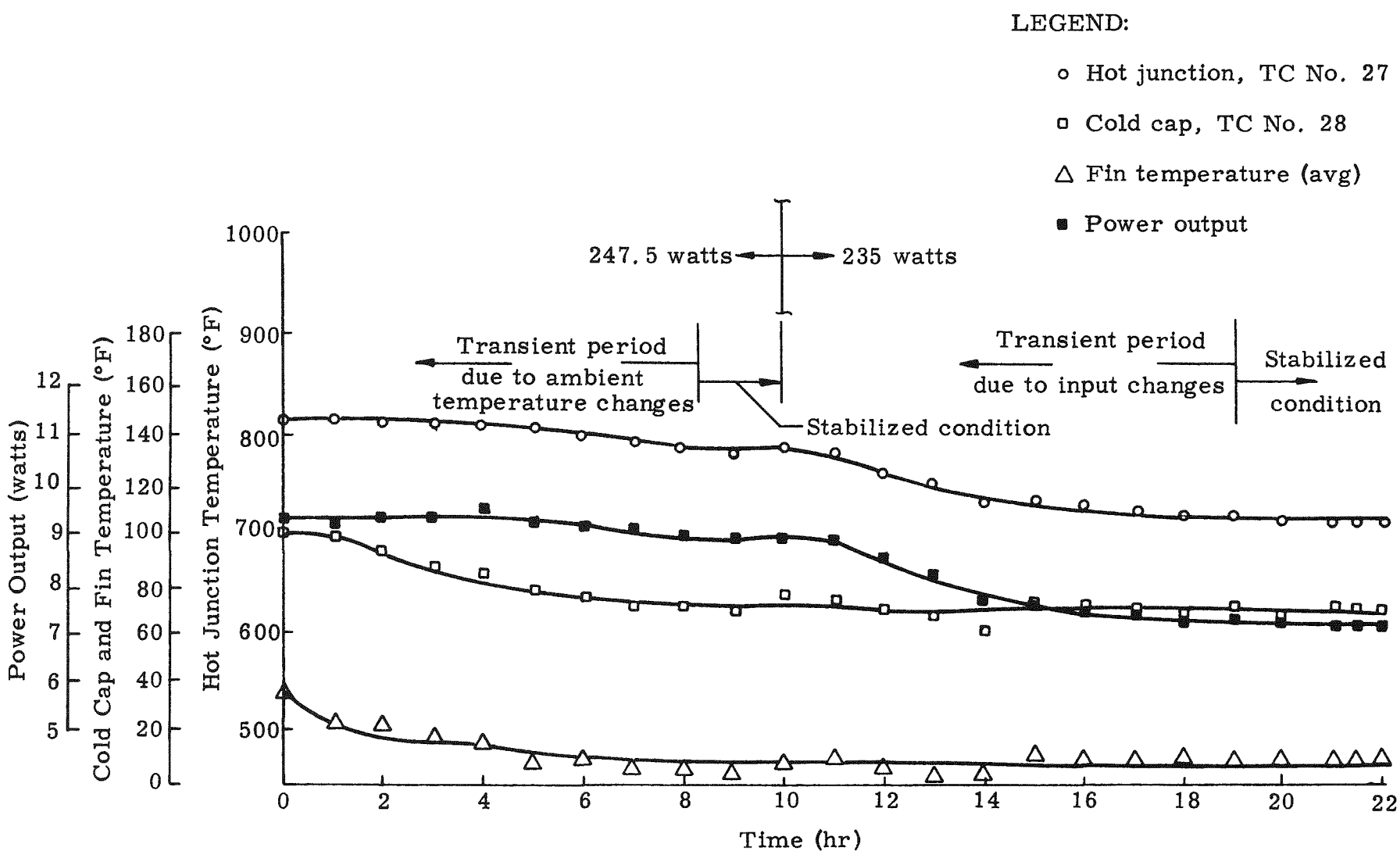

Fig. IX-22. Results of SNAP 7A and SNAP 7C Generator Temperature Chamber Tests, Where Nominal Power Input Was 247.5 and 235 Watts, Ambient Air Temperature Was 0° F, and Generator Atmosphere Was 50% Argon and 50% Hydrogen

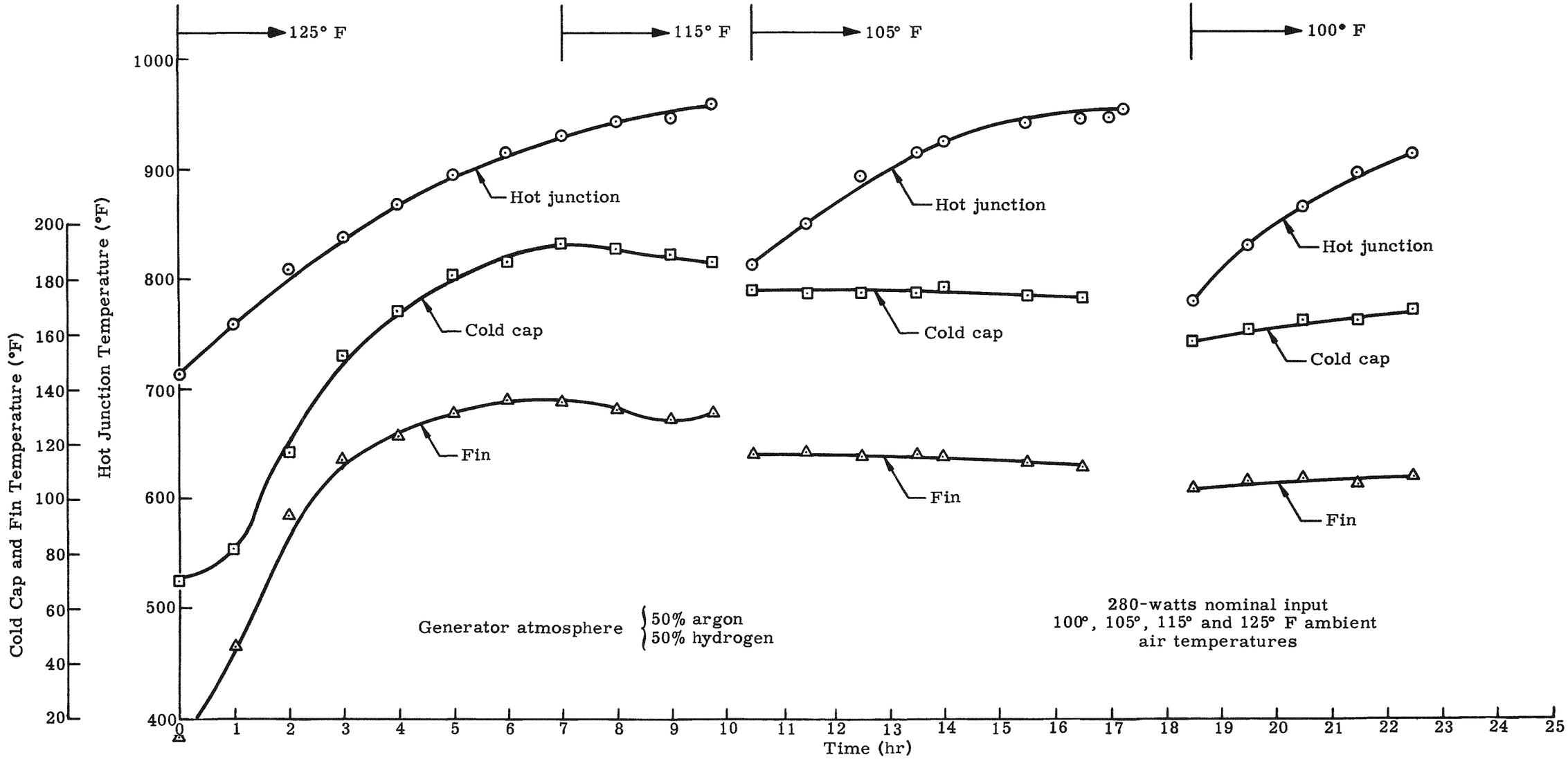

Fig. IX-23. SNAP 7A-7C Thermoelectric Generator Output Short-Circuit Shipping Condition

TABLE IX-5

Snap 7A-7C Thermoelectric Generator Temperature Test Data

		Power		Thermocouple Number*								
	Time	In (watts)	Out (watts)	25	26	27	28	29	30	31	Fin	Fin
				Temperature (°F)								
8/24	4:00 pm	240	5.91	726	649	702	121	118	108	101	--	72
	5:00	255	6.52	765	683	739	126	124	112	107	--	77
	6:00	255	7.07	813	730	785	130	124	113	105	--	72
	7:00	257	8.46	841	762	812	127	122	111	103	--	67
	8:00	257	9.12	859	786	831	123	119	108	101	--	67
	9:30	257	9.56	894	814	864	133	127	115	109	--	75
	10:30	257	9.75	899	822	871	134	126	115	106	--	70
	11:30	257	10.04	907	830	879	132	126	113	106	--	69
8/25	12:30 am	257	--	907	836	878	130	124	112	102	--	71
	2:00	257	--	919	842	890	136	132	119	112	--	76
	3:00	257	--	920	842	891	135	130	119	110	--	74
	4:00	257	--	920	844	891	135	126	119	106	--	69
	5:00	257	--	921	845	892	130	125	114	106	--	70
	6:00	256	--	917	845	888	130	124	112	104	--	67
	7:00	257	--	926	853	899	139	132	112	113	--	81
	8:00	258	--	926	852	900	138	133	119	114	--	80
	9:00	257	--	928	851	899	138	131	119	112	--	75
	9:45	257	10.45	932	852	901	136	130	118	111	--	67
	10:30	257	10.65	934	855	906	128	122	111	103	--	61
	11:00	257	10.75	929	851	900	124	120	106	99	--	57
	11:30	257	10.75	935	853	902	125	120	108	99	--	70
	12:30	257	10.55	929	850	899	131	125	111	103	--	74
	1:00	void										
	1:30	258	10.40	931	853	899	132	128	114	107	--	76
	2:00	258	10.40	929	854	899	136	130	117	110	79	79
	2:30	258	10.40	929	851	900	136	130	117	110	75	77
	3:00	257	10.45	929	851	901	137	131	118	111	77	79

*See Table IX-9 for TC locations.

TABLE IX-6

Snap 7A-7C Thermoelectric Generator Temperature Test Data

		Power		Thermocouple Number*								
	Time	In (watts)	Out (watts)	25	26	27	28	29	30	31	Fin	Fin
				Temperature (°F)								
8/25	3:30 pm	247.5	10.50	924	848	895	132	128	114	108	59	64
	4:00	247.5	10.40	918	842	889	125	120	107	100	50	56
	4:30	247.5	10.60	909	836	881	117	102	99	93	45	49
	5:00	248	10.45	904	830	875	112	107	94	86	40	45
	6:00	247.5	10.45	898	827	870	111	106	93	86	42	45
	7:00	246	10.15	890	820	861	110	104	89	81	40	43
	8:00	248	10.09	881	811	851	104	101	87	80	40	42
	8:30	247.5	9.875	873	803	845	102	99	84	76	37	40
	9:30	247.5	9.875	868	799	839	100	95	80	73	35	37
	10:30	248.5	9.80	860	793	831	96	91	77	70	32	34
	11:30	247.5	9.50	860	787	830	101	96	81	74	36	36
8/26	1:00 am	246	9.55	856	786	826	97	91	80	72	34	34
	2:00	245	9.55	853	782	823	97	93	80	72	32	35
	3:00	245	9.46	850	781	821	96	92	79	71	34	35
	4:00	245	9.36	848	778	818	96	91	77	71	32	35
	5:00	245	9.36	846	778	818	97	91	77	69	34	35
	6:00	245	9.36	846	773	815	95	91	78	71	33	34
	7:00	245	9.36	844	772	815	95	91	77	72	33	33
	8:00	--	--	842	775	811	95	91	78	71	33	33
	9:00	248	9.26	842	773	813	94	89	76	69	32	32
	10:00	248	9.24	844	775	814	96	91	79	72	34	34
	11:00	248	9.24	845	776	816	99	93	80	73	36	36
	12:00	248	9.24	845	776	816	99	93	80	73	36	36

*See Table IX-9 for TC locations.

TABLE IX-7

Snap 7A-7C Thermoelectric Generator Temperature Test Data

		Power		Thermocouple Number*								
	Time	In (watts)	Out (watts)	25	26	27	28	29	30	31	Fin	Fin
				Temperature (°F)								
8/26	1:00 pm	248	9.24	844	776	816	99	95	81	74	26	20
	2:00	248	9.30	843	774	814	93	88	75	67	21	25
	3:00	248	9.36	842	773	813	87	82	69	60	15	19
	4:00	248	9.40	841	772	812	84	79	65	58	14	17
	5:00	247.5	9.24	834	768	804	78	74	53	51	8	9
	6:00	248	9.12	828	766	798	75	72	57	50	8	10
	7:00	247.5	9.08	823	758	794	72	67	54	45	5	8
	8:00	247	8.93	816	754	787	71	68	54	45	5	7
	9:00	248	8.88	811	751	780	68	65	50	42	3	5
	10:00	248	8.88	817	761	787	76	72	57	50	6	11
	11:00	235	8.83	812	748	782	74	70	55	47	8	11
	12:00	234	8.46	792	733	763	70	67	53	44	4	8
8/27	1:00 am	235	8.10	770	720	747	67	62	49	40	3	4
	2:00	235	7.70	761	710	734	61	57	47	38	3	3
	3:00	235	7.66	763	700	735	73	68	55	48	12	12
	4:00	234	7.45	757	690	729	71	67	55	46	9	9
	5:00	235	7.35	754	687	723	70	66	51	44	9	9
	6:00	235	7.35	749	684	720	70	66	54	47	10	10
	7:00	235	7.28	749	682	718	70	66	53	47	8	8
	8:00	235	7.20	744	680	715	67	63	51	45	9	9
	9:00	235	7.16	743	675	714	71	67	54	46	8	10
	9:30	235	7.16	743	676	714	71	67	54	45	10	11
	10:00	235	7.16	743	675	714	70	66	53	45	9	11

*See Table IX-9 for TC locations.

TABLE IX-8

Snap 7A-7C Thermoelectric Generator Temperature Test Data

		Power		Thermocouple Number*								
	Time	In (watts)	Out (watts)	25	26	27	28	29	30	31	Fin	Fin
				Temperature (°F)								
8/27	11:00 am	278	7.84	790	718	758	81	78	64	57	49	43
	11:30	278	8.23	817	748	786	98	95	82	74	77	69
	12:00	278	8.48	839	768	808	117	114	101	93	98	90
	12:30	280	--	853	782	823	138	134	120	111	112	102
	12:45	280	--	862	791	833	147	143	127	120	117	108
	1:00 pm	280	--	870	798	839	152	147	134	126	119	110
	1:30	280	--	883	813	854	161	156	143	136	124	117
	2:00	280	8.80	897	828	869	168	163	149	142	125	122
	2:30	280	9.09	914	844	885	176	171	158	152	133	129
	3:00	280	9.12	925	854	895	181	175	162	156	132	131
	3:30	280	9.35	934	864	906	183	178	165	159	134	133
	4:00	280	9.56	944	874	915	186	181	168	162	136	136
	4:30	279	--	954	884	923	192	185	172	165	138	138
	5:00	280	--	960	892	931	193	188	174	167	134	136
	5:30	280	--	968	898	938	192	186	173	166	131	134
	6:00	280	--	970	901	943	191	184	173	165	131	134
	6:30	279	--	973	908	947	189	182	169	162	130	130
	7:00	279	--	978	913	949	189	182	168	162	129	129
	7:30	279	--	979	918	950	186	179	165	158	127	127
	7:45	279	--	984	918	954	193	186	173	166	131	131
	8:30	279	--	839	781	814	176	170	157	150	116	116
	9:30	280	--	891	824	850	175	169	157	149	117	117
	10:30	280	--	922	849	895	174	167	153	146	115	115
	11:30 pm	280	--	945	878	915	175	169	154	148	116	116

*See Table IX-9 for TC locations.

TABLE IX-8 (continued)

		Power		Thermocouple Number*								
	Time	In (watts)	Out (watts)	25	26	27	28	29	30	31	Fin	Fin
				Temperature (°F)								
8/28	12:00	280	--	956	890	926	177	170	156	148	115	115
	12:40 am	280	--	963	899	935	175	168	154	147	112	114
	1:30	280	--	973	908	943	174	168	154	147	111	114
8/28	2:30 am	280	--	976	913	946	173	166	153	145	110	112
	3:00	280	--	--	--	947	--	--	--	--	--	--
	3:15	280	--	--	--	952	--	--	--	--	--	--
	4:30	280	--	808	744	780	157	152	141	135	103	104
	5:30	280	--	861	795	830	161	156	143	136	107	107
	6:30	280	--	896	832	867	165	159	145	138	106	108
	7:30	280	--	925	862	896	165	159	145	138	104	107
8/28	8:30 am	240	--	944	878	914	169	162	150	142	107	110
	9:00	240	10.20	934	869	906	165	161	148	141	108	110
	9:30	240	10.00	922	858	896	161	157	144	138	102	106
	1:00 pm	240	8.79	880	813	856	160	155	144	136	109	109

*See Table IX-9 for TC locations.

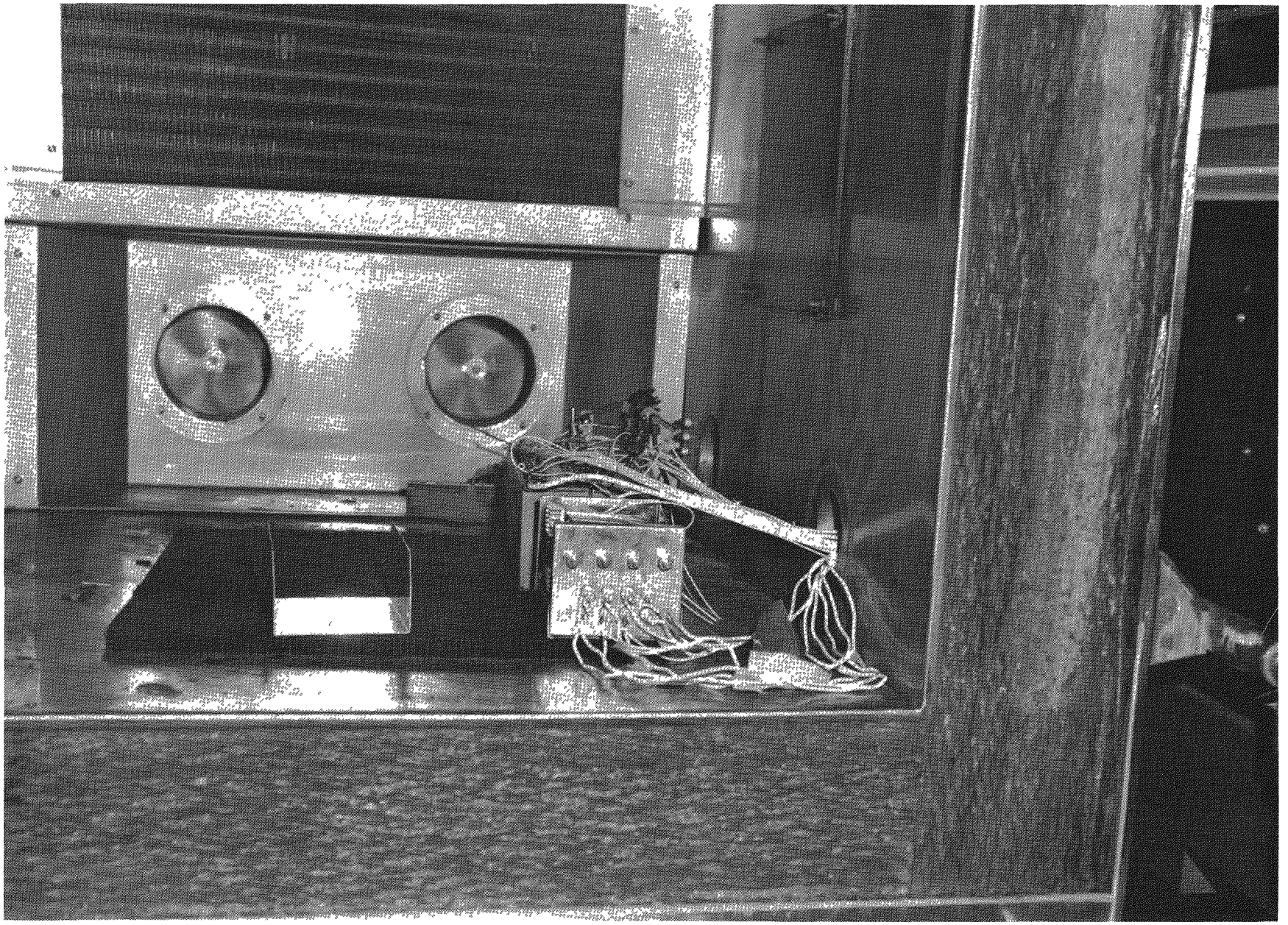

Fig. IX-24. SNAP 7C Battery and Converter Positioned in the Temperature Chamber for Temperature Output Tests

TABLE IX-9

Snap 7A-7C Generator Thermocouple Locations

Thermocouple Number	Location
25	Fuel Block No. 3 Couple, No. 5 Module, No. 2 Section Fuel Block
26	Hot Shoe, Center No. 1 Couple, No. 5 Module
27	Hot Shoe, Center No. 5 Couple, No. 5 Module
28	Cold Cap, No. 1 Couple, P Element, No. 5 Module
29	Cold Cap, No. 5 Couple, N Element, No. 5 Module
30	Heat Sink Bar L, No. 3 Couple, No. 5 Module
31	Heat Sink Top, Between Heat Sink Bars A and M
	Fin No. 1
	Fin No. 2

REFERENCES

1. "Instruction Manual--SNAP 7C Electric Generation System," MND-P-2640, The Martin Company, October 1, 1961, changed October 25, 1961.

2. Schneider, P. J., "Conduction Heat Transfer," Addison-Wesley, Reading, Massachusetts, 1955.

3. Perry, J. H., "Chemical Engineers' Handbook," McGraw-Hill, New York, 1950.

4. MN-SW-1013, "Statement of Work for SNAP 7 Generators," Revision C, The Martin Company, September 27, 1961.

5. "Final Safety Analysis, SNAP 7C Generator," MND-P-2614, The Martin Company.

6. Giedt, W. H., "Principles of Engineering Heat Transfer," D. Van Nostrand, 1957.

7. "U. S. Navy Arctic Engineering Technical Publication," NAVDOCKS TP-PW-11, March 15, 1955.

8. Evans, R. D., "The Atomic Nucleus," McGraw-Hill Book Company, Incorporated, New York, 1955.

9. Marshall, J. H., "How to Figure Shapes of Beta Ray Spectra," Nucleonics, Vol 13, No. 8, p 34, August 1955.

10. Marinelli, L. O., Quimby, E. H. and Hine, G. J., Nucleonics, Vol. 2, No. 4, p 60, April 1948.

11. Haybittle, Phys. in Med. Biol. 1, 3:270, 1956.

12. ORNL-CF-61-1-25.

APPENDIX A

THERMAL ANALYSIS OF BURIED CONTAINER SNAP 7C EMPLACEMENT

Figure A-1 is a sketch of the model to be analyzed.

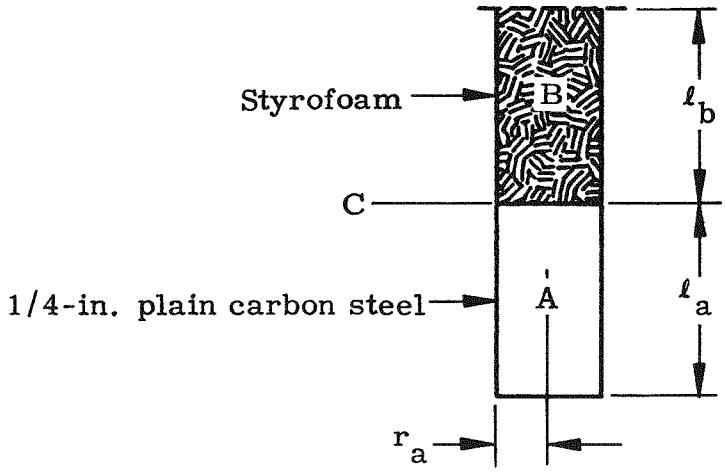

Fig. A-1. Buried Container Model

Section A will be treated as a constant-temperature (T_a) surface, losing heat in all directions below Plane C by conduction through the ice. The ice temperature at infinite distance will be taken as a constant (T_∞) at any particular time.

The steady-state heat loss from Section A by this mechanism is then given by the equation

$$q_a = -k_e A(r) \frac{dT(r)}{dr} \qquad (1)$$

where

q_a = heat loss from Section A

k_e = thermal conductivity of the ice

A(r) = area of heat flow path at a distance r from equivalent center of heat source

T(r) = temperature at distance r.

The shape of a constant-temperature surface at distance r will be taken as a hemisphere with center on the intersection of Plane C and the cylinder centerline. This implies that, for the purpose of analysis, Surface A will be treated as a hemisphere with area equal to the cylindrical Surface A.* The variable area A(r) of the surface will then be given by

$$A(r) = 2\pi r^2 . \tag{2}$$

Equation (1) then becomes

$$q_a = -2\pi k_e r^2 \frac{dT(r)}{dr}$$

which becomes, when integrated,

$$\frac{1}{r_2} - \frac{1}{r_1} = \frac{-2\pi k_e}{q_a} (T_2 - T_1) . \tag{3}$$

It is desired to determine the temperature at the surface (T_a) relative to the temperature T_∞ at $r_1 = \infty$. The radius r_2 is chosen equal to the radius of a hemisphere whose surface area is equal to that of the cylindrical Section A, having a radius of r_a and length ℓ_a.

$$r_2 = \sqrt{r_a \ell_a + \frac{r_a^2}{2}} \tag{4}$$

Substituting Eq (4) for r_2, $r_1 = \infty$, T_a for T_2 and T_∞ for T_1 gives

$$T_a - T_\infty = \frac{q_a}{2\pi k_e \sqrt{r_a \ell_a + \frac{r_a^2}{2}}} = \Delta T$$

*This will become apparent later in the analysis.

$$q_a = 2\pi k_e \sqrt{r_a \ell_a + \frac{r_a^2}{2}} \ (\Delta T). \tag{5}$$

In Section B of the cylinder, the side wall will act as a fin losing heat to the surroundings according to the relation derived in Ref. 6.

$$q_b = \sqrt{UPkA} \ (T_b - T_\infty) \ \frac{\left(1 - pe^{-2m\ell_b}\right)}{\left(1 + pe^{-2m\ell_b}\right)} \tag{6}$$

where

$$p = \frac{km - U}{km + U}$$

$$m = \sqrt{\frac{UP}{kA}}$$

U = heat transfer coefficient from surface

P = perimeter = $2\pi r_b$

A = $2\pi r_b t$

t = thickness of side wall

k = thermal conductivity of side wall

T_b = temperature on root of fin at Plane C.

According to the definition of the problem, $T_b = T_a$. Equation (6) may be rewritten

$$q_b = \sqrt{UPkA} \ \frac{\left(1 - pe^{-2m\ell_b}\right)}{\left(1 + pe^{-2m\ell_b}\right)} \ \Delta T. \tag{7}$$

All quantities in Eq (7) are defined and determinable except the effective surface heat transfer coefficient U. Such a coefficient would be expected to be the same in Sections B and A. U is defined in the heat conduction equation as follows.

$$q = UA\Delta T \tag{8}$$

Substituting into Eq (8) the heat loss for Section A given by Eq (5) and the area A for Section A given by

$$A = 2\pi r_a \ell_a + \pi r_a^2 \tag{8a}$$

and solving for U gives

$$U = \frac{k_e}{\sqrt{r_a \ell_a + \frac{r_a^2}{2}}} \tag{9}$$

The total heat production q_p must equal the heat loss $q_a + q_b$

$$q_p = \left[2\pi k_e \sqrt{r_a \ell_a + \frac{r_a^2}{2}} + \sqrt{UPkA} \; \frac{\left(1 - pe^{-2m\ell_b}\right)}{\left(1 + pe^{-2m\ell_b}\right)} \right] \Delta T \tag{10}$$

In order to determine the container surface temperature, the temperature rise (Δ T) in the ice pack must be evaluated from Eq (10).

The following geometry is assumed:

r_a = 1.5 ft

ℓ_a = 4.1 ft

ℓ_b = 3.33 ft

k_e = 1.3 Btu/hr-ft-°F

k = 28 Btu/hr-ft-°F.

The heat input to the system at the beginning of life is 256 watts, and the calculated temperature rise in the ice is 33° F. At the end of life the heat input decays to 200 watts and the temperature rise becomes 25.5° F. Reference 7 indicates a maximum ice temperature for Antarctica as follows:

	Temperature (°F)	
	Maximum	Minimum
At a 1-meter depth	20	- 30

Based on these values and the above estimates, the minimum container wall temperature will be -4.5° F. The maximum wall temperature is 53° F, but since this is above the ice freezing point, the above analysis does not hold. In this condition the problem reduces to that of a cylinder submerged in water at 32° F. In summary, the container wall temperature will range from -4.5° F to +36° F, depending on time of year and fuel age.

The generator will transfer heat to the container by both radiation and natural air convection.

$$q_{total} = q_{rad} + q_{conv}$$

$$q_{rad} = h_r A_r \Delta T_0$$

$$q_{conv} = h_{c_1} A_{gen} \Delta T_1 = h_{c_2} A_{con} \Delta T_2$$

$$\Delta T_1 + \Delta T_2 = \Delta T_0$$

where

h_r = radiation heat transfer coefficient

h_{c_1} = convection heat transfer coefficient for generator surface

h_{c_2} = convection heat transfer coefficient for inside container walls

A_r = effective radiation area, generator to container

A_{con} = area of inside container wall

A_{gen} = convective surface area of generator

ΔT_0 = temperature difference between generator and container wall

ΔT_1 = temperature difference between generator and surrounding air

ΔT_2 = temperature difference between container wall and enclosed air.

$$q_{conv} = \frac{h_{c_1} h_{c_2} A_{gen} A_{con}}{h_{c_1} A_{gen} + h_{c_2} A_{con}} \Delta T_0$$

$$q_{total} = \left(h_r A_r + \frac{h_{c_1} h_{c_2} A_{gen} A_{con}}{h_{c_1} A_{gen} + h_{c_2} A_{con}} \right) \Delta T_0$$

Evaluating this equation for G = 874 Btu/hr (maximum heat input) and for the appropriate geometry results in

$$\Delta T = 73.5^\circ F.$$

The maximum surface temperature of the generator is then 73.5° + 36° = 109.5° F. At the end of life the total temperature difference will be 57.3° F and the minimum generator surface temperature will be approximately 53° F.

Air temperature within the steel container housing will range from a maximum of 60° F to a minimum of 20° F.

APPENDIX B

SHIELDING KILOCURIE AMOUNTS OF STRONTIUM-90*

I. INTRODUCTION

Strontium-90 is one of the radioactive isotopes used to generate heat for small auxiliary power systems. Kilocurie amounts of this isotope are required to produce several watts of heat. Since the decay sequence of Strontium-90 contains no nuclear gamma radiation, it would be easy to believe that no shielding is required. However, bremsstrahlung X-rays are present, and shielding must be provided for them. Most of the bremsstrahlung are generated when the beta rays are slowed down in the compound or mixture of which the fuel pellet is made. A smaller number are generated by the betas which escape the pellet and are slowed down in the cladding material.

Bremsstrahlung from Strontium-Yttrium-90 are usually measured by using small sources in the microcurie and millicurie range. These results invariably stress the large quantity of low energy gamma rays produced but do not give adequate distributions for the high energy end of the spectrum. These results are wholly inadequate for use in designing shields for high kilocurie amounts of Strontium-90. Calculated bremsstrahlung distributions indicate that heavier shielding is required than is indicated by experimental results obtained in measuring microcurie and millicurie amounts of Strontium-90.

To obtain a confirmation of the amount of shielding required for large Strontium-90 sources, Oak Ridge National Laboratory was requested to measure the attenuation by lead absorbers of the radiation from a 1000-curie source of strontium titanate. The purpose of this report is to compare the experimental results with calculated values.

II. BREMSSTRAHLUNG

The total intensity (number of photons times the photon energy) of bremsstrahlung from monoenergetic beta rays in thick targets is given by

$$I = kZE^2$$

---

*A. M. Spamer

where

I = bremsstrahlung intensity

k = constant

Z = atomic number of absorber

E = beta energy (mev).

The spectral distribution of photons is a straight line function with the maximum photon energy equal to the beta ray energy (Ref. 8). The number of photons at the maximum energy is, however, zero. By equating the total intensity to the area of the triangle formed by the distribution curve and the coordinate axes, the number of photons at zero energy is easily found to be equivalent to 2EkZ. If the photon distribution is divided into energy groups, the average number of photons in each group is equal to the area under the distribution curve bounded by the energy limits of the range, divided by the energy increment.

Beta rays from isotope decay are not emitted monoenergetically but in spectral distributions which vary greatly for different isotopes (Ref. 9).

If the distribution of betas is known for a particular isotope, it may be broken into energy groups and the photon production for each group found.

By use of the curves in Ref. 9, the beta distribution of the nominal 2.2-mev beta from the disintegration of Yttrium-90 was found. The results were normalized to have the area under the curve represent the distribution from one Yttrium-90 disintegration. As a check of these results, the average energy of the betas calculated from this curve was found to be 0.876 mev, which compares favorably with the value 0.90 mev given in Ref. 10.

The beta distribution was divided into 10 equal energy groups; the number of betas in each group per Yttrium-90 disintegration is given in Table B-1. This grouping of betas was then used to calculate bremsstrahlung distribution. The energy grouping for the bremsstrahlung was chosen to be the same as that for the betas. The number of gammas for each group and the number of gammas divided by kZ are listed in Table B-1.

TABLE B-1

Grouped Spectral Distribution of Betas and Bremsstrahlung from Yttrium-90

Energy Group	Number of Betas per Yttrium-90 Disintegration	Number of Gammas + kZ	Number of Gammas per Yttrium-90 Disintegration: As Used k = 0.0007 Z = 26	Number of Gammas per Yttrium-90 Disintegration: Adjusted k = 0.000175 Z = 26
2.2-1.98	0.0068	0.000157	2.97×10^{-6}	7.42×10^{-7}
1.98-1.76	0.0349	0.00143	2.70×10^{-5}	6.75×10^{-6}
1.76-1.54	0.0696	0.00611	1.155×10^{-4}	2.89×10^{-5}
1.54-1.32	0.1013	0.0180	3.404×10^{-4}	8.51×10^{-5}
1.32-1.10	0.1231	0.0425	8.035×10^{-4}	2.09×10^{-4}
1.10-0.88	0.1389	0.0924	1.747×10^{-3}	4.37×10^{-4}
0.88-0.66	0.1482	0.188	3.550×10^{-3}	8.87×10^{-4}
0.66-0.44	0.1469	0.385	7.286×10^{-3}	1.82×10^{-3}
0.44-0.22	0.1308	0.887	1.677×10^{-2}	4.19×10^{-3}
0.22-0	0.0993	3.50	6.612×10^{-2}	1.65×10^{-2}

Published values for the constant k vary widely from 0.4×10^{-3} to 1.1×10^{-3} (Ref. 8). One theoretical determination gives values one order of magnitude lower. The value 0.7×10^{-3} was used in the calculations presented here.

An effective value of Z = 26 was obtained for strontium titanate by using the following relation, found in Ref. 8:

$$Z_{eff} = \frac{N_1 Z_1^{\,2} + N_2 Z_2^{\,2} + N_3 Z_3^{\,2} + \ldots}{N_1 Z_1 + N_2 Z_2 + N_3 Z_3 + \ldots}$$

where N_1, N_2, N_3, . . . are the atoms per cm^3 of the mixture having atomic numbers Z_1, Z_2, Z_3, . . .

The total intensity of bremsstrahlung from a distribution of beta energies is expressed by

$$I = kZ(E_{rms})^2 \doteq \sum_{\substack{\text{all} \\ \text{groups}}} N_i \overline{E}_i$$

or

$$(E_{rms})^2 \doteq \sum_{\substack{\text{all} \\ \text{groups}}} \frac{N_i}{kZ} \overline{E}_i$$

E_{rms} is the root mean square energy of the beta distribution; $\overline{E}_i$ is the average group energy of the bremsstrahlung, and N_i is the number of bremsstrahlung in the group. The root mean square energy of the betas was calculated and found to be 1.015 mev. The sum of the number of gammas, divided by kZ, multiplied by the average energy, was calculated and found to have a value of 1.217 mev. This is about 18% higher than the calculated $(E_{rms})^2$.

Reference 11 states that the dose rate from one curie of Strontium-90 is about the same as that from 12 mgm of radium, and the average energy of the bremsstrahlung is about 300 kev. The dose rate at one meter from 12 mgm of radium is 12 mr/hr. Using the distribution of bremsstrahlung given in Table B-1, the bare (without self-absorption and shielding) dose rate at one meter from one curie of Strontium-Yttrium-90 was found to be 12.53 mr/hr, and the average energy of the bremsstrahlung was calculated to be 236 kev.

The bremsstrahlung from the 0.5-mev beta of Strontium-90 were not included since they will be in the low kilovolt range and will be attenuated rapidly in the first few mils of shielding.

III. SHIELDING PROGRAM

Dose rates were calculated by means of a generalized shielding program coded for the IBM 709. The source is divided into a number of point sources, and the program calculates the dose rate from each of these points. The program was coded to accommodate up to 400 source points and a maximum of 10 initial source energies. Path lengths through the various materials, along a line joining a point source and the dose point, are found and used to calculate relaxation lengths and buildup for each of the materials between these two points. The individual relaxation lengths are added to obtain the total relaxation length. Buildup along the individual path segments is defined as the infinite medium buildup factor minus one. The total buildup factor along the path from the source to the dose point is assumed to be one plus the sum of the individual buildups. Infinite media buildup factors are approximated by the sum of two exponentials.

The direct energy flux at the dose point is evaluated for each source energy and source position and converted to dose rates by the appropriate flux-to-dose conversion factor. The total dose rate is, of course, equal to the sum of the dose rates from each individual source point.

IV. DESCRIPTION OF EXPERIMENTS*

Dose rates from a 1000-curie source of Strontium-Yttrium-90 were measured by ORNL personnel. The kilocurie of Strontium-90 was contained in 65 grams of titanate powder which had been compacted and sintered to a density of 4.5 grams per cubic centimeter. The only radioactive contamination in the pellet was 305 millicuries of Cerium-144 at the time the measurements were made.

Measurements were made with a Cutie Pie Model 740 (Vectoreen Instrument Company) and a survey meter No. 2610A (Nuclear Instrument and Chemical Company) which had been calibrated by the ORNL Health Physics Department, using standard radium gamma sources.

The physical arrangement used when the measurements were made is shown in Fig. B-1. Two sets of measurements were made. Case I was made with the detector located 16-3/8 inches above the pellet when the pellet was shielded with a 1/8-inch Hastelloy C plate and lead plates which varied in increments of 1/2 inch up to 6-1/2 inches. The measurements for Case II were made with the detector 19-1/4 inches above the

*This information was drawn freely from an advance copy of Ref. 12.

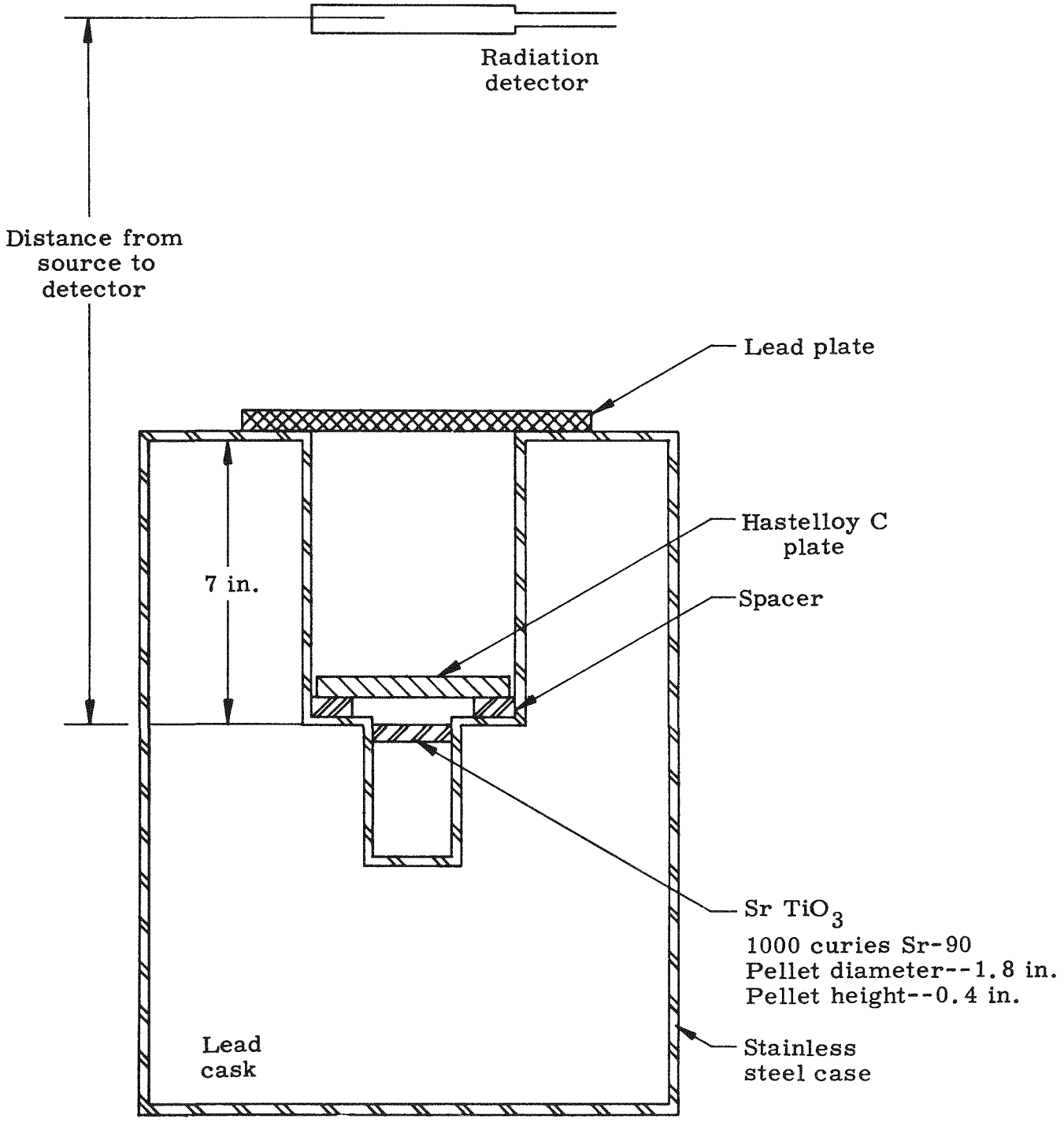

Fig. B-1. Physical Arrangement Used in Measuring Dose Rates

pellet when it was shielded with 1/2 inch of Hastelloy C and various thicknesses of lead. The results of these experiments are plotted in Fig. B-5 and B-6.

V. RESULTS OF CALCULATIONS

The accuracy of point-by-point approximations to integrals depends upon the number of points used. To determine the number of points to use to obtain reasonably accurate results, several problems are run with different numbers of points. Experience has shown that comparatively few points are required to have the third and fourth significant figures in agreement with the results from a greater number of points. To determine the number of source points to use for the present problem, the source was divided into 5, 10, 20 and 40 points. The circular cross section of the fuel pellet was divided into 5 and 10 approximately equal areas, as shown in Fig. B-2 and B-3, and the height was divided into 1, 2 and 4 equal divisions. Calculated results are given in Table B-2. After examining these results, it was decided to run the remainder of the problems with 20 source points. Dose rates versus thickness of lead shielding are tabulated in Table B-3 and are plotted in Figs. B-5 and B-6. Table B-3 also contains the contribution to total dose rate from the 305 millicuries of Cerium-144 present in the strontium pellet. As with Strontium-90, most of the gamma radiation associated with Cerium-144 is bremsstrahlung radiation. The bremsstrahlung radiation from Cerium-144 results from the 2.97-mev beta of Praseodymium-144. The higher energy beta of Praseodymium-144 causes the bremsstrahlung to be more penetrating than the bremsstrahlung of Yttrium-90. If the contribution from Cerium-144 to Strontium-90 dose rates were limited to a percentage of the Strontium-90 dose rate, the allowable amount of cerium would vary with the shield thickness. To illustrate this point, it was assumed that a 10% increase in dose rate would be acceptable. The curies of Cerium-144 per curie of Strontium-90 were calculated for various thicknesses of lead shielding and are plotted in Fig. B-4.

VI. COMPARISON OF RESULTS AND CONCLUSIONS

Examination of Figs. B-5 and B-6 shows that the calculated results are higher than the experimental results by an almost constant amount. Analysis of the data shows the calculated results are higher than the experimental results by a factor of about 4.

This could be caused by either of two items used in the calculations. One of these could be the curie strength, and the second, the product

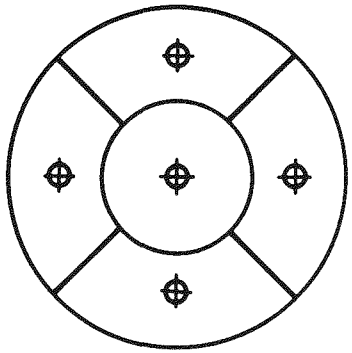

Fig. B-2.
Source Point Configuration--
Five Divisions

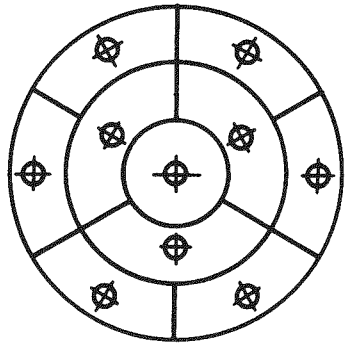

Fig. B-3.
Source Point Configuration--
10 Divisions

TABLE B-2

Comparison of Dose Rates for Various Numbers of Source Points

Number of Divisions in Circular Area	Number of Divisions in Height	Total Number of Source Points	Dose Rate*		
			No Lead (mr/hr)	1/2-in. Lead (mr/hr x 10^4)	5-in. Lead (mr/hr)
5	1	5	38.181	1.0144	6.6837
	2	10	38.318	1.0146	6.6937
	4	20	38.354	1.0146	6.6963
10	1	10	38.175	1.0142	6.6787
	2	20	38.311	1.0143	6.6890
	4	40	38.347	1.0144	6.6914

*Detector--16-3/8in. from pellet;
Self absorption in pellet and 1/8-in. Hastelloy

TABLE B-3

Calculated Dose Rates Versus Thickness of Lead
for Comparison with ORNL Data--

Self Absorption + Hastelloy C + Lead

Thickness of Lead (in.)	Dose Rates (mr/hr) Sr-Y-90* 1000 Curies	Ce-144* 305 Millicuries	Sr-Y-90** 1000 Curies
1/2	1.015×10^{4}	23.6	5.61×10^{3}
1	3.828×10^{3}	12.0	2.08×10^{3}
1-1/2	1.575×10^{3}	6.4	8.47×10^{2}
2	6.81×10^{2}	3.5	3.62×10^{2}
2-1/2	3.03×10^{2}	1.9	1.60×10^{2}
3	1.38×10^{2}	1.045	7.26×10
3-1/2	6.38×10	0.575	3.34×10
4	2.98×10	0.316	1.55×10
5	6.70	0.0952	3.47
6	1.54	0.0285	8.00×10^{-1}
7	3.64×10^{-1}	0.00851	1.87×10^{-1}

*Distance, source to detector = 16-3/8 in.
Hastelloy C thickness = 1/8 in.

**Distance, source to detector = 19-1/4 in.
Hastelloy C thickness = 1/2 in.

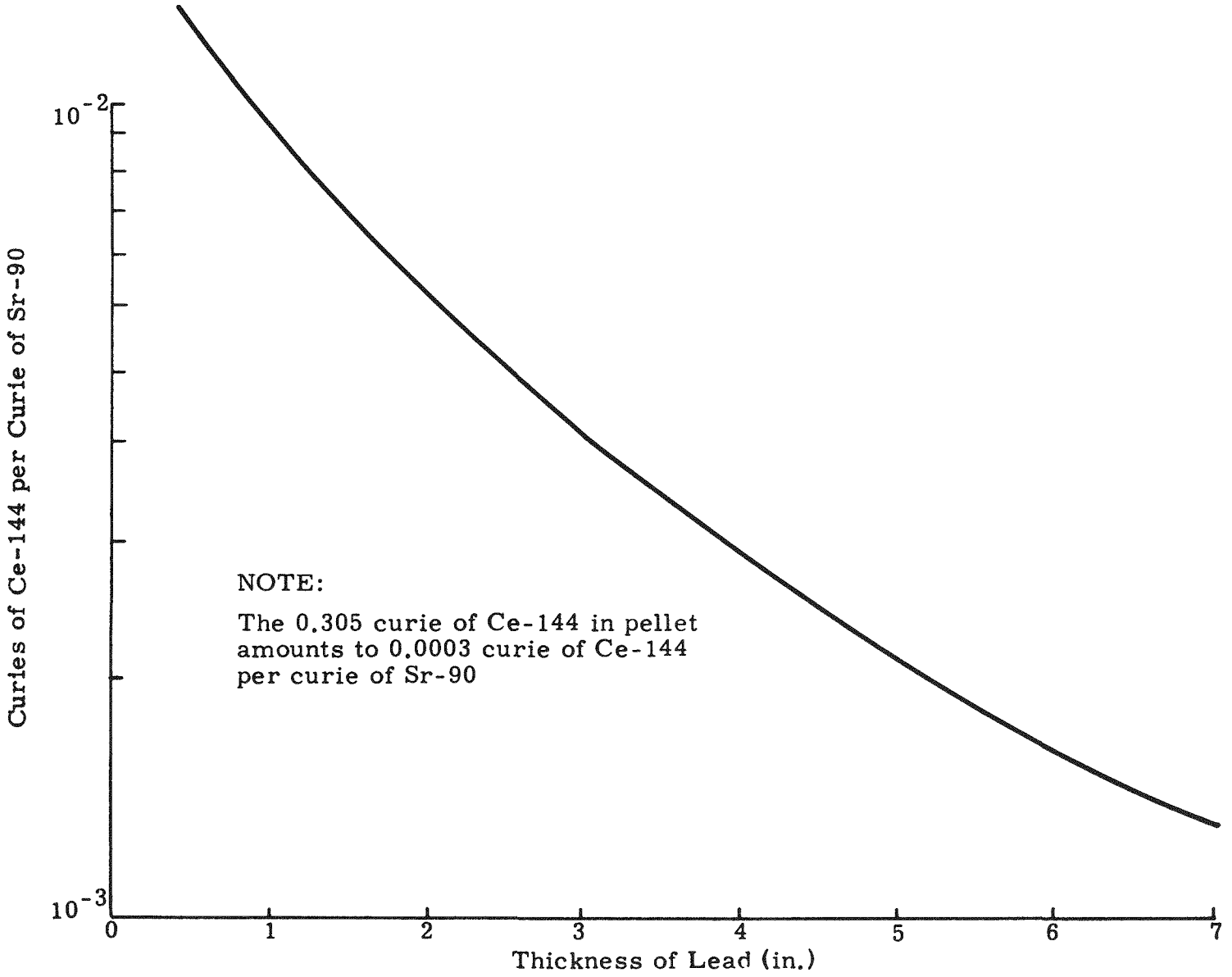

Fig. B-4. Curies of Ce-144 per Curie of Sr-90 Required to Increase Strontium-90 Dose Rate by 10%

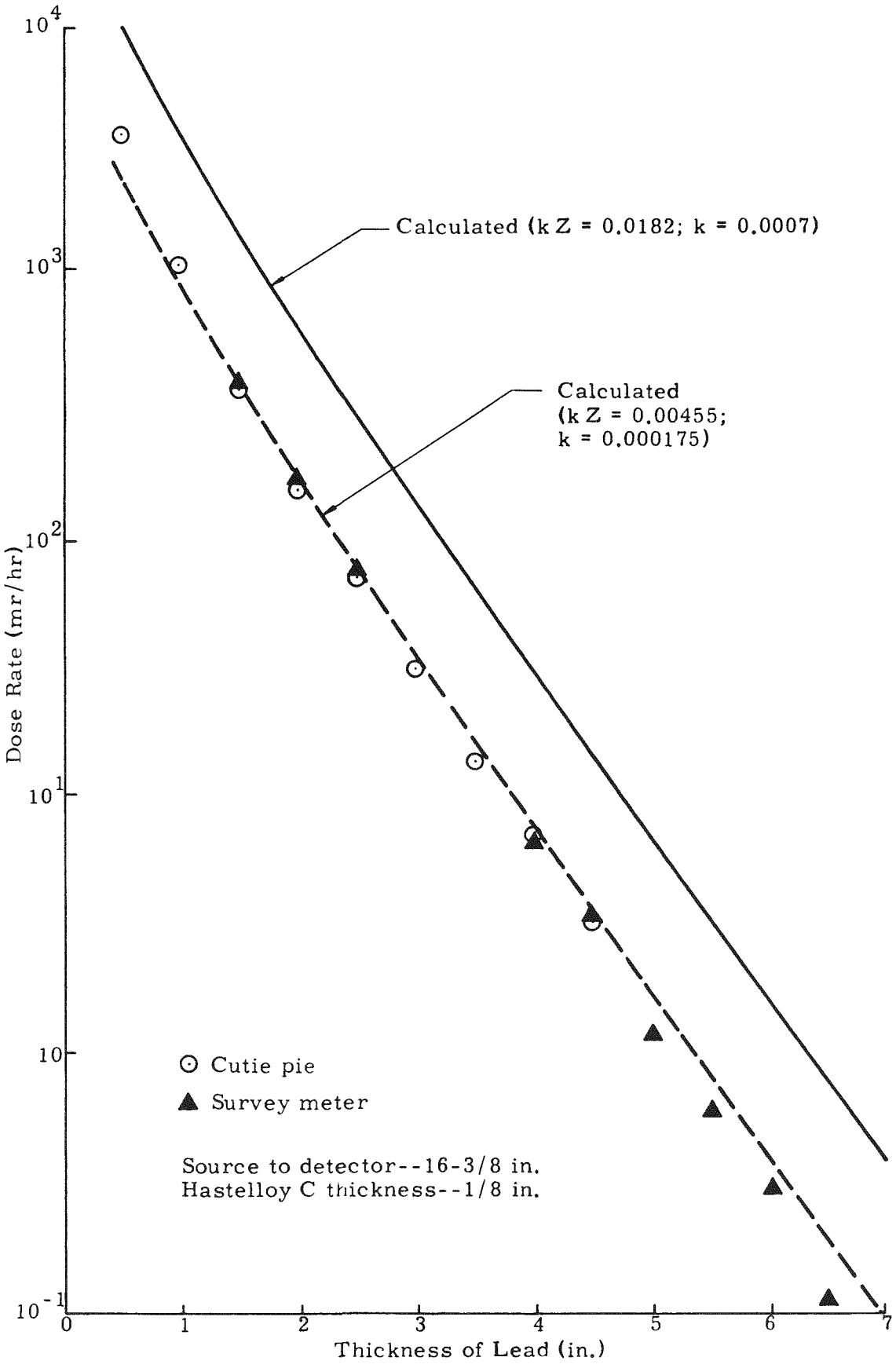

Fig. B-5. Measured and Calculated Dose Rates for Case 1

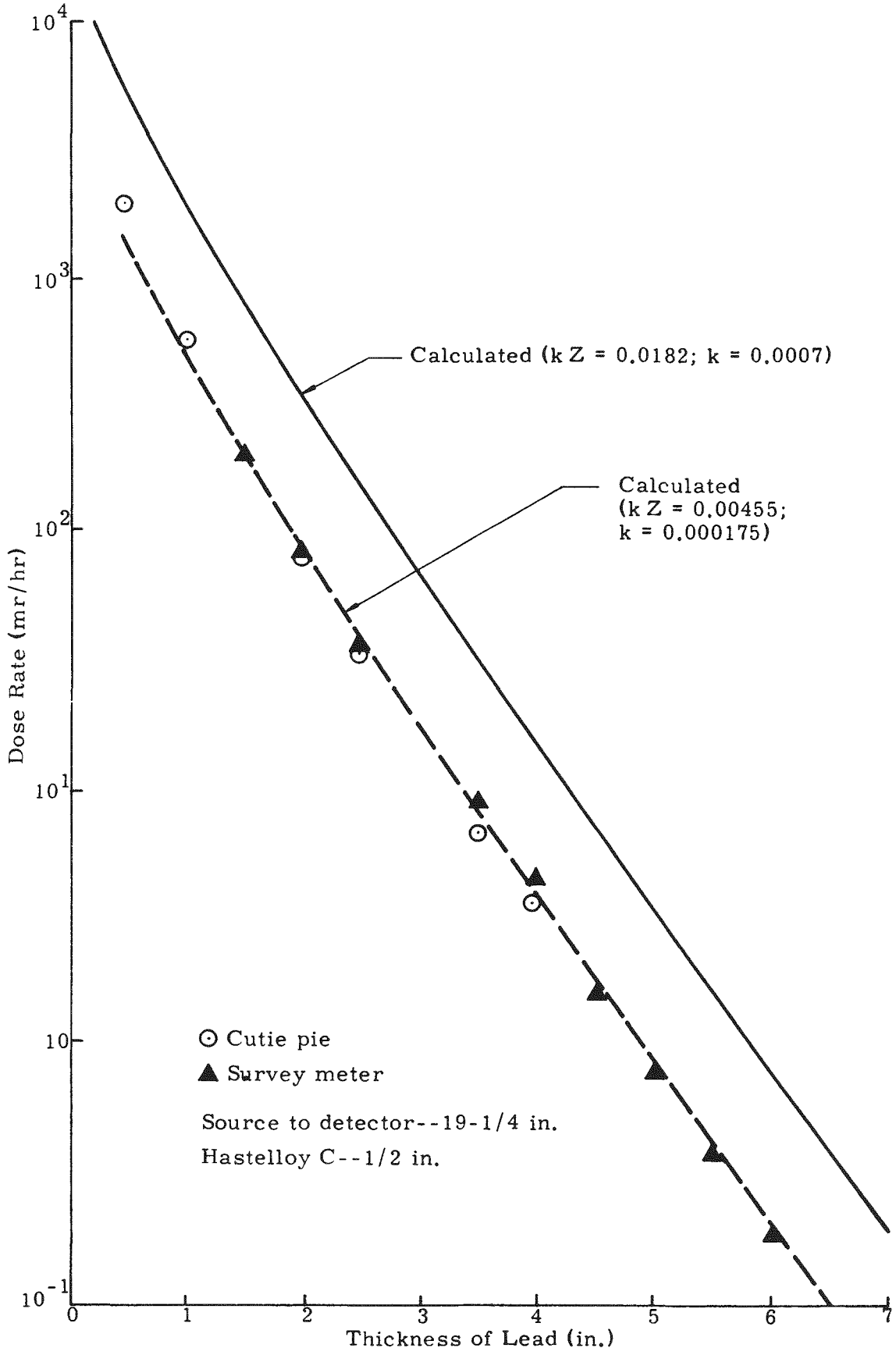

Fig. B-6. Measured and Calculated Dose Rates for Case 2

kZ which enters into the bremsstrahlung calculation. The curie strength used should be close to the stated amount since care was exercised to determine the amount of Strontium-90 present in the pellet. When the spread of values given the k is considered (Ref. 8) it would be safe to assume that the factor kZ used in the calculations is incorrect. The factor kZ will be corrected to obtain agreement between calculated and experimental results.

The originally calculated values were divided by 4 and plotted as the dashed curves in Figs. B-5 and B-6. These curves are in close agreement with the experimental points.

The value of kZ used to make the original calculations is 0.0007 x 26 = 0.0182, and the value which gave the dashed curve is 0.00455. If it is assumed that the calculated effective Z of 26 is correct, the value of k would become 1.75×10^{-4}. The number of gammas per disintegration of Yttrium-90, using the adjusted value of kZ, is tabulated in Table B-1.

The Cerium-144 present in the pellet while the experiments were being performed did not contribute appreciably to the Strontium-90 dose rates. Depending upon the shield thickness, the amount of cerium present in the pellet could be increased by factors between 4 and 40 to have a 10% increase in dose rate.

APPENDIX C

SNAP 7C ENGINEERING DRAWINGS, WEIGHTS AND DIMENSIONS

Title	Number
SNAP 7C--5-Watt Electric Generation System Drawings	
Installation--USN Weather Station	398C1080052
Container	398C1080050
Outrigger	398C1080051
Battery--Converter Enclosure Assembly	398C1080053
Generator Cover Assembly	398C1080054
Thermoelectric Generator Assembly	398C1080055
Supports--SNAP 7C Container	398C1080056
Interconnection Block Diagram	398C1080057
Schematic--Battery and Converter Compartment	398C1080058
Schematic--dc to dc Converter	398C1080059
Schematic--Antenna Coupler	398C1080060
SNAP 7C Thermoelectric Generator Drawings	
Generator--Biological Shield Assembly	398-3021000
Cylinder	398-3021001
End Plate	398-3021002
Fuel Capsule Assembly	398-3021003
Fuel Block	398-3021004
Details--Fuel Block	398-3021005
Shield	398-3021006

Title	Number
SNAP 7C Thermoelectric Generator Drawings (continued)	
Shield Block	398-3021007
Insulation Strip	398-3021008
Insulation Block	398-3021009
Thermoelectric Elements	398-3021010
Shoe--Hot Junction	398-3021011
Details--Cold Junction	398-3021012
Piston	398-3021013
Washer	398-3021014
Frame--Heat Sink	398-3021015
Bars--Heat Sink	398-3021016
Insulation--Corner Strip	398-3021017
Insulation--Spacer	398-3021018
Insulation--Plate	398-3021019
Wire Guide	398-3021020
Plug	398-3021021
Electrical Connector	398-3021022
Connector Mount	398-3021023
Connecting Bar	398-3021025
Shipping Pallet	398-3021026
Nameplate	398-3021027
Cover, Generator Test	398-3021028
Cap Screw	398-3021029

Title	Number
SNAP 7C Thermoelectric Generator Drawings (continued)	
Fuel Capsule Shipping Cask	398-3021040
Biological Shield Container	398-3021041
Generator Assembly	398-3021042
Generator Cover Assembly	398-3021043
Details and Assembly--Fuel Shipping Cask	398-3021044
Hot Shoe--Element Assembly	398-3021045
Cold Cap Assembly	398-3021046
Thermoelectric Module Assembly	398-3021047
Heat Sink Assembly	398-3021048
Generator Shell Assembly	398-3021049
Generator--Pallet, Shipping Assembly	398-3021050

SNAP 7C Weights and Dimensions

Name	Dimensions (in. approximate) Length	Width	Height	Weight (lb approximate)
Thermoelectric Generator and Biological Shield		19 (dia)	21	1840
Battery and Converter Compartment	20	16	6	100
Bottom Container Section	49-1/2	36 (dia)		550
Top Container Section	45-1/2	36 (dia)		550
Outriggers (4)	36	4	7-1/2	40 each
Antenna Coupler and Top Deck Assembly		36 (dia)	1/2	160

SNAP 7C Weights and Dimensions (continued)

Name	Dimensions Length (in. approximate)	Width (in. approximate)	Height (in. approximate)	Weight (lb approximate)
Marman Clamps and Gaskets (2 each)		36 (dia)		26 each
Shipping Pallet	60	48	6	360
Electrical Cables				
398C1080057-19	36			
398C1080057-29	36			
Shorting Plug				
398C1080055-1	2-1/2			
Battery and Converter Compartment Shelf	24-1/2	15-1/2	1	
U. S. Navy PAWS Instrument Package Shelf	29-1/2	22-1/2	1	
Styrofoam Insulation	36	35 (dia)		
U. S. Navy PAWS (GFE)				
RF Cables (2) (GFE)	72			
Control Cable (GFE)	72			
Barometer Hose (GFE)	72			

Total system weight minus shipping pallet = 3412 pounds.